The Hong Kong Polytechnic University
Department of Electronic and Information Engineering

Relaying Methods for Cooperative Communication Networks

PhD candidate: Zhou, Qingfeng

Supervisor: Dr. Francis C. M. Lau

A thesis submitted in partial fulfilment
of the requirements for the
Degree of Doctor of Philosophy

February 2010

CERTIFICATE OF ORIGINALITY

I hereby declare that this thesis is my own work and that, to the best of my knowledge and belief, it reproduces no material previously published or written, nor material that has been accepted for the award of any other degree or diploma, except where due acknowledgement has been made in the text.

__________________________ (Signed)

Zhou, Qingfeng (Name of student)

To my family

this page is left blank intentionally

Abstract

A cooperative communication system is generally referred to as a wireless communication system in which the transmission between a source node and a destination node is improved by the participation of one or more relay(s). The main interest of the academia and the industry on cooperative communications is to optimally harness the available relays to enhance the robustness of the desired transmission to fading and interference. For a single-relay system, the simplest relaying protocols are the decode-and-forward (DF) and amplify-and-forward (AF) protocols. These well-known relaying schemes are usually fulfilled in the time-division-duplexing platform. Specifically, in the first time slot, the source node broadcasts a frame of information signals to the relay and the destination; then the relay processes the received signal by amplifying it in the AF scheme or re-encoding the decoded result of the received signal in the DF scheme, and goes on to transmit the processed signal frame to the destination in the second time slot. Finally the destination decodes the information frame based on the combination of the received signals from the source node and the relay node.

In this thesis, we will explore the relaying schemes for single-relay networks, multi-relay networks, and multi-relay two-way networks, and further analyze the performance of those schemes. Firstly, two new relaying protocols will be proposed for single-relay systems, namely incremental selection amplify-and-forward (ISAF) and jointly incremental selection relaying (JISR) protocols. It will be shown that both protocols improve the reliability of the desired transmission compared with existing relaying protocols.

Secondly, we will systematically study a multi-relay network in which only one of the relays that satisfies a selection criterion will be allowed to re-transmit the signal in the second time-slot. If the AF, DF, selection decode-and-forward (SDF), IAF, ISAF or JISR protocol is further used, the relaying scheme is called opportunistic AF, (OAF), opportunistic DF (ODF), opportunistic SDF (OSDF),

opportunistic IAF (OIAF), opportunistic ISAF (OISAF), and opportunistic JISR (OJISR), respectively. We will derive closed-form expressions of the asymptotic outage performances for all these opportunistic relaying schemes and compare their capabilities. We will also show that the OIAF, OISAF and OJISR schemes outperform the OAF, ODF and OSDF schemes in terms of diversity-multiplexing tradeoff (DMT). Moreover, the OISAF and OJISR schemes have accomplished better outage performance than the OIAF scheme.

Thirdly, we will analyze the performance of the channel-state-information-assisted OAF (CSI-assisted OAF) scheme in terms of outage performance, ergodic achievable rate and average symbol error rate. Previous analysis of the CSI-assisted AF scheme has approximated $(\bar{\gamma}^2 xy)/(\bar{\gamma}x + \bar{\gamma}y + 1)$ by $(\bar{\gamma}^2 xy)/(\bar{\gamma}x + \bar{\gamma}y)$, where $\bar{\gamma}$ represents the signal-to-noise ratio (SNR); x and y are the squares of the magnitudes of the channel fading coefficients. However, this approximation is invalid for the CSI-assisted OAF system. In this part, we will derive more accurate upper- and lower-bounds of the performance of the CSI-assisted OAF system.

Finally, we will extend the opportunistic relaying notion to multi-relay two-way networks. In a two-way relaying system, the channel accommodates the transmissions from the source to the destination and vice versa simultaneously. In this kind of system, the source and the destination are usually called Source One and Source Two. Suppose that there is no direct link between the sources, and that multiple relays are located between the sources. To reach a high overall throughput in the two-way system, a pair of information frames is exchanged during two time slots by using physical-layer network coding. During the first time slot, both the sources broadcast their information frames to the relay nodes. Then during the second time slot, the relays broadcast some network-coded and temporally aligned information-bearing frames back to the sources. Subsequently, the sources decode the information frame from their counterparts based on the received frames from the relays. Here, we will propose a new relaying protocol, namely opportunistic two-way relaying (O-TR), in which only the best/opportunistic relay is active in performing the relaying duty. It will be proved that the proposed O-TR outperforms the case when all the available relays are used to construct the distributed space-time code.

Acknowledgements

Since graduated from University of Science and Technology of China in 2000, I had been seizing every opportunity to pursue a PhD degree. The path had been winded and filled with pitfalls and difficulties. Without the help and support from many others, it would not be possible for me to get through and complete my PhD degree.

First of all, I am cordially grateful to my supervisor, Dr. Francis Lau for his unwavering support and encouragement, which had made my PhD study also a joyful journey. Whenever I knocked on his office door, he would put aside what he was working on and would eagerly discuss with me about my work. He also granted me the freedom of choosing a research topic that interested me, guided me throughout the whole study and provided me with his unconditional support. Moreover, he was tolerant of my on-and-off ignorant and arrogant characters. He further helped me enhancing the mathematical derivations and my English writing skills with great patience.

Next, I would like to express my gratitude to Dr. Yonghui Li and Prof. Branka Vucetic of the School of Electrical and Information Engineering, University of Sydney. During the three-month visit to their Telecommunications Laboratory in 2009, I had been generously furnished with invaluable comments and advices. Moreover, the collaboration with Dr. Li and Prof. Vucetic had greatly improved my capability in performing research. I should also thank the colleagues in the Laboratory for their assistance on research and my stay in Sydney. Even though we had spent a short time together, the friendship that built among us would last forever.

My grateful acknowledgement is also made to the leader of our Applied Nonlinear Circuits and Systems Research Group, Prof. Chi. K. Tse. He always shared with us his views on career development, research directions and even lifestyle in various seminars and social gatherings. In addition, thanks are expressed to groupmates and colleagues, such as Dr. Rongtao Xu, Dr. Xia Zheng, Dr. Feng Xu, Dr. Waiman Tam, Dr. Yi Zhao, Dr. Jie Zhang, Dr. Junfeng Sun, Dr. Sufen Chen, Dr.

Xiaohui Qu, Dr. Hongbin Chen, Dr. Ben C. T. Cheng, Dr. Yongxiang Xia, Dr. Xi Chen, Dr. Guangjian Tian, Mr. Shixiong Zhang, Mr. Chi Xu, Mr. Xuhua Sheng, Miss Ruoxi Xiang, Miss Xiujuan Zheng, Miss Zhen Liang (just to name a few in an arbitrary order), for encouraging me and decorating my PhD study with happiness and friendship.

Last but not least, I am deeply indebted to my parents, my sister, and my brother-in-law. I do not believe that I could have overcome all the hard times during these years without the lasting support from them. I also owe my deep appreciation to my wife for taking such a good care of our newborn baby, and for her enduring support and patience that made this PhD thesis possible.

Publications

Journal papers

1. Q. F. Zhou, Y. Li, F. C. M. Lau, and B. Vucetic, "Decode-and-forward two-way relaying with network coding and opportunistic relay selection," *IEEE Trans. Commun.*, to appear.

2. Q. F. Zhou and F. C. M. Lau, "Performance analysis of opportunistic cooperative communications with CSI-assisted amplify-and-forward relaying and MRC reception," *IEEE Trans. Veh. Technol.*, to appear.

3. Q. F. Zhou, F. C. M. Lau, and S. F. Hau, "Asymptotic analysis of opportunistic relaying protocols," *IEEE Trans. Wireless Commun.*, vol. 8, no. 8, pp. 3915–3920, Aug. 2009.

4. Q. F. Zhou and F. C. M. Lau, "Two incremental relaying protocols for cooperative networks," *IET Communications*, vol. 2, no. 10, pp. 1272–1278, Nov. 2008.

Conference paper

1. Q. F. Zhou and F. C. M. Lau, "Novel Incremental Relaying Protocols for Cooperative Networks," *Proceedings, 14th China Symposium on Information Theory 2007 (CSIT'2007)*, December 2007, Guangzhou, China, pp. 257-260.

Contents

List of Tables

List of Figures

Acronyms

AF	Amplify-and-forward
AWGN	Additive white Gaussian noise
BER	Bit error rate
BPSK	Binary phase-shift-keying
cdf	Cumulative distribution function
CDMA	Code division multiple access
C-MRC	Cooperative maximal ratio combing
CP	Cyclic prefix
CSCG	Circularly symmetric complex Gaussian
CSI	Channel state information
dB	Decibel
DF	Decode-and-forward
DFE	Decision feedback equalizer
DMT	Diversity-multiplexing tradeoff
DRT	Direct repeat-transmission
DT	Direct transmission
EADST	Error aware distributed space-time
EGC	Equal gain combining
FD	Frequency division
FDST-TR	Fully-distributed space-time coded two-way relaying

FER	Frame error rate
FFT	Fast Fourier transformation
Gb	Gigabit
IAF	Incremental amplify-and-forward
IFFT	Inverse fast Fourier transformation
iid	Independent and identically distributed
ISAF	Incremental selection amplify-and-forward
ISI	Inter-symbol interference
JISR	Joint incremental selection relaying
LDPC	Low density parity check
LOS	Line-of-sight
MAC	Medium access control
Mb	Megabit
MC-CDMA	Multi-carrier code division multiple access
M-PSK	M-ary phase-shift-keying
MGF	Moment generating function
MIMO	Multiple-input multiple-output
MMSE	Minimum mean-squared-error
MRC	Maximal ratio combining
OAF	Opportunistic amplify-and-forward
ODF	Opportunistic decode-and-forward
OFDM	Orthogonal frequency division modulation
OIAF	Opportunistic incremental amplify-and-forward
OSDF	Opportunistic selection decode-and-forward
OISAF	Opportunistic incremental selection amplify-and-forward
OJISR	Opportunistic joint incremental selection relaying
O-TR	Opportunistic two-way relaying

pdf	Probability density function
PEP	Pairwise error probability
PSK	Phase-shift-keying
P2P	Point-to-point
QAM	Quadrature amplitude modulation
QPSK	Quadrature phase-shift-keying
RV	Random variable
SDF	Selection decode-and-forward
SER	Symbol error rate
SNR	Signal-to-noise ratio
STBC	Space-time block coding, or space-time block codes
STC	Space-time coding, or space-time codes
TD	Time division
VLSI	Very-large-scale integration
WiMAX	Worldwide interoperability for microwave access

Notations

Set

$\mathcal{R}$	Real number
$\mathcal{C}$	Complex number
$\mathcal{R}^n$	Real column vector
$\mathcal{C}^n$	Complex column vector
$\mathcal{R}^{n\times m}$	Real $n \times m$ matrix
$\mathcal{C}^{n\times m}$	Complex $n \times m$ matrix

Vector and matrix

x	Scalar value $x \in \mathbb{R}$ or $x \in \mathbb{C}$
$\boldsymbol{x}$	Column vector of $\mathcal{R}^{n\times 1}$ or $\mathcal{C}^{n\times 1}$
$\boldsymbol{I}$	Identity matrix
$\boldsymbol{X}$	Matrix $[x_{ij}]$ of $\mathcal{R}^{n\times m}$ or $\mathcal{C}^{n\times m}$
$\boldsymbol{X}^*$	Hermitian transpose of matrix $\boldsymbol{X}$
$\boldsymbol{X}^T$	Transpose of matrix $\boldsymbol{X}$
$\lvert x\rvert$	Absolute value of scalar x, or amplitude of complex x
$\det(\boldsymbol{X})$	Determinant of square matrix $\boldsymbol{X}$

Operation and function

$\binom{m}{n}$	Binomial coefficient

$\mathbf{B}(\cdot,\cdot)$	Beta function
$\mathrm{E}[\cdot]$	Mathematical expectation
$\\|\boldsymbol{x}\\|_2$	l_2-norm of vector $\boldsymbol{x}$
$\mathrm{erfc}(x)$	Complementary error function
$\mathrm{Ei}(x)$	Exponential integral function
$\exp(x)$	Exponential function
${}_2F_1(\boldsymbol{a};\boldsymbol{b};x)$	Gauss hypergeometric function
$\Gamma(x)$	Gamma function
$\Im(z)$	Imaginary part of complex variable z
$K_1(\cdot)$	The first order modified Bessel function of the second kind
$\ln(x)$	Natural logarithm, base e
$\log(x)$	Logarithm on base 2
$\max\{x_1,\ldots,x_n\}$	Maximum of the elements $x_1,\ldots,x_n$
$\min\{x_1,\ldots,x_n\}$	Minimum of the elements of $x_1,\ldots,x_n$
$\mathcal{L}(f(t))$	Laplace transform
$\mathcal{O}(x^3)$	Big O notation
$n!$	Factorial of n
$\mathrm{mod}\{\boldsymbol{x},M\}$	Modulo-M operation
$Q(x)$	Gaussian Q-function
$\Re(z)$	Real part of complex variable z
$\sim$	Asymptotically equal

Probability

$\mathcal{CN}(\mu,\sigma^2)$	Complex circularly symmetric Gaussian distribution with mean μ and variance σ^2
$\Pr(\mathcal{A})$	Probability of an event $\mathcal{A}$

$p_X(x)$	Probability density function of RV X

Chapter 1

Introduction

The first cellphone in human history, Motorola DynaTAC 8000X, which was built in 1973 but not available for sale until 1983, weighed two pounds with the size of a brick and cost $3995 per piece. Nevertheless, it only provided the voice service through the first generation (1G) wireless network, in particular, via the analog modulation technique. Now, merely three decades later, cellular technology has come to its fourth generation (4G). In the next few years, the 4G network will be deployed worldwide, and subscribers can watch high-definition television (HDTV), play online games, check real-time stock information, and keep connected everywhere all the time, of course wirelessly. In the 4G network, any mobile device can achieve a downlink speed up to 1 Gb/s if it is stationary with respect to the base station, or up to 100 Mb/s if it is moving in high speed. In contrast to the booming of the transmission rate, the size and cost of mobile devices actually plunge, thanks to the advanced very-large-scale integration (VLSI) technology.

The striking progress of wireless technology is really a tribute to the breakthrough work of Shannon in 1948 [1]. In this work, Shannon shown that the capacity, or the maximal achievable rate, of an additive white Gaussian noise (AWGN) channel is given by

$$C = \frac{1}{2}\log_2\left(1 + \frac{P}{N}\right) \tag{1.1}$$

where P is the received signal power and N is the noise power, the unit of C can be bits/s/Hz, or bits/sample [2], or bits/transmission [3], or bits/channel use [3], or bits/symbol [4]. Here, Shannon's world-famous formula tells us that given an AWGN channel and a fixed signal-to-noise ratio (SNR), there is a transmission rate limit which we can never beat. However, nowadays the data transmission rate supported by cellular networks is still increasing year-after-year. Consequently, a question that one may ask is: "When we will reach the limit of the transmission rate, if there is a transmission-rate limit according to the Shannon's theorem?"

The answer to the above question is likely to be: *The Shannon limit of point-to-point (P2P) channels has almost been achieved, however, the transmission-rate limits of many multi-node networks are to be determined.*

We say that the Shannon limit has been nearly achieved for P2P channels because the latest low-density parity-check (LDPC) coding technique can almost reach the Shannon limit, with a gap as small as 0.0045 dB [5]. As a reference, according to the Shannon's formula, the minimum signal-to-noise ratio (SNR) to achieve a transmission rate of 0.5 bits/s/Hz is 0.188 dB. However, the capacities of many multi-point channels, except multiple access channels, broadcast channels and multiple-input multiple-output channels, are still unknown. For instance, in the network shown in Fig. 1.1, what is the capacity of the channel connecting the source $\mathbb{S}$ and the destination $\mathbb{D}$? Clearly, if we consider only the link directly connecting $\mathbb{S}$ and $\mathbb{D}$, the conditional capacity is that of a traditional P2P fading channel and is given by

$$C(h) = \frac{1}{2}\log_2\left(1 + |h|^2\frac{P}{N}\right) \tag{1.2}$$

where h is the channel coefficient of the $\mathbb{S} - \mathbb{D}$ link. However, if we further take the

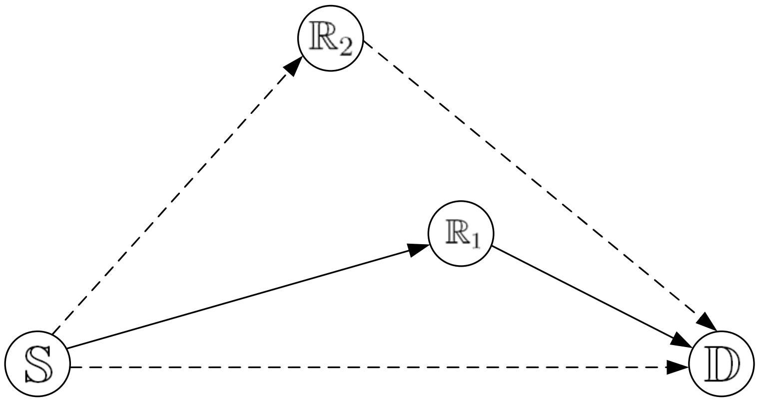

Figure 1.1: A source-destination $\mathbb{S} - \mathbb{D}$ transmission pair with two intermediate nodes $\mathbb{R}_1, \mathbb{R}_2$.

two nodes $\mathbb{R}_1$ and $\mathbb{R}_2$ into consideration, two questions will follow.

Question (i): What is the capacity of the $\mathbb{S} - \{\mathbb{R}_1, \mathbb{R}_2\} - \mathbb{D}$ channel?

Question (ii): Will the transmission between $\mathbb{S}$ and $\mathbb{D}$ benefit from the involvement of $\mathbb{R}_1$ and $\mathbb{R}_2$?

Question (i) was first tackled back in the 70's of the last century by van der Muelen [6] and Thomas Cover [7]. In [7], only an upper bound of the capacity of a P2P channel with one intermediate node has been obtained. *The intermediate node is generally called a relay node, or simply a relay.* Consequently, the P2P channel associated with one intermediate node is usually called a single-relay network, while the network shown in Fig. 1.1 is called a multi-relay network. Unfortunately, the exact capacity of a single-relay channel has been an unsolved problem. While Question (i) has attracted a broad range of attention, a lot of scholars attempt to comprehend this special kind of channel from the perspective of engineering via answering Question (ii) [8–11]. Having found out that the answer to the question is positive, they further raise the third question: "How can the intermediate relay nodes $\mathbb{R}_1$ and $\mathbb{R}_2$ contribute to the transmission between $\mathbb{S}$ and $\mathbb{D}$?" The answer to this question is critical to understanding how the overall throughput of a multi-node network can be improved by utilizing the relaying notion.

1.1 Relay Channels

According to the conventional shortest-path routing scheme, the transmission from $\mathbb{S}$ to $\mathbb{D}$ in Fig. 1.1 should be fulfilled via the direct $\mathbb{S}-\mathbb{D}$ link since this path has the least number of hops compared to the other paths such as the $\mathbb{S}-\mathbb{R}_1-\mathbb{D}$ link and the $\mathbb{S}-\mathbb{R}_2-\mathbb{D}$ link. However this shortest-path routing scheme is not robust to channel fluctuation. For instance, if the direct link $\mathbb{S}-\mathbb{D}$ suffers from deep fading, then the transmission to the destination node will be highly impaired, i.e., the power of the received signal at the destination may be so low that the error rate of the received signal is well above the required level.

However, the intermediate nodes $\mathbb{R}_1$ and $\mathbb{R}_2$ can provide a solution to circumvent the drawback of the shortest path strategy. At the moment when the direct link is deeply distorted, there is a certain possibility that one of the $\mathbb{S}-\mathbb{R}_1-\mathbb{D}$ and $\mathbb{S}-\mathbb{R}_2-\mathbb{D}$ links is good enough to allow reliable transmission to the destination node. Intuitively, transmitting the information frames via all the three paths, i.e., $\mathbb{S}-\mathbb{D}$, $\mathbb{S}-\mathbb{R}_1-\mathbb{D}$ and $\mathbb{S}-\mathbb{R}_2-\mathbb{D}$, will be more robust to channel fading than via the path $\mathbb{S}-\mathbb{D}$ solely. This is the motivation to raise a new transmission strategy. This kind of new transmission strategy is frequently called "cooperative communications" or "cooperative diversity" or "relaying". In Fig. 1.1, the relays $\mathbb{R}_1$ and $\mathbb{R}_2$ can be idle mobile units in the cellular networks, or users in the ad-hoc networks, or transmit units in the sensor networks.

In [8,9] the first cooperative communication system was studied. In this cooperative system, two adjacent users transmit their information packets to the common destination. The two users transmit alternately by using time-division multiple access (TDMA). When one user transmits, the other user listens and records the received signal. Afterwards, the other user will transmit the first data frame from its buffer and suffixes the frame with the signal received previously from its peer user.

In this way each data frame is received twice at the destination, one from its source user, one from the other user. The implementation issues and the performance of such a user-cooperative communication has also been discussed and studied in the literature.

Almost in the same period, Laneman *et.al.* studied the cooperative communication system from the information theoretic point of view [10, 11]. They mainly studied a single-relay cooperative system consisting of a source node, a destination node and a relay node. They also proposed two relaying protocols, namely amplify-and-forward (AF) and decode-and-forward (DF) protocols. In the AF protocol, the source transmits one information frame, which is listened by both the relay and the destination, during the first time slot. On the reception of the information frame from the source, the relay amplifies the received signal according to its power constraint. Then during the second time slot, the relay forwards the amplified signal to the destination, while the source keeps idle. Finally, the destination decodes the information frame based on the received signal from the source and that from the relay. It has been proved that the AF protocol achieves the full cooperative diversity, i.e., diversity of two for a single-relay system with the direct $\mathbb{S} - \mathbb{D}$ link. In the DF protocol, after receiving the frame from the source, the relay decodes the received signal, and then re-encodes the output of the decoder. During the second time slot, the relay forwards the re-encoded frame to the destination. The diversity of the DF protocol is only one for a single-relay system. However, some derivatives of the DF protocol, e.g., the selection decode-and-forward (SDF) protocol [10], can achieve the full diversity.

In this thesis, we will study the relaying schemes for single-relay one-way networks, multi-relay one-way networks, and multi-relay two-way networks. In a one-way network, the channel only accommodates the directional information flow from the source to the destination. In a two-way network, the channel accommodates the bidirectional information flowing from the source to the destination and vice versa at the same time. For simplicity, in the rest of this thesis, a single-relay network refers to a single-relaying one-way network, and a multi-relay network refers to a multi-relay one-way network, unless otherwise mentioned.

1.2 Thesis Organization

The rest of this thesis is divided into six chapters.

In Chapter 2, the motivation for studying cooperative relaying systems will be reviewed. Essentially, one of the challenges of designing efficient communication systems over wireless channels is to mitigate the impairment caused by fading. We will first present several fading-mitigation methods, and describe the similarity between the multiple-input multiple-output (MIMO) and relaying from the aspect of fading-mitigation. This similarity gains academic attention, and leads to the mounting studies on the relay channels. Then the relaying networks which will be considered in this thesis will be introduced. They are single-relay networks, multi-relay networks and multi-relay two-way relaying networks. The relaying methods for these scenarios will also be briefly reviewed. They are amplify-and-forward (AF), decode-and-forward (DF), selection decode-and-forward (SDF) and incremental amplify-and-forward (IAF) protocols for single-relay networks; orthogonal relaying, distributed space-time relaying and opportunistic relaying protocols for multi-relay networks; distributed space-time relaying for multi-relay two-way relaying networks.

In Chapter 3, we will study single-relay cooperative systems. We will propose two new relaying protocols, namely incremental selection amplify-and-forward (ISAF) and jointly incremental selection relaying (JISR) protocols. Both of them can achieve the full diversity and can accomplish better outage performance than the IAF scheme.

In Chapter 4, we focus on the opportunistic relaying protocols for multi-relay systems. Instead of coordinating a number of relays to forward the received signals, an opportunistic relaying protocol always selects a "best" relay according to certain criteria, and allows only this relay to forward its received signals. We will study the performance of several opportunistic relaying protocols with the maxmin selection criterion. These opportunistic relaying protocols include opportunistic decode-and-forward (ODF), opportunistic amplify-and-forward (OAF), opportunistic selection decode-and-forward (OSDF), opportunistic incremental amplify-and-forward (OIAF), opportunistic incremental selection amplify-and-forward (OISAF) and opportunistic jointly incremental selection relaying (OJISR) protocols. We will show that the OIAF, OISAF and OJISR schemes outperform the OAF, ODF and OSDF schemes in terms of diversity-multiplexing tradeoff (DMT). Moreover, the OISAF and OJISR schemes have accomplished better outage performance than the OIAF scheme.

In Chapter 5, we will study the performance of the channel-state-information assisted (CSI-assisted) opportunistic amplify-and-forward (OAF) relaying protocol associated with the maxmin relay selection criterion. In previous works that evaluate the performance of the CSI-assisted AF protocol, the amplification term $(\bar{\gamma}^2 xy)/(\bar{\gamma}x + \bar{\gamma}y + 1)$ is always approximated by $(\bar{\gamma}^2 xy)/(\bar{\gamma}x + \bar{\gamma}y)$ so as to simplify the performance analysis, where $\bar{\gamma}$ is the average signal-to-noise ratio (SNR), x and y are randomly distributed channel gains. However, we will demonstrate that this approximation fails to predict accurately the outage probability performance of the CSI-assisted OAF with maxmin relay selection. To the best of our knowledge, there is also a lack of such an analysis for the associated opportunistic relaying protocol, i.e., CSI-assisted opportunistic OAF relaying protocol. In this chapter, we will derive the upper and lower performance bounds of such a relaying protocol. Moreover, we will study the asymptotic performance of the protocol.

In Chapter 6, we will go on to study the multi-relay two-way relaying systems with no direct link connecting the source node and the destination node. In a two-way relaying system, the destination node also needs to transmit its information to the source node. This two-way transmission can be easily fulfilled with four time slots. During the first two time slots, the source transmits and the relay performs the relaying transmission to the destination. Then during the other two time slots, the destination and the relay collaboratively convey the transmission to the source. However, this simple transmission scheme is poor in spectral efficiency. Recently, a method called physical-layer network coding has been proposed to improve the spectral efficiency of the two-way transmission. In the physical-layer network coding, the source node and the destination node send out their information frames simultaneously during the first time slot while the relay node receives the signals. Then the relay network-encodes the received frames from the source and the destination, and broadcasts the network-coded frame to the source and the destination during the second time slot. The source and the destination finally decode the information frame of the other party based on the coded-frame from the relay. Here, we will propose a new two-way relaying scheme which integrates the physical-layer network coding and the opportunistic relaying scheme. Subsequently, we will evaluate the performance of the new relaying protocol, and compare it with other two-way relaying protocols.

Finally, Chapter 7 concludes this thesis and outlines some possible future directions.

Chapter 2

Cooperative Relaying

In this chapter, we first review some fading mitigation methods for use in wireless communications as well as some performance measures of such channels. Then we introduce the relaying notion — an attractive approach to suppress the impairment of channel fading. We will further present research works on cooperative relaying networks, including single-relay networks, multi-relay networks and multi-relay two-way networks, which are the focuses of this thesis. At the same time, the motivation of our study will be given.

2.1 Fading Channel

When a wireless communication channel suffers from a flat fading, the error rate of the communication link will usually increase. Yet, there are ways to reduce the effect of fading. In the following, we introduce several such methods, including channel coding, diversity, adaptive modulation, and multi-input multi-output (MIMO) method.

Channel coding The essence of channel coding is to correct or detect the bit errors at the receiver by adding some redundancy bits in the transmission. The simplest channel coding method is the repetition coding. In repetition coding, a frame of symbols is transmitted repeatedly for a number of times. Assume that the channel coefficient varies from frame to frame. By taking the average of all the received frames, the fading effect can be reduced and there is a good chance that the decoded result becomes correct. Well-known and good channel codes include Reed-Solomon (R-S) codes, convolutional codes, turbo codes and low-density parity-check (LDPC) codes. However, channel coding can only correct or detect errors which occupy only a small fraction of the entire frame. If a large part of the frame is erroneous, like error burst caused by a slowly fading channel, channel coding may not work satisfactorily. Therefore, channel coding is quite effective in mitigating the fast-fading effect, but may not be so when combating slow fading.

Diversity The basic idea of diversity is to transmit several duplicates of the same frame of symbols. Since each duplicate experiences different channel fading, the effect of deep fading can be compensated by the strong signals in other good channels. This technique is usually employed to tackle slow fading. General diversity methods are time diversity, frequency diversity and spatial diversity. However, time and frequency diversity will reduce the spectral efficiency of the channel. Therefore, spatial diversity is more attractive in practice. One of the well-known diversity technique is the reception diversity provided by maximal-ratio-combining (MRC) the independently received signals arriving at the multiple antennas of the receiver.

Adaptive modulation In adaptive modulation, the modulation scheme changes according to the channel condition. If the channel is in a good condition, one can transmit with a higher-order modulation scheme such as quadrature amplitude modulation (QAM) so as to increase the spectral efficiency. However, when the channel suffers from a deep fading, a lower-order modulation such as binary phase-shift-keying (BPSK) should be used to reduce the error rate.

MIMO/space-time coding The notion of MIMO was inspired by the proposal of transmit diversity by Alamouti [12], and also by the study of the capacity of multi-antenna systems by Foschini [13] and Telatar [14]. Multi-input multi-output transmission technique is indeed a systematic application of spatial diversity. With the introduction of the space-time coding method [12, 15–17], the MIMO concept has been made much more feasible. As of today, MIMO technique is the most attractive method to suppress slow fading impairment.

Consider a communication link with a fading channel, the instantaneous signal-to-noise ratio (SNR) at the receiver, denoted by γ, varies with time and space. To measure the performance of such a communication link, two metrics, namely the outage probability and the average symbol error rate (SER) are commonly used [18]. In addition, diversity order can be used to further characterize the link performance at the high SNR region. In the following, we briefly describe each of these characteristics.

2.1.1 Outage probability

In wireless communications, if the channel coherence time T_c is much larger than the symbol duration T_s, i.e. $T_c \gg T_s$, a deep fade will generate a burst of error symbols, which is very difficult for channel codes to correct. The percentage of time that the received SNR falls under a certain threshold γ_{th}, i.e. $\gamma < \gamma_{th}$, is called the outage probability and is expressed as

$$P_{\text{out}}(\gamma_{th}) = \Pr(\gamma < \gamma_{th}) = \int_0^{\gamma_{th}} f(\gamma)\mathrm{d}\gamma \tag{2.1}$$

where $f(\gamma)$ is the probability density function (pdf) of the random variable RV γ.

We can also define the outage probability from the information-theoretic perspective. Suppose that a capacity-approaching channel code is exploited in the fading channel. Since the instantaneous SNR γ is a time-varying RV, the instantaneous mutual information $I(\gamma)$ is also time varying. If the required transmission rate $\mathtt{R}$ is fixed, then a reliable transmission is not achievable at the instance when the mutual information is less than the required transmission rate $\mathtt{R}$. Note that the channel coefficient is assumed to be constant within the channel coherence time. Therefore, each time when the mutual information falls below the required transmission rate $\mathtt{R}$, it will last for the duration of the channel coherence time, i.e., T_c. Consequently, the probability that the mutual information $I(\gamma)$ is smaller than the required transmission rate $\mathtt{R}$ can be regarded as the outage probability. Mathematically, it is expressed as

$$P_{\text{out}} = \Pr(I(\gamma) < \mathtt{R}) = \Pr(\gamma < I^{-1}(\mathtt{R})). \tag{2.2}$$

Comparison between (2.2) and (2.1) clearly shows that both definitions are equivalent.

2.1.2 Average symbol error rate (SER)

On the other hand, if $T_c \approx T_s$, the detection error for each symbol is independent, and a burst of errors occurs with a very low probability. In this case, channel coding is an effective way to recover the fading-induced symbol errors of a codeword. We denote the instantaneous symbol error rate by $P_{\text{ser}} = e(\gamma)$, where $e(\cdot)$ is determined by the modulation scheme being used over AWGN channel. For instance, $e(x) = \mathrm{Q}(\sqrt{2x})$ for the binary phase-shift-keying (BPSK) modulation scheme where $\mathrm{Q}(\cdot)$ denotes the Q-function. Here, the appropriate figure-of-merit is the average SER, which can be evaluated using

$$\bar{P}_{\text{ser}} = \int_0^\infty e(\gamma) f(\gamma) \mathrm{d}\gamma. \tag{2.3}$$

2.1.3 Diversity order

Diversity order is a metric which measures how fast the outage probability or the average SER decreases with the SNR at the high SNR region. Mathematically, the diversity order d is defined as

$$d = -\lim_{\bar{\gamma}\to\infty} \frac{\log P_{\text{out}}(\bar{\gamma})}{\log \bar{\gamma}} \quad \text{or} \quad d = -\lim_{\bar{\gamma}\to\infty} \frac{\log P_{\text{ser}}(\bar{\gamma})}{\log \bar{\gamma}} \tag{2.4}$$

where $\bar{\gamma} = P/N_0$ with P being the transmitted power and N_0 the power density of additive white Gaussian noise (AWGN) at the receiving end.

2.2 MIMO and Relaying

The MIMO technique can not only improve the reliability of the channel between the transmitter and the receiver [12, 15–17], but also boost the capacity of the channel [13]. It can further achieve diversity and multiplexing flexibly so as to meet the demands of different users [19]. Due to its promising features, the MIMO technique has been adopted in the IEEE 802.11n (Wireless Local Area Networks, WLANs) and the IEEE 802.16 (Worldwide Interoperability for Microwave Access, WiMAX) standards.

The use of the MIMO technique normally requires the installation of multiple antennas as well as a large amount of processing power. Consequently, small-size and/or power-limited devices such as mobile phones, personal digital assistants and sensors may not be able to make use of the MIMO technique. Alternatively, by

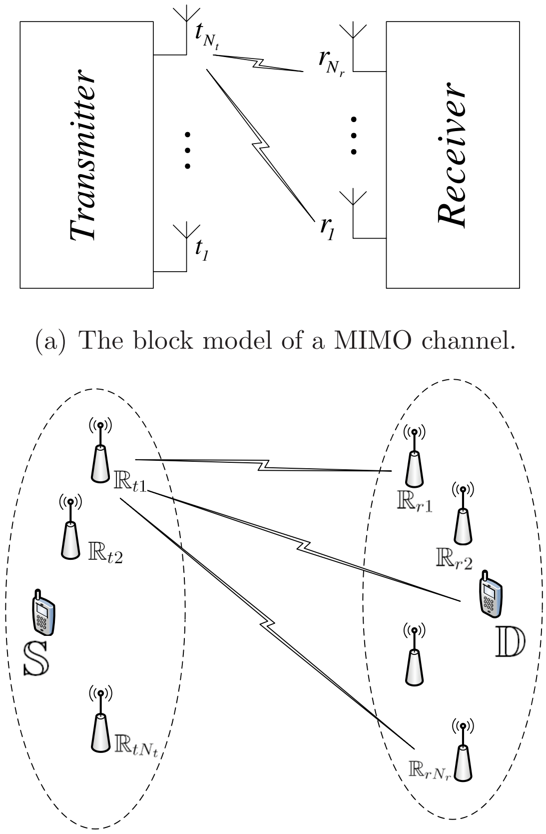

(a) The block model of a MIMO channel.

(b) The imitation of MIMO a channel by using relays.

Figure 2.1: Comparison of a MIMO channel and a relay channel.

forming a "virtual" MIMO network, even devices with a single antenna can enjoy the benefits of a MIMO system. Fig. 2.1(a) shows the model of a MIMO channel with N_t transmitting antennas and N_r receiving antennas; while Fig. 2.1(b) shows the model of a virtual MIMO channel consisting of a transmit cluster with one transmitter and N_t transmit relays, and a receiver cluster with one destination and N_r receive relays. Furthermore, in Fig. 2.1(b), each device is equipped with a single antenna. In the virtual MIMO network, the transmitter can first transmit the information to the relays in the transmit cluster. Assuming that these relays can successfully decode the received signal, the transmitter can then work in collaboration with these relays to perform beamforming or space-time coding. At the same time, the receive cluster will form a virtual multi-antenna array to coordinate the signal reception process. Such a virtual MIMO network can technically fulfill the functions of a MIMO channel, but in a distributed way. As we can observe, the virtual MIMO network is very much similar to a relay channel, which was first studied three decades ago [7]. Consequently, the development of MIMO technologies early this century have re-drawn academic interest to the study of relay channels.

Moreover, in a portable device, the power of the transmitted signal is tens of dB higher than that of the received signal. Therefore, receiving incoming signals and transmitting signal simultaneously requires a very high isolation between the receiving RF module and the transmitting RF module. This is very difficulty and expensive to achieve, if not impossible. For most portable devices, the price and the circuit complexity are the main concerns. It is especially true for simple devices like sensor nodes. Therefore most portable devices do not support simultaneous transmission and reception in the same bandwidth. This constraint is conventionally called the half-duplex constraint. To overcome this constraint, the transmission and the reception tasks are fulfilled orthogonally in time, like time-division (TD), or in frequency, like frequency-division (FD).

Mainly focusing on small devices with simple communication circuits, most relaying-related research works assume that all nodes including sources, relays and destinations are only equipped with a single antenna, and all the antennas work on the half-duplex mode. The same assumption is applied in this thesis, unless mentioned otherwise. We also assume that the source sends information frame by frame, and the time period occupied by the transmission of an information frame is denoted as one time slot. Based on the above assumptions, direct transmission (DT) and direct repeat-transmission (DRT) are defined as follows.

Direct transmission (DT) Direct transmission refers to the transmission of one information frame via the direct source-destination link during one time slot.

Direct repeat-transmission (DRT) Direct repeat-transmission refers to the transmission of one information frame via the direct source-destination link during one time slot followed by a retransmission of the same information frame via the direct link in a consecutive time slot. Subsequently, the destination decodes the information frame based on the maximum-ratio-combining (MRC) of the received signals from both time slots.

2.3 Relaying Methods

Even though the channel capacity of general relaying channels is still an open problem [7], researchers have found that by making use of the relays, which are located somewhere between the source and the destination, the reliability of the transmission from the source to the destination can be improved, and the transmission range of the source will be increased [8–10]. The present research concerning the relaying networks has been mainly focused on the design of the forwarding method in the relay. In the following we will briefly review some of the relaying methods designed for relaying networks.

2.3.1 Relaying methods for single-relay networks

We consider a single-relay network consisting of a source, a destination and a relay, as shown in Fig. 2.2. We suppose that the source needs to send information frames to the destination. According to the conventional shortest-path(hop) routing scheme of Ad hoc networks, the information transmission should be allocated via the direct $\mathbb{S}-\mathbb{D}$ link. However, the shortest-path transmission scheme may not be robust to channel fading. For instance, the $\mathbb{S}-\mathbb{D}$ link may undergo a deep fading and the received signal-to-noise ratio (SNR) at the destination side becomes lower than the

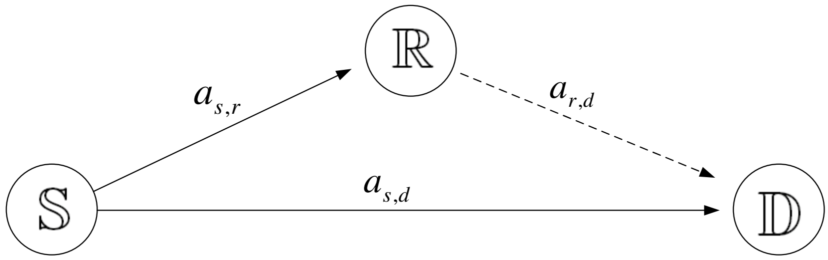

Figure 2.2: The system model of a user-cooperation system with one relay. $\mathbb{S}$ denotes the source, $\mathbb{R}$ denotes the relay and $\mathbb{D}$ denotes the destination. All terminals are equipped a single antenna.

minimum required SNR for successful signal-frame decoding. Subsequently, the automatic repeat-request (ARQ) protocol at the destination will signal the source to retransmit the same frame repeatedly, until the frame can be decoded successfully at the destination. If the deep fading of the $\mathbb{S} - \mathbb{D}$ link lasts for a long time, the re-transmissions via the deep fading link will continue, thus reducing the spectral efficiency of the communication system. In the relaying notion, the source can make use of the relay to forward the information frame to the destination. The transmission from the source and the forwarding from the relay accomplish a diversity of two, which is more robust than the direct transmission which has a diversity of only one.

We further review some relaying methods which consume make use of a single relay to assist forwarding the information frame to the destination. It is assumed that the source broadcasts one information frame in the first time slot, and both the relay and the destination listen to the broadcast, as illustrated in Fig. 2.3.

Decode-and-forward (DF) In the decode-and-forward protocol, the relay attempts to decode the received signal from the source during the first time slot. It then re-encodes the decoded frame (may or may not decoded successfully) and forwards it to the destination in the second time slot.

Amplify-and-forward (AF) In the amplify-and-forward protocol, the relay am-

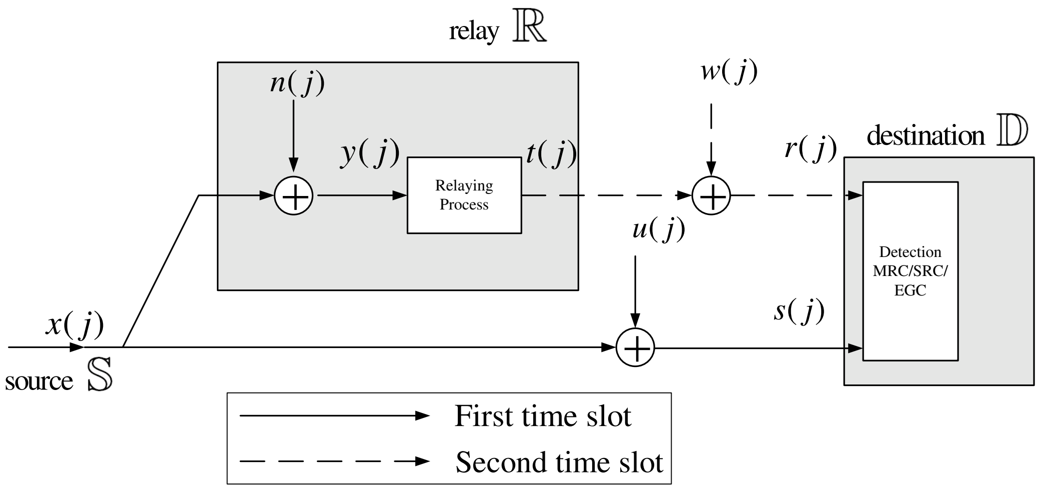

Figure 2.3: Signal flowing of a single-relay network. Solid line represent the signal flow during the first time slot; dashed line represent the signal flow during the second time slot.

plifies the received signal and forwards it to the destination in the second time slot.

Selection decode-and-forward (SDF) In the selection DF (SDF) protocol, either DF or DT is chosen in the second time slot according to the link quality between the source and the relay. Specifically, if the $\mathbb{S}-\mathbb{R}$ link is good so that the relay can successfully decode the received signal frame in the first time slot, then the relay forwards the information frame to the destination in the second time slot. If the relay fails to decode the received frame, the source will retransmit the same information frame to the destination directly in the second time slot. Fig. 2.4 illustrates the flow of the SDF protocol.

The relaying methods mentioned above consume two time slots to transmit one information frame. Consequently, the effective information rate reduces to half of the transmission rate. To achieve a higher information rate, the incremental amplify-and-forward protocol has been proposed [10].

Incremental amplify-and-forward (IAF) In the incremental AF (IAF) proto-

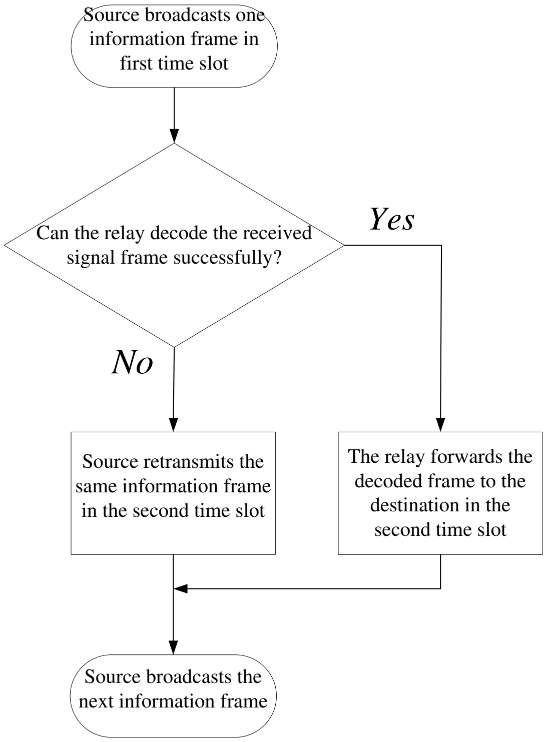

Figure 2.4: The flow chart of the SDF relaying protocol.

col, the source performs broadcasting during the first time slot. Then, depending on the destination being or not being able to decode the received frame correctly, the destination will broadcast a one-bit information message, success or failure, to the source and the relay. It is assumed that this feedback message is encoded with low-rate codes such that it can always be correctly decoded by the source and the relay. In particular, if the destination is unable to correctly decode the received frame during the first time slot, it sends out a "failure" feedback. After receiving the "failure" feedback from the destination, the relay will amplify-and-forward what it has received from the source to the destination. Otherwise, the destination sends out a "success" message. After receiving the "success" feedback, the relay does nothing during the following time slot while the source will make use of the time slot to transmit the next information frame to the destination. Since there are occasions that some in-

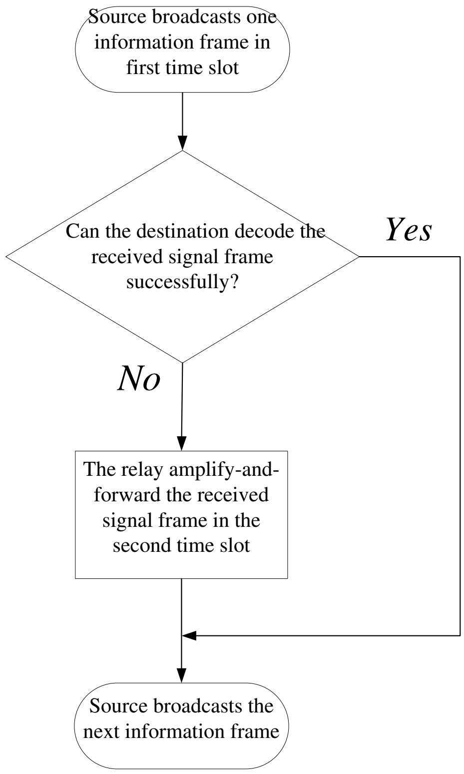

Figure 2.5: The flow chart of the IAF relaying protocol.

formation frame might be successfully transmitted during the first time slot, the second time slot can be spared, resulting in a better spectral efficiency. Fig. 2.5 shows the flow chart of the IAF protocol.

2.3.2 Relaying methods for multi-relay networks

Under some conditions, such as in dense sensor networks, each source-destination pair is surrounded by a number of nodes. These nodes are potential relays as long as they locate within the transmission ranges of both the source and the destination. The multiplicity of relays adds more challenges to design efficient, effective and relatively simple relaying methods that can allow simple detecting method to be used at the destination. In particular, the following factors should be taken into consideration when designing the protocols.

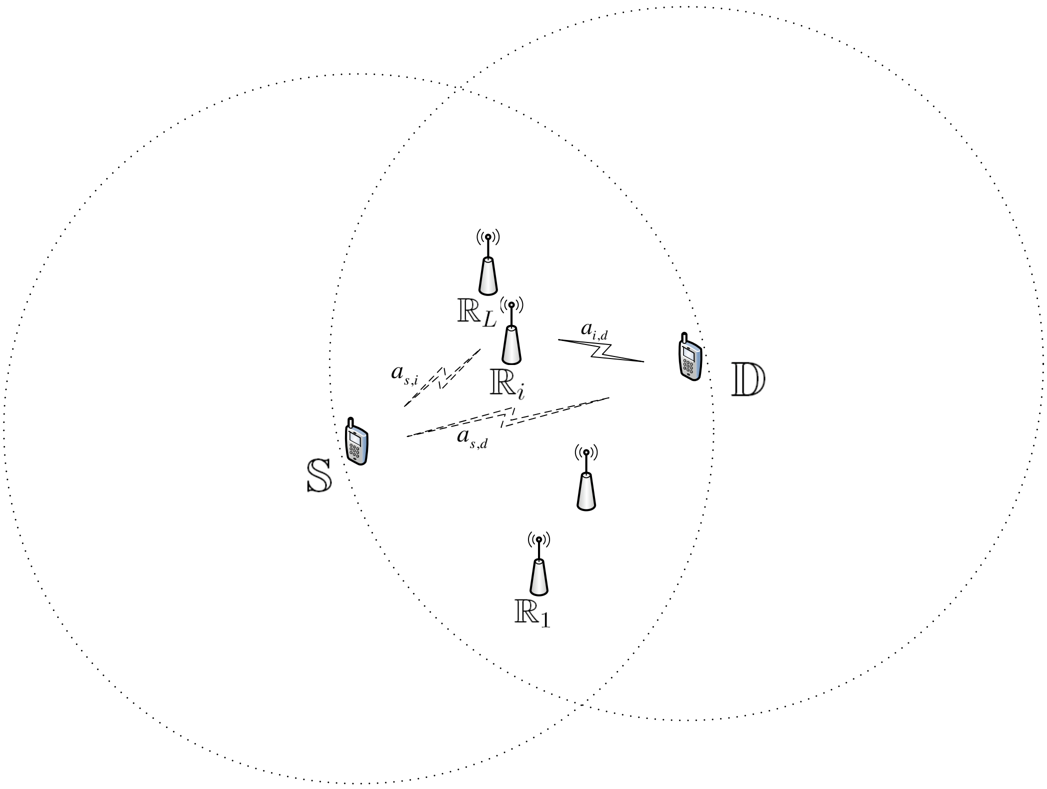

Figure 2.6: The system model of a user-cooperation system with multiple relays. $\mathbb{S}$ denotes the source, $\mathbb{R}_i, (i = 1, \dots, L)$ denotes the relays and $\mathbb{D}$ denotes the destination. All terminals are equipped a single antenna.

1. Diversity order that the relaying scheme can achieve.
2. Spectral efficiency of the relaying scheme.
3. Complexity of the signal detection and combining methods used at the relays and the destination.
4. Robustness to synchronization errors.
5. Interference among the transmissions from the source and the relays.
6. Power allocation among the relays.

In the following, we will review some relaying protocols designed for a multi-relay system with L relays, such as the one shown in Fig. 2.6. In the figure, the

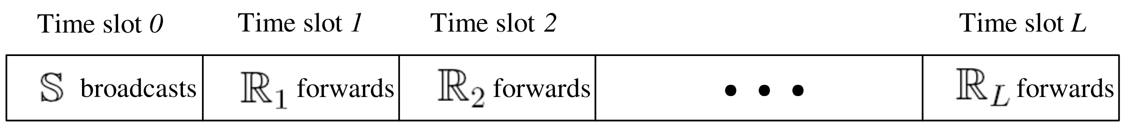

Figure 2.7: The temporally orthogonal relaying scheme for a multi-relay system.

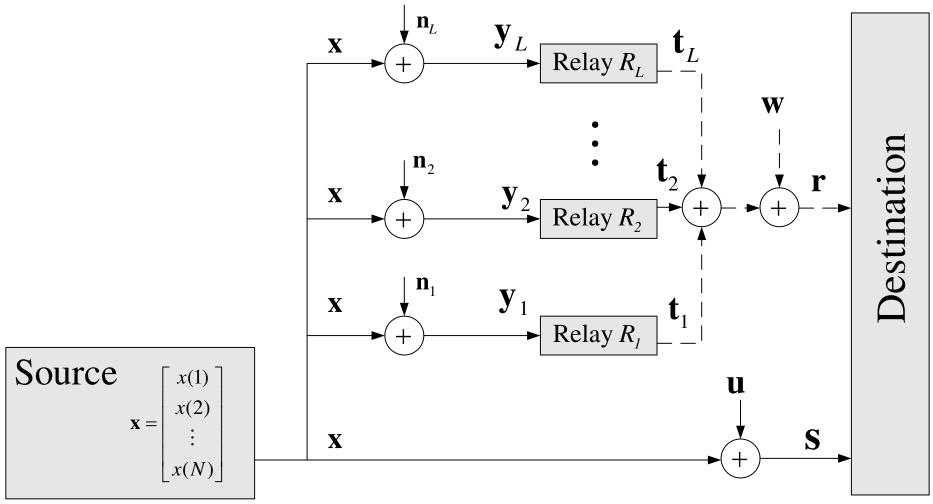

Figure 2.8: Distributed space-time coding for a multi-relay system.

relays are indexed; specifically, $\mathbb{R}_i, (i = 1, \ldots, L)$ denotes the ith relay.

Orthogonal relaying The simplest way to exploit the L relays is to assign orthogonal transmission slots – time slots or frequency slots – to the relays to avoid any transmission interference. For instance, the L relays can sequentially forward the information frame in L consecutive time slots. In this relaying mode, each transmission occupies $L + 1$ time slots with the first one assigned to the source and the other L time slots assigned to the L relays, as shown in Fig. 2.7. This protocol, known as orthogonal relaying, is simple but has very poor spectral efficiency [11, 20–28].

Distributed space-time coding One way to maintain the same spectral efficiency as a single-relay system is that the L relays transmit simultaneously based on the distributed space-time coding technique [29–36]. As shown in Fig. 2.8, dur-

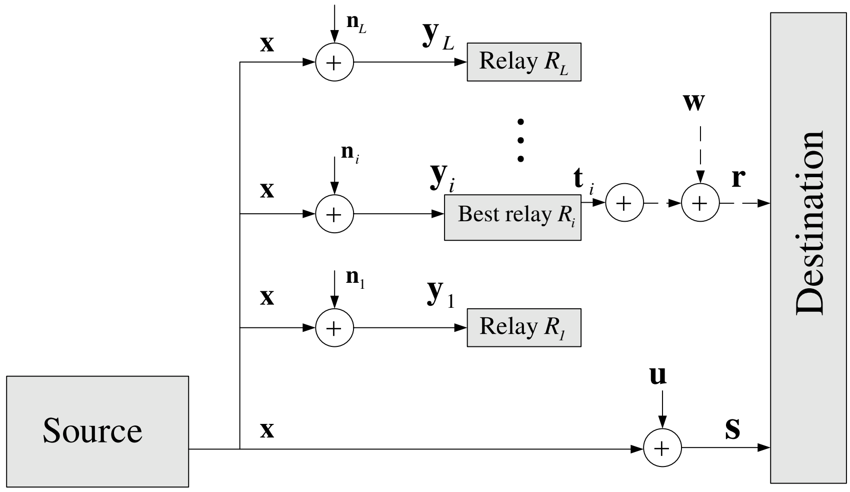

Figure 2.9: The opportunistic relaying for a multi-relay system.

ing the first time slot, the source broadcasts one information frame; during the second time slot the L relays encode the received signals into L frames, which form a distributed space-time codeword, and then transmit the L frames simultaneously to the destination. Finally, the destination decodes the received signals by using similar decoding techniques for conventional space-time coding. The key challenge here is to ensure synchronization among the relays. Recently, some distributed space-time coding robust to the asynchronous multi-relay channels have also been proposed and studied [37–42].

Opportunistic relaying Another way to improve the spectral efficiency is to endorse only the "best" relay to transmit for each transmission. Specifically, during the second time slot, only the "best" relay can forward the received information frame to the destination, while the other relays remain idle, as illustrated in Fig. 2.9. This relaying strategy is called opportunistic relaying. Bletsas *et. al.* [43, 44] conceived a best-relay selection algorithm which can be easily implemented in a distributed maner. Since then, the opportunistic relaying methods have been further studied [45–53]

2.3.3 Relaying methods for multi-relay two-way communication networks

Compared to the MIMO communication method, the cooperative relaying not only preserves the benefits inherent from the MIMO technique, but also possesses a few more remarkable advantages. However, implanting the benefit of the MIMO systems to the relaying systems is not a trivial work because of the technical challenges faced by the relaying methodology, such as relaying methods, synchronization, resource allocation, and encoder and decoder design. As described previously, distributed space-time codes [31, 34, 54–58] and opportunistic relaying [43, 52, 59, 60] are initiatives that tackle these challenges and possess the inherent advantages.

At the same time, network coding is a promising technique aiming to improve the throughput of communication systems [61–63]. Motivated by this innovative throughput-boosting method, physical-layer network coding has been proposed to improve the information transmission efficiency in wireless communication systems [64, 65]. The improvement of system throughput can be demonstrated by a simple example. Referring to Fig. 2.10, we assume that $\mathbb{S}$ and $\mathbb{D}$ have one information frame for each other. Subject to the conventional medium access control (MAC) strategy of wireless communications, $\mathbb{S}$ will send its frame to the intermediate node $\mathbb{R}$ first, then $\mathbb{R}$ forwards the frame to $\mathbb{D}$. Afterwards, $\mathbb{D}$ sends its frame to $\mathbb{R}$, and $\mathbb{R}$ passes it to $\mathbb{S}$. In this way, to fulfill the two-way transmission, totally four time slots will be consumed. The overall throughput is 0.5 frame/time slot. In the transmission scheme when network coding is used, $\mathbb{S}$ and $\mathbb{D}$ will send their information frames simultaneously to $\mathbb{R}$ in the first time slot. Then having received the superposition of these two frames, $\mathbb{R}$ broadcasts it back to both $\mathbb{S}$ and $\mathbb{D}$. Subsequently, $\mathbb{S}$ and $\mathbb{D}$ can decode the information frame from the other party based on this broadcasted signal. Such a transmission scheme requires only two time slots to send one frame.

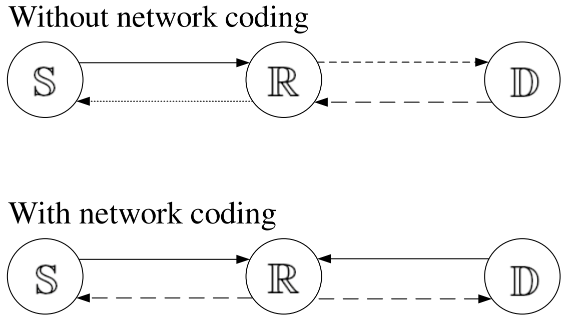

Figure 2.10: The two-way transmission without network coding versus the two-way transmission with network coding.

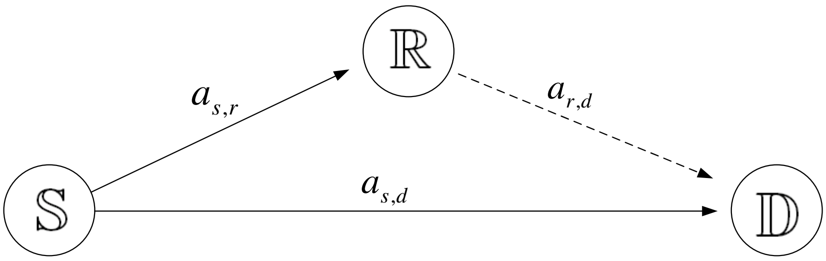

Figure 2.11: The system model of a user-cooperation system with one relay. $\mathbb{S}$ denotes the source, $\mathbb{R}$ denotes the relay and $\mathbb{D}$ denotes the destination. All terminals are equipped a single antenna.

Thus, it achieves an overall throughput of 1 frame/time slot, which is two times higher than that of the transmission scheme without network coding. With an aim to integrating the benefits of relaying and network coding, distributed space-time coding (STC) with modular network coding for two-way relaying systems has been proposed [66].

2.4 System Model and Performance

We re-draw Fig. 2.2 as Fig. 2.11. Referring to Fig. 2.11, $a_{i,j}$ represents the channel coefficient between terminal i and terminal j. We assume that $a_{s,d}$, $a_{s,r}$ and $a_{r,d}$ are independent of one another and are Rayleigh distributed[1], i.e., $a_{i,j}$ follows

[1]In this thesis, all channel amplitudes $|a_{i,j}|$ are assumed to be Rayleigh distributed random variables unless specified otherwise.

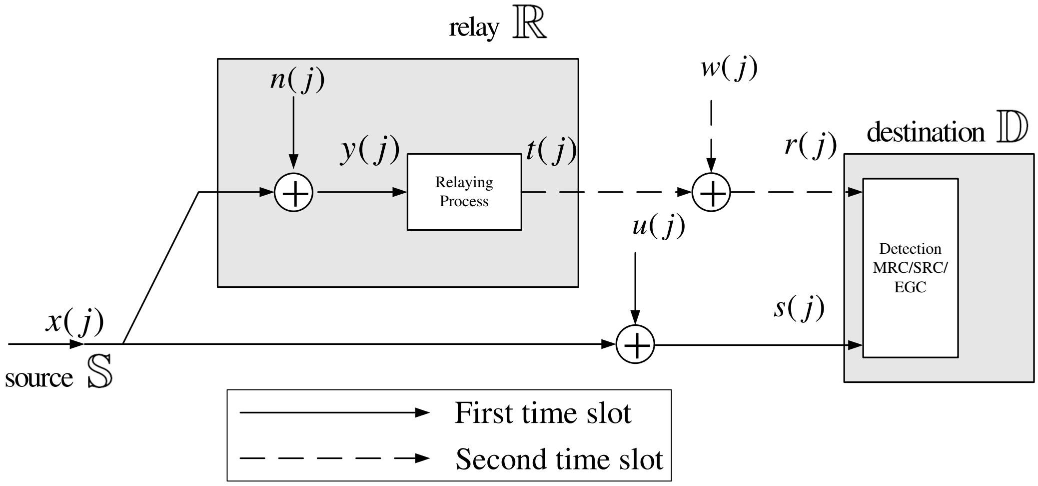

Figure 2.12: Signal flowing of a single-relay network. Solid line represent the signal flow during the first time slot; dashed line represent the signal flow during the second time slot.

$\mathcal{CN}(0, \sigma_{i,j}^2)$. Thus, $|a_{i,j}|^2$ are exponentially distributed random variables with parameter $\sigma_{i,j}^{-2}$. Let the received SNR be $\gamma_{i,j} = |a_{i,j}|^2\bar{\gamma}_{i,j}$, where $\bar{\gamma}_{i,j}$ denotes the received SNR when $|a_{i,j}|^2 = 1$, i.e., no channel gain. Let P_s be the transmitted power of the source, and P_r be the transmitted power of the relay. We assume that the variance of the zero-mean complex AWGN at the receiver side (the relay/the destination) is N_0. Then the SNRs $\bar{\gamma}_{i,j}$ can be explicitly expressed by $\bar{\gamma}_{s,r} = \bar{\gamma}_{s,d} = P_s/N_0$ and $\bar{\gamma}_{r,d} = P_r/N_0$. For simplicity, we set $\bar{\gamma}_s = \bar{\gamma}_{s,r} = \bar{\gamma}_{s,d}$.

2.4.1 Single-relay networks

We re-draw Fig. 2.3 as Fig. 2.12. As shown in Fig. 2.12, signal frames are sequentially broadcasted from the source $\mathbb{S}$, and transmitted through the $\mathbb{S} - \mathbb{D}$ link and the $\mathbb{S} - \mathbb{R} - \mathbb{D}$ link. We assume that the transmission from the source and the signal forwarding from the relay are fulfilled during two consecutive time slots (except for the IAF protocol).

During the first time slot, the source broadcasts the first buffered signal frame.

This transmission is also called direct transmission (DT). We assume that each signal frame contains N symbols and we denote the frame by the column vector $\boldsymbol{x} = [x(1), x(2), \cdots, x(N)]^T$, where the element $x(j)$ represents the jth transmitted symbol (such as a QPSK symbol) in baseband form. Denoting the received vector at the relay by $\boldsymbol{y} = [y(1), y(2), \cdots, y(N)]^T$, we have

$$y(j) = a_{s,r}\sqrt{P_s}x(j) + n(j), \quad \text{for} \quad j = 1, 2, \ldots, N \tag{2.5}$$

where $n(j)$ is a complex AWGN with distribution $\mathcal{CN}(0, N_0)$. The relay will process the received signal frame and then, dependent on the protocol used, may or may not forward the processed signal frame to the destination in the second time slot.

2.4.1.1 Decode-and-forward (DF) protocol

After the broadcasting of $\boldsymbol{x}$ from the source $\mathbb{S}$, the relay $\mathbb{R}$ is required to decode the received frame of symbols if it is operated in the DF mode. We assume that the channel state information is known to the receiver. Then, each received frame is decoded with the maximal-likelihood detection, and the decoded frame at the relay $\hat{\boldsymbol{x}} = [\hat{x}(1), \hat{x}(2), \cdots, \hat{x}(N)]^T$ is determined in the favor of

$$\hat{\boldsymbol{x}} = \arg \min_{\boldsymbol{x} \in \mathcal{X}^N} \|\boldsymbol{y} - a_{s,r}\sqrt{P_s}\boldsymbol{x}\|_2^2 \tag{2.6}$$

or

$$\hat{x}(j) = \arg \min_{x \in \mathcal{X}} |y(j) - a_{s,r}\sqrt{P_s}x| \tag{2.7}$$

where $\mathcal{X}$ is the modulation constellation of each input signal, $\|\boldsymbol{x}\|_2$ represents the l_2-norm of the vector $\boldsymbol{x}$, and $|x|$ denotes the amplitude of x. Then in the second time slot, the relay $\mathbb{R}$ forwards the detected signal packet $\hat{\boldsymbol{x}}$ to the destination $\mathbb{D}$.

At the end of the second time slot, the destination $\mathbb{D}$ will perform decoding based on the two received frames from the source $\mathbb{S}$ and from the relay $\mathbb{R}$. The received signal from $\mathbb{S}$ is given by

$$s(j) = a_{s,d}\sqrt{P_s}x(j) + u(j) \tag{2.8}$$

and the received signal from $\mathbb{R}$ is given by

$$r(j) = a_{r,d}t(j) + w(j) = a_{r,d}\sqrt{P_r}\hat{x}(j) + w(j) \tag{2.9}$$

where $t(j) = \sqrt{P_r}\hat{x}(j)$ is the forwarded signal from the relay, $u(j)$ and $w(j)$ are independent and identically distributed AWGNs with the distribution $\mathcal{CN}(0, N_0)$. Denoting the decoded frame at the destination by $\tilde{\boldsymbol{x}} = [\tilde{x}(1), \tilde{x}(2), \cdots, \tilde{x}(N)]^T$, the optimal detection rule, which is the maximum likelihood (ML) detection and minimizes the symbol error rate, is [67]

$$\begin{aligned}
&\tilde{x}(j) \\
&= \arg\max_{x\in\ \mathcal{X}} \Bigg\{ p(|a_{s,r}|^2\bar{\gamma}_s) \exp\left(-\frac{[(a_{s,d}^* s(j) + a_{r,d}^* r(j)) - (|a_{s,d}|^2\sqrt{P_s}x - |a_{r,d}|^2\sqrt{P_r}x)]^2}{2\sigma^2} \right) \\
&\quad +(1 - p(|a_{s,r}|^2\bar{\gamma}_s)) \exp\left(-\frac{[(a_{s,d}^* s(j) + a_{r,d}^* r(j)) - (|a_{s,d}|^2\sqrt{P_s}x + |a_{r,d}|^2\sqrt{P_r}x)]^2}{2\sigma^2} \right) \Bigg\}.
\end{aligned}$$

where $p(|a_{s,r}|^2\bar{\gamma}_s)$ is the detection error of $\hat{x}(j)$ at the relay, the * sign denotes the conjugate operation, and $\sigma^2 = (|a_{s,d}|^2 + |a_{r,d}|^2)N_0$. However, the optimal detection is difficult to realize. Instead, simpler demodulation methods are employed to detect the transmitted symbol. These methods are unified by [67]

$$\tilde{x}(j) = \arg\min_{x\in\mathcal{X}} |k_{s,d}s(j) + k_{r,d}r(j) - k_{s,d}a_{s,d}x - k_{r,d}a_{r,d}x| \tag{2.10}$$

where $k_{s,d}$ and $k_{r,d}$ are the decoding weights to be designed.

2.4.1.1.1 $k_{s,d} = a^*_{s,d}$ **and** $k_{r,d} = a^*_{r,d}$ **:** The simplest way is to assign $k_{s,d} = a^*_{s,d}$ and $k_{r,d} = a^*_{r,d}$. Then the instantaneous mutual information is given by [10]

$$I_{\text{DF}} = \frac{1}{2}\min\{\log(1+\gamma_{s,r}), \log(1+\gamma_{s,d}+\gamma_{r,d})\} \tag{2.11}$$

and the outage probability is equal to

$$\begin{aligned} P_{\text{out,DF}} &= \Pr(I_{\text{DF}} < \mathtt{R}/2) = \Pr(\min\{\gamma_{s,r}, \gamma_{s,d}+\gamma_{r,d}\} < 2^{\mathtt{R}} - 1) \\ &\sim \sigma_{s,r}^{-2}\frac{\gamma_{th}}{\bar{\gamma}_s} \end{aligned} \tag{2.12}$$

where $\gamma_{th} = 2^{\mathtt{R}} - 1$, and the $\sim$ sign denotes the asymptotic equivalence [2]. Since two consecutive time slots are occupied by the transmission of one information frame, the effective information rate is half of the transmission rate of each time slot, i.e., $\mathtt{R}/2$. The equation (2.12) implies that an outage event occurs whenever the instantaneous mutual information cannot maintain the effective information rate, i.e., $I_{\text{DF}} < \mathtt{R}/2$. Clearly, the simple detection method of assigning $k_{s,d} = a^*_{s,d}$ and $k_{r,d} = a^*_{r,d}$ is not able to achieve the full diversity of two [67][25].

2.4.1.1.2 $k_{s,d} = a^*_{s,d}$ **and** $k_{r,d} = \min\{|a_{s,r}|^2, |a_{r,d}|^2\}/a_{r,d}$ **:** To utilize the full diversity advantage, Wang *et. al.* [67][25] proposed a suboptimal demodulation method, namely cooperative maximal-ratio-combining (C-MRC) detection. In C-MRC, the weights are set to $k_{s,d} = a^*_{s,d}$ and $k_{r,d} = a^2_{\text{eq}}/a_{r,d}$, where $a^2_{\text{eq}} = \min\{|a_{s,r}|^2, |a_{r,d}|^2\}$. The instantaneous mutual information is then

$$I_{\text{DF,C-MRC}} = \frac{1}{2}\log(1+\gamma_{s,d}+\min\{\gamma_{s,r}, \gamma_{r,d}\}) \tag{2.13}$$

[2]Since the outage probability P_{out} is a decreasing function of average SNR $\bar{\gamma}$, it can be expanded into a polynomial of $1/\bar{\gamma}$, that is, $P_{\text{out}} = \sum_{i=d}^{\infty} c_i(1/\bar{\gamma})^i$ with $c_d > 0$ and $c_i \geq 0$ for $i \geq d+1$. When $\bar{\gamma}$ is large, P_{out} would be dominated by the first term $c_d(1/\bar{\gamma})^d$. Therefore, we say $c_d(1/\bar{\gamma})^d$ is the asymptotic equivalence of P_{out}, denoting as $P_{\text{out}} \sim c_d(1/\bar{\gamma})^d$.

and the outage probability is given by

$$P_{\text{out,DF,C-MRC}} = \Pr(I_{\text{DF,C-MRC}} < \mathtt{R}/2) \sim (\sigma_{s,r}^{-2} + \sigma_{r,d}^{-2})\sigma_{s,d}^{-2}\frac{\gamma_{th}^2}{\bar{\gamma_s}^2} \tag{2.14}$$

Furthermore, when BPSK modulation scheme is employed, the average bit error rate (BER) $\bar{P}_{\text{ber,C-MRC}}$ is bounded above by [67]

$$\bar{P}_{\text{ber,C-MRC}} \leq f(\bar{\gamma}) \sim (k_{\text{C-MRC}} \cdot \bar{\gamma}_s)^{-2} \tag{2.15}$$

where $k_{\text{C-MRC}}$ is a constant dependent on $\sigma_{s,d}^2$, $\sigma_{s,r}^2$ and $\sigma_{r,d}^2$.

2.4.1.2 Amplify-and-forward (AF) protocol

In the AF protocol, the received signal at the relay is merely amplified and then forwarded. The amplification is determined such that the transmitted power from the relay meets the power constraint. Recall that the frame received by the relay is denoted by $\boldsymbol{y} = [y(1), y(2), \cdots, y(N)]^T$. In the AF relaying mode, the signal frame forwarded by the relay is expressed as

$$t(j) = \sqrt{\frac{P_r}{\alpha P_s + N_0}}y(j) \tag{2.16}$$

where α equals $|a_{s,r}|^2$ for the CSI-assisted AF relaying method [10, 20, 68, 69], or equals a constant for the fixed-gain AF relaying method [70, 71]. The fixed-gain AF relaying is further classified into two categories — blind relaying and semi-blind relaying. In the blind relaying, α is an arbitrary positive constant [72]; while in the semi-blind relaying, α equals $\mathrm{E}[|a_{s,r}|^2]$.

Combining (2.5) and (2.16), the received signal $r(j)$ at the destination during the second time slot can be expressed as

$$
\begin{aligned}
r(j) &= a_{r,d}t(j) + w(j) \\
&= a_{r,d}\sqrt{\frac{P_r}{\alpha P_s + N_0}}a_{s,r}\sqrt{P_s}x(j) + a_{r,d}\sqrt{\frac{P_r}{\alpha P_s + N_0}}n(j) + w(j). \quad (2.17)
\end{aligned}
$$

Denoting γ_r as the equivalent SNR of the received signal $r(j)$, we can obtain [68]

$$
\gamma_r = \frac{|a_{r,d}|^2 P_r |a_{s,r}|^2 P_s}{(|a_{r,d}|^2 P_r + \alpha P_s + N_0)N_0} = \frac{\gamma_{r,d}\gamma_{s,r}}{\gamma_{r,d} + \alpha\bar{\gamma}_s + 1}. \quad (2.18)
$$

The instantaneous mutual information is then given by [10]

$$
I_{\mathrm{AF}} = \frac{1}{2}\log(1 + \delta_{s,d}\gamma_{s,d} + \gamma_r) = \frac{1}{2}\log(1 + \gamma_{srd}) \quad (2.19)
$$

where $\delta_{s,d} = 1$ if the direct $\mathbb{S} - \mathbb{D}$ link is available, otherwise $\delta_{s,d} = 0$; and

$$
\gamma_{srd} = \delta_{s,d}\gamma_{s,d} + \gamma_r \quad (2.20)
$$

denotes the equivalent SNR of the single-relay network. Furthermore, the outage probability can be calculated by

$$
P_{\mathrm{out,AF}} = \Pr(I_{\mathrm{AF}} < \mathtt{R}/2) = \Pr(\gamma_{srd} < 2^{\mathtt{R}} - 1) = \Pr(\gamma_{srd} < \gamma_{th}) \quad (2.21)
$$

where $\gamma_{th} = 2^{\mathtt{R}} - 1$.

2.4.1.2.1 Case I: CSI-assisted AF relaying scheme is employed and the direct link is not available : The equivalent SNR γ_{srd} becomes

$$
\gamma_{srd,\mathrm{I}} = \frac{\gamma_{r,d}\gamma_{s,r}}{\gamma_{r,d} + \gamma_{s,r} + 1} \approx \frac{\gamma_{r,d}\gamma_{s,r}}{\gamma_{r,d} + \gamma_{s,r}} \quad (2.22)
$$

and the outage probability can be derived using [68][20]

$$P_{\text{out,AF,I}} = 1 - \frac{2\gamma_{th}}{\sqrt{\bar{\gamma}_s \bar{\gamma}_{r,d}}} K_1\left(\frac{2\gamma_{th}}{\sqrt{\bar{\gamma}_s \bar{\gamma}_{r,d}}}\right) \exp\left(-\gamma_{th}\frac{\bar{\gamma}_s + \bar{\gamma}_{r,d}}{\bar{\gamma}_s \bar{\gamma}_{r,d}}\right) \tag{2.23}$$

where $K_1(\cdot)$ is the first order modified Bessel function of the second kind [73]. Furthermore, by using the approximation $\frac{\gamma_{r,d}\gamma_{s,r}}{\gamma_{r,d}+\gamma_{s,r}+1} \approx \frac{\gamma_{r,d}\gamma_{s,r}}{\gamma_{r,d}+\gamma_{s,r}}$, the moment generation function (MGF) of the equivalent SNR $\gamma_{srd,\text{I}}$ has been derived as [68]

$$\begin{aligned}
\mathcal{M}_{\gamma_{srd,\text{I}}}(s) &= \frac{16}{3\bar{\gamma}_s\bar{\gamma}_{r,d}\left(\frac{1}{\bar{\gamma}_s} + \frac{1}{\bar{\gamma}_{r,d}} + \frac{2}{\sqrt{\bar{\gamma}_s\bar{\gamma}_{r,d}}} + s\right)^2} \\
&\times \left[\frac{4(\frac{1}{\bar{\gamma}_s} + \frac{1}{\bar{\gamma}_{r,d}})}{\left(\frac{1}{\bar{\gamma}_s} + \frac{1}{\bar{\gamma}_{r,d}} + \frac{2}{\sqrt{\bar{\gamma}_s\bar{\gamma}_{r,d}}} + s\right)} \;{}_2F_1\left(3, \frac{3}{2}; \frac{5}{2}; \frac{\frac{1}{\bar{\gamma}_s} + \frac{1}{\bar{\gamma}_{r,d}} - \frac{2}{\sqrt{\bar{\gamma}_s\bar{\gamma}_{r,d}}} + s}{\frac{1}{\bar{\gamma}_s} + \frac{1}{\bar{\gamma}_{r,d}} + \frac{2}{\sqrt{\bar{\gamma}_s\bar{\gamma}_{r,d}}} + s}\right)\right. \\
&\qquad \left. + \;{}_2F_1\left(2, \frac{1}{2}; \frac{5}{2}; \frac{\frac{1}{\bar{\gamma}_s} + \frac{1}{\bar{\gamma}_{r,d}} - \frac{2}{\sqrt{\bar{\gamma}_s\bar{\gamma}_{r,d}}} + s}{\frac{1}{\bar{\gamma}_s} + \frac{1}{\bar{\gamma}_{r,d}} + \frac{2}{\sqrt{\bar{\gamma}_s\bar{\gamma}_{r,d}}} + s}\right)\right]
\end{aligned} \tag{2.24}$$

where ${}_2F_1(\cdot, \cdot; \cdot; \cdot)$ is the Gauss hypergeometric function [73]. Note that a similar result can be found in [20], but not expressed in terms of the Gauss hypergeometric function.

For the BPSK modulation scheme, the average SER can then be calculated by exploiting the MGF $\mathcal{M}_\gamma(\cdot)$ of the equivalent SNR and using

$$P_{\text{ser}} = \frac{1}{\pi}\int_0^{\pi/2} \mathcal{M}_\gamma\left(-\frac{1}{\sin^2\theta}\right) \mathrm{d}\theta. \tag{2.25}$$

For other sophisticated modulation schemes, please refer to Sections 5.1 and 8.2 of [74] for the detailed relationship between the average SER and the MGF of the SNR. (Note that under the same approximation $\frac{\gamma_{r,d}\gamma_{s,r}}{\gamma_{r,d}+\gamma_{s,r}+1} \approx \frac{\gamma_{r,d}\gamma_{s,r}}{\gamma_{r,d}+\gamma_{s,r}}$, the outage performance and the MGF of the equivalent SNR for the same system over Nakagami-m fading channels have also been studied in [69].)

2.4.1.2.2 Case II: Fixed-gain AF relaying scheme is employed and the direct link is not available : The equivalent SNR becomes

$$\gamma_{srd,\mathrm{II}} = \frac{\gamma_{r,d}\gamma_{s,r}}{\gamma_{r,d} + \alpha\bar{\gamma}_s + 1} \tag{2.26}$$

and the outage probability is given by [70]

$$P_{\mathrm{out,AF,II}} = 1 - 2\sqrt{\frac{(\alpha\bar{\gamma}_s + 1)\gamma_{th}}{\bar{\gamma}_s\bar{\gamma}_{r,d}}} K_1\left(2\sqrt{\frac{(\alpha\bar{\gamma}_s + 1)\gamma_{th}}{\bar{\gamma}_s\bar{\gamma}_{r,d}}}\right)\exp\left(-\frac{\gamma_{th}}{\bar{\gamma}_s}\right). \tag{2.27}$$

Further, the MGF of the equivalent SNR $\gamma_{srd,\mathrm{II}}$ is calculated by [70]

$$\mathcal{M}_{\gamma_{srd,\mathrm{II}}}(s) = \frac{1}{\bar{\gamma}_s s + 1} + \frac{(\alpha\bar{\gamma}_s + 1)\bar{\gamma}_s s \exp(\frac{(\alpha\bar{\gamma}_s+1)}{\bar{\gamma}_{r,d}(\bar{\gamma}_s s+1)})}{\bar{\gamma}_{r,d}(\bar{\gamma}_s s + 1)^2}\mathrm{Ei}\left(\frac{(\alpha\bar{\gamma}_s + 1)}{\bar{\gamma}_{r,d}(\bar{\gamma}_s s + 1)}\right). \tag{2.28}$$

By substituting (2.28) into (2.25), the average BER of the system can be found under BPSK modulation.

2.4.1.2.3 Case III: CSI-assisted AF relaying scheme is employed and the direct link is available : The equivalent SNR is given by

$$\gamma_{srd,\mathrm{III}} = \frac{\gamma_{r,d}\gamma_{s,r}}{\gamma_{r,d} + \gamma_{s,r} + 1} + \gamma_{s,d}. \tag{2.29}$$

Recall that the pdf of $\gamma_{s,d}$ is expressed as $p(\gamma_{s,d}) = \frac{1}{\bar{\gamma}_s}\exp\left(-\frac{\gamma_{s,d}}{\bar{\gamma}_s}\right)$. Using (2.21) and (2.23), we can obtain the outage probability as

$$\begin{aligned} P_{\mathrm{out,AF,III}} &= \int_0^{\gamma_{th}}\left[1 - \frac{2(\gamma_{th} - \gamma)}{\sqrt{\bar{\gamma}_s\bar{\gamma}_{r,d}}}K_1\left(\frac{2(\gamma_{th} - \gamma)}{\sqrt{\bar{\gamma}_s\bar{\gamma}_{r,d}}}\right)\exp\left(-\frac{(\gamma_{th} - \gamma)(\bar{\gamma}_s + \bar{\gamma}_{r,d})}{\bar{\gamma}_s\bar{\gamma}_{r,d}}\right)\right] \\ &\quad \times \frac{1}{\bar{\gamma}_s}\exp\left(-\frac{\gamma}{\bar{\gamma}_s}\right)\mathrm{d}\gamma \end{aligned} \tag{2.30}$$

Note that the result is derived by exploiting the approximation $\frac{\gamma_{r,d}\gamma_{s,r}}{\gamma_{r,d}+\gamma_{s,r}+1} \approx \frac{\gamma_{r,d}\gamma_{s,r}}{\gamma_{r,d}+\gamma_{s,r}}$. Further, the equivalent SNR $\gamma_{srd,\mathrm{III}}$ equals $\gamma_{srd,\mathrm{I}} + \gamma_{sd}$. Since γ_{sd} and $\gamma_{srd,\mathrm{I}}$ are independent, the MGF of $\gamma_{srd,\mathrm{III}}$ can be calculated by

$$\mathcal{M}_{\gamma_{srd,\mathrm{III}}}(s) = \mathcal{M}_{\gamma_{sd}}(s)\mathcal{M}_{\gamma_{srd,\mathrm{I}}}(s) = \frac{1}{1+\bar{\gamma}_s s}\mathcal{M}_{\gamma_{srd,\mathrm{I}}}(s). \tag{2.31}$$

By substituting (2.31) into (2.25), the average BER of the system can be found under BPSK modulation.

2.4.1.2.4 Case IV: Fixed-gain AF relaying scheme is employed and the direct link is available : The equivalent SNR is given by

$$\gamma_{srd,\mathrm{IV}} = \frac{\gamma_{r,d}\gamma_{s,r}}{\gamma_{r,d} + \alpha\bar{\gamma}_s + 1} + \gamma_{s,d}. \tag{2.32}$$

Similar to the derivation of (2.30), by using the pdf of $\gamma_{s,d}$ and (2.27), we obtain the outage probability as

$$\begin{aligned} P_{\mathrm{out,AF,IV}} = \int_0^{\gamma_{th}} &\left[1 - 2\sqrt{\frac{(\alpha\bar{\gamma}_s+1)(\gamma_{th}-\gamma)}{\bar{\gamma}_s\bar{\gamma}_{r,d}}}K_1\left(2\sqrt{\frac{(\alpha\bar{\gamma}_s+1)(\gamma_{th}-\gamma)}{\bar{\gamma}_s\bar{\gamma}_{r,d}}}\right)\right. \\ &\left.\times \exp\left(-\frac{(\gamma_{th}-\gamma)}{\bar{\gamma}_s}\right)\right]\frac{1}{\bar{\gamma}_s}\exp\left(-\frac{\gamma}{\bar{\gamma}_s}\right)\mathrm{d}\gamma \end{aligned} \tag{2.33}$$

Since the equivalent SNR $\gamma_{srd,\mathrm{IV}} = \gamma_{srd,\mathrm{II}} + \gamma_{sd}$, and $\gamma_{srd,\mathrm{II}}$ and γ_{sd} are independent, the MGF of $\gamma_{srd,\mathrm{IV}}$ is given by

$$\mathcal{M}_{\gamma_{srd,\mathrm{IV}}}(s) = \mathcal{M}_{\gamma_{sd}}(s)\mathcal{M}_{\gamma_{srd,\mathrm{II}}}(s) = \frac{1}{1+\bar{\gamma}_s s}\mathcal{M}_{\gamma_{srd,\mathrm{II}}}(s). \tag{2.34}$$

By substituting (2.34) into (2.25), the average BER of the system can be found under BPSK modulation.

2.4.1.3 Selection decode-and-forward (SDF) protocol

The SDF protocol is the selective combination of the DF relaying and the DRT. Therefore, the mutual information of the SDF protocol is derived based on those of the DF and the DRT. The mutual information of the DF protocol is given by (2.11), i.e.,

$$\begin{aligned} I_{\text{DF}} &= \frac{1}{2}\min\{\log(1+\gamma_{s,r}), \log(1+\gamma_{s,d}+\gamma_{r,d})\} \\ &= \frac{1}{2}\min\{\log(1+\bar{\gamma}_s|a_{s,r}|^2), \log(1+\bar{\gamma}_s|a_{s,d}|^2+\bar{\gamma}_{r,d}|a_{r,d}|^2)\} \end{aligned} \tag{2.35}$$

while the mutual information of DRT can be calculated using

$$I_{\text{DRT}} = \frac{1}{2}\log(1+2\bar{\gamma}_s|a_{s,d}|^2). \tag{2.36}$$

The switching between the DF relaying and the DRT depends on the qualify of the $\mathbb{S}-\mathbb{R}$ link. Specifically, if the relay can successfully decoded the received signal, i.e., $\log(1+\bar{\gamma}_s|a_{s,r}|^2) > \mathtt{R}$, the DF relaying will be applied. Otherwise, the DRT will be used. Thus, it can be readily shown that the instantaneous mutual information of SDF is given by [10]

$$I_{\text{SDF}} = \begin{cases} I_{\text{DF}}, & \text{if} \quad |a_{s,r}|^2 \geq g(\bar{\gamma}_s) \\ I_{\text{DRT}}, & \text{if} \quad |a_{s,r}|^2 < g(\bar{\gamma}_s) \end{cases} \tag{2.37}$$

where

$$g(\bar{\gamma}_s) = \frac{2^{\mathtt{R}}-1}{\bar{\gamma}_s}. \tag{2.38}$$

In (2.37), $|a_{s,r}|^2 \geq g(\bar{\gamma}_s)$ is derived from $\log(1+\bar{\gamma}_s|a_{s,r}|^2) > \mathtt{R}$. It represents the scenario that the SNR of the received signal frame at the relay is strong enough for the relay to successfully decoded the received frame. The outage probability of SDF is hence given by [10]

$$P_{\text{out,SDF}} \;=\; \Pr(I_{\text{SDF}} < \mathtt{R}/2) \sim \frac{1}{2\sigma_{s,d}^2}\frac{\sigma_{s,r}^2+\sigma_{r,d}^2}{\sigma_{s,r}^2\sigma_{r,d}^2}\left(\frac{2^{\mathtt{R}}-1}{\bar{\gamma}_s}\right)^2 \tag{2.39}$$

2.4.1.4 Incremental amplify-and-forward (IAF) protocol

The IAF protocol is the selective combination of the AF relaying and the DT transmission. The mutual information of the DT transmission is given by

$$I_{\text{DT}} = \log(1+\bar{\gamma}_s|a_{s,d}|^2) \tag{2.40}$$

and the mutual information of the AF relaying is given by (2.19) when the direct link is available, i.e.,

$$I_{\text{AF}} = \frac{1}{2}\log(1+\gamma_{s,d}+\gamma_r). \tag{2.41}$$

The quality of the direct $\mathbb{S}-\mathbb{D}$ link determines the switching between these two transmission schemes. If the DT transmission fails, i.e., $I_{\text{DT}} < \mathtt{R}$, the AF relaying is activated. Therefore, the instantaneous mutual information of IAF is expressed by [10]

$$I_{\text{IAF}} = \begin{cases} I_{\text{DT}}, & \text{if} \quad |a_{s,d}|^2 \geq g(\bar{\gamma}_s) \\ I_{\text{AF}}, & \text{if} \quad |a_{s,d}|^2 < g(\bar{\gamma}_s) \end{cases} \tag{2.42}$$

and the outage probability is given by [10]

$$P_{\text{out,IAF}} \;=\; \Pr(I_{\text{IAF}} < \mathtt{R}/2) \sim \frac{1}{2\sigma_{s,d}^2}\frac{\sigma_{s,r}^2+\sigma_{r,d}^2}{\sigma_{s,r}^2\sigma_{r,d}^2}\left(\frac{2^{\mathtt{R}}-1}{\bar{\gamma}_s}\right)^2. \tag{2.43}$$

In the IAF protocol, whenever the destination fails decoding the received signal in the first time slot, the relay is asked to amplify-and-forward the received signal to the destination in the second time slot. However, there is a possibility that one

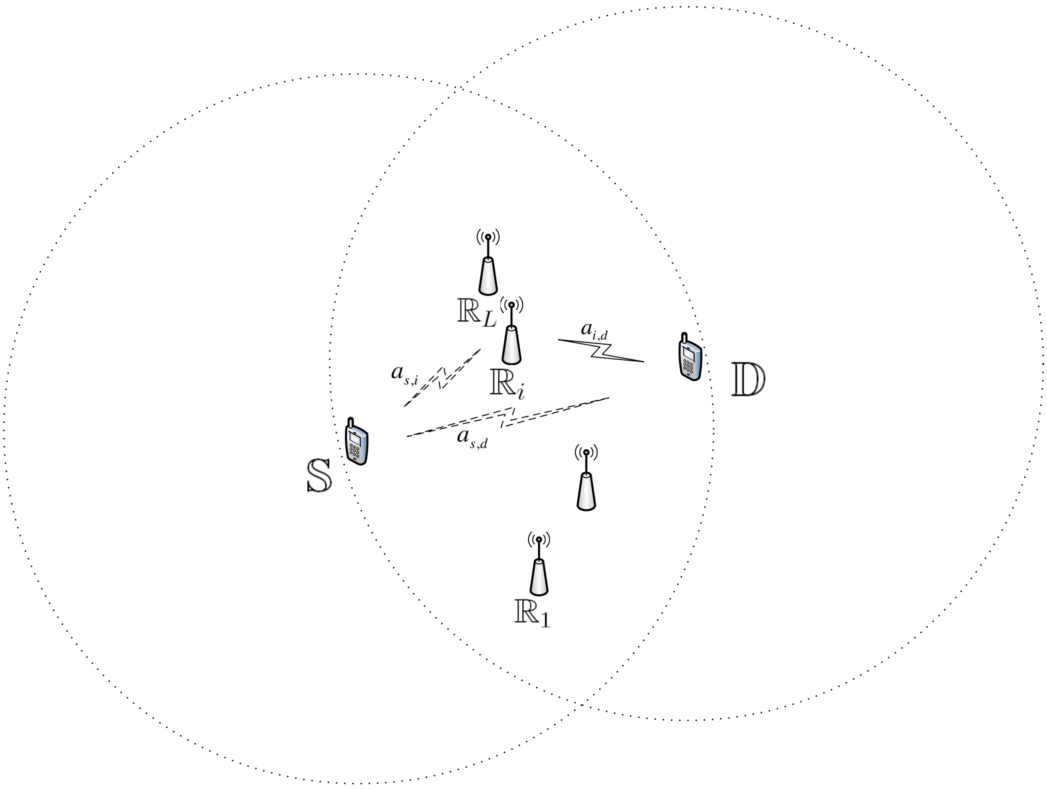

Figure 2.13: The system model of a user-cooperation system with multiple relays. $\mathbb{S}$ denotes the source, $\mathbb{R}_i, (i = 1, \ldots, L)$ denotes the relays and $\mathbb{D}$ denotes the destination. All terminals are equipped a single antenna.

round of re-transmission of the same information frame from the source will provide enough extra information for the destination to achieve successful decoding. In this case, the DRT scheme should be used. Motivated by this observation and based on the IAF protocol, we have proposed two new relaying protocols, namely the incremental selection amplify-and-forward (ISAF) and joint incremental selection relaying (JISR), which will be described and analyzed in Chapter 3.

2.4.2 Multi-relay networks

We re-draw the multi-relay network in Fig. 2.6 as Fig. 2.13. In Fig. 2.13, $a_{s,i}$ and $a_{i,d}$ denote the channel coefficients of the $\mathbb{S} - \mathbb{R}_i$ link and the $\mathbb{R}_i - \mathbb{D}$ link, respectively $(i = 1, 2, \ldots, L)$.

2.4.2.1 Orthogonal relaying

In the orthogonal relaying, the L relays transmit orthogonally. In this simplest relaying scheme for use in multi-relay systems, each relay occupies one exclusive time slot or frequency slot.

2.4.2.1.1 Orthogonal DF relaying : When the orthogonal relaying scheme uses DF, the outage probability is given by [11]

$$P_{\text{out,DF},\perp} = \Pr(I_{\text{DF},\perp} < \frac{\mathtt{R}}{L+1}) = \sum_{\mathcal{D}(r)} \Pr(\mathcal{D}(r)) \Pr\left(I_{\text{DF},\perp} < \frac{\mathtt{R}}{L+1} | \mathcal{D}(r)\right) \quad (2.44)$$

where $\mathcal{D}(r)$ is the set of relays which can successfully decode the signal received from the source during the first time slot. The mutual information conditioned on $\mathcal{D}(r)$ is further given by

$$I_{\text{DF},\perp} = \frac{1}{L+1} \log \left(1 + \gamma_{s,d} + \sum_{i \in \mathcal{D}(r)} \gamma_{i,d}\right) \quad (2.45)$$

where $\gamma_{i,d}$ is the SNR of the $\mathbb{R}_i - \mathbb{D}$ link. The asymptotic outage probability of this relaying scheme, which is derived as (12) in [11], indicates that this scheme can achieve the full diversity. Apart from the asymptotic analysis, an exact expression of the outage probability has been provided in [23]. In this relaying scheme, each relay has to be intelligent enough to determine whether it can successfully decoded the received signal or not. Furthermore, the destination should be informed to ignore the received signals during the corresponding time slots assigned to those relays which cannot decode unsuccessfully.

To make a complete use of the information of all relays, two other full-diversity-achieving DF relaying methods have been proposed [25, 27]. For example, in [25], the L relays make a hard decision on each of the symbols in the received frame and forward them to the destination without checking whether successful decoding is achieved or not. Then the destination decodes the received signals by assigning each received signal a relay-associated weight and using maximal ratio combining (MRC). Such a relaying scheme is called cooperative MRC (C-MRC) reception (cf. Sect. 2.4.1.1.2). In this relaying scheme, the duty of each relay is much simpler because there is no need to distinguish the decodability of the received frame.

2.4.2.1.2 Orthogonal AF relaying When each relay uses the AF relaying, the equivalent SNR of the MRC received signal at the destination is given by [24]

$$\begin{aligned} \gamma_{\mathrm{AF},\perp} &= \gamma_{s,d} + \sum_{i=1}^{L} \gamma_i \\ &= \gamma_{s,d} + \sum_{i=1}^{L} \frac{\gamma_{s,i}\gamma_{i,d}}{\gamma_{i,d} + \alpha_i \bar{\gamma}_s + 1} \end{aligned} \tag{2.46}$$

where γ_i is the equivalent SNR of the $\mathbb{S} - \mathbb{R}_i - \mathbb{D}$ link; and $\alpha_i = |a_{s,i}|^2$ for the CSI-assisted AF relaying method, $\alpha_i = \mathrm{E}[|a_{s,i}|^2]$ for the semi-blind fixed-gain AF relaying method, and α_i is an arbitrary constant for the blind fixed-gain AF relaying method. Since γ_i $(i = 1, 2, \ldots, L)$ are independent, the MGF of $\gamma_{\mathrm{AF},\perp}$ is given by

$$\mathcal{M}_{\gamma_{\mathrm{AF},\perp}}(s) = \mathcal{M}_{\gamma_{s,d}}(s) \sum_{i=1}^{L} \mathcal{M}_{\gamma_i}(s). \tag{2.47}$$

For the fixed-gain AF scheme, $\mathcal{M}_{\gamma_i}$ can simply be calculated using (2.28). With the approximation $\frac{\gamma_{i,d}\gamma_{s,i}}{\gamma_{i,d}+\gamma_{s,i}+1} \approx \frac{\gamma_{i,d}\gamma_{s,i}}{\gamma_{i,d}+\gamma_{s,i}}$, $\mathcal{M}_{\gamma_i}$ is given by (2.24) for the CSI-assisted AF scheme [20, 68, 69]. Then, based on the MGF of the equivalent SNR $\gamma_{\mathrm{AF},\perp}$, the average BER could be easily evaluated using (2.25) in the case of BPSK modulation. In addition, the outage probability can be obtained by making use of the inverse Laplace transform, i.e.,

$$P_{\mathrm{out}} = \mathcal{L}^{-1}(\mathcal{M}_{\gamma}(s)/s)|_{\gamma_{th}}. \tag{2.48}$$

where $\mathcal{L}^{-1}(\cdot)$ is the inverse Laplace transform operator.

Furthermore, for the CSI-assisted AF scheme, the equivalent SNR $\gamma_{\mathrm{AF},\perp}$ can be approximated by its upper bound, i.e.,

$$\gamma_{\mathrm{AF},\perp} \leq \gamma_{s,d} + \sum_{i=1}^{L} \min(\gamma_{s,i}, \gamma_{i,d}). \tag{2.49}$$

With this approximation, the MGF of $\gamma_{\mathrm{AF},\perp}$ is more tractable. This approximation has been used to derive the MGF of the equivalent SNR over Nakagami-m fading channels [24]. Besides an upper bound, a lower bound is also found and is equal to [20]

$$\gamma_{s,d} + \sum_{i=1}^{L} \frac{1}{2} \min(\gamma_{s,i}, \gamma_{i,d}) \leq \gamma_{\mathrm{AF},\perp} \leq \gamma_{s,d} + \sum_{i=1}^{L} \min(\gamma_{s,i}, \gamma_{i,d}) \tag{2.50}$$

Note that these bounds are satisfied only under the approximation $\gamma_i \approx \frac{\gamma_{i,d}\gamma_{s,i}}{\gamma_{i,d}+\gamma_{s,i}}$. Also, for the CSI-assisted AF relaying scheme, a simple method has been proposed [22] to calculate the asymptotic outage probability if the underlying fading channel gain has a non-zero probability density at the value 0, i.e. $p(|a_{i,j}| = 0) > 0$. Examples satisfying such a condition include Rayleigh distribution and Rician distribution. However, the method does not work for Nakagami-m distributed fading channels because Nakagami-m distribution does not guarantee $p(|a_{i,j}| = 0) > 0$.

2.4.2.1.3 Serial orthogonal relaying : In the orthogonal relaying, suppose the relay $\mathbb{R}_i$ can receive not only the signal transmitted from the source, but also the signals forwarded by other relays before the transmission by $\mathbb{R}_i$. In this way, the relay $\mathbb{R}_i$ can decode the information frame from the source based on more signals, improving the error performance of the network [21, 26, 28]. This kind of orthogonal relaying is usually called serial relaying. However, the serial relaying still suffers from the same low spectral efficiency as other orthogonal relaying schemes.

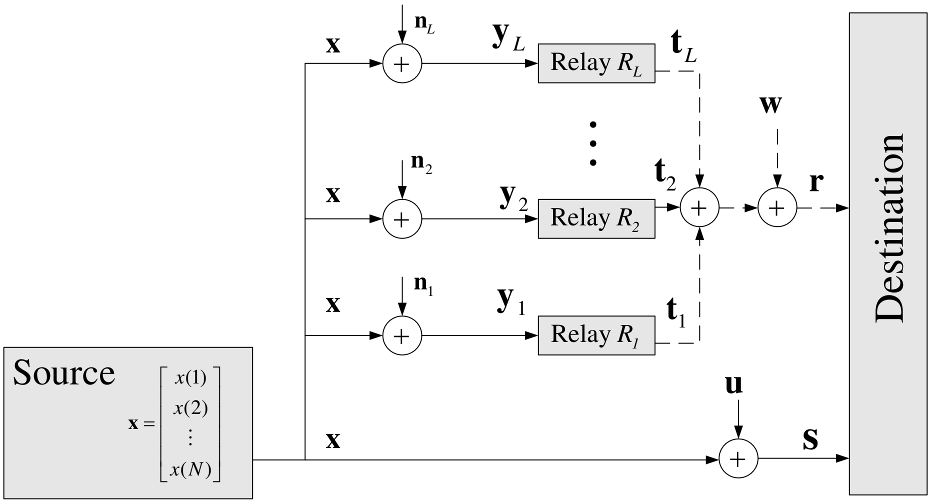

Figure 2.14: Distributed space-time coding for a multi-relay system.

2.4.2.2 Distributed space-time coding

Here, we re-draw Fig. 2.8 as Fig. 2.14, which shows a multi-relay system using distributed space-time coding. As shown in Fig. 2.14, the frame of symbols transmitted from the source is denoted by $\boldsymbol{x} = [x(1), x(2), \ldots, x(N)]^T$, the received signal at the relay R_i $(i = 1, 2, \ldots, L)$ is represented by $\boldsymbol{y}_i = [y_i(1), y_i(2), \ldots, y_i(N)]^T$, the transmitted signal from the relay R_i after some signal processing is given by $\boldsymbol{t}_i = [t_i(1), t_i(2), \ldots, t_i(N)]^T$; and the received signal at the destination is denoted as $\boldsymbol{r} = [r(1), r(2), \ldots, r(N)]^T$.

2.4.2.2.1 Distributed DF relaying In the distributed DF relaying space-time coding scheme [11], during the first time slot the source broadcasts one information frame to the relays and the destination (if the direct link is available). During the second time slot, each of the relays that can successfully decode the received signal transmits a space-time codeword to the destination. Then the destination decodes the information frame based on the received codewords [17, 54]. To construct the space-time codes, it is assumed that all relays work under a centralized control, or each relay is fully aware of the channel states of the entire network. Given a fixed set of channel states, the mutual information of the distributed-space-time relaying system is given by [11]

$$I_{\text{DF,DST}} = \frac{1}{2}\log\left(1 + \frac{2}{L}\gamma_{s,d}\right) + \frac{1}{2}\log\left(1 + \frac{2}{L}\sum_{i\in\mathcal{D}(r)}\gamma_{i,d}\right) \tag{2.51}$$

where $\mathcal{D}(r)$ is the set of relays which can successfully decode the signal received from the source during the first time slot. The outage probability can therefore be calculated using

$$P_{\text{out,DF,DST}} = \Pr(I_{\text{DF,DST}} < \mathtt{R}) = \sum_{\mathcal{D}(r)} \Pr(\mathcal{D}(r)) \times \Pr(I_{\text{DF,DST}} < \mathtt{R}|\mathcal{D}(r)). \tag{2.52}$$

In this discussion, no specific channel coding method has been taken into account, and the outage probability has been obtained from the information-theoretic point of view. To gain the same transmit diversity as the MIMO communications, a lot of distributed space-time codes have been constructed [29–32].

For single-relay networks, the distributed Alamouti space-time code has been investigated. Specifically, the source and the relay collaborate to form a distributed Alamouti space-time code. Maximum-likelihood (ML) detection, which is the optimal detection and provides full diversity order, is then applied at the destination. However, in order to perform the ML detection, the destination needs to know the error probability at the relay, which is not practical. Also, the ML detection becomes too complicated to implement when the number of relays is large. In [30], another distributed Alamouti code with DF relaying called Error Aware Distributed Space-Time (EADST) codes has been proposed. In this scheme, the detected error rates at the relays are monitored to determine whether the relays are healthy or not. If a relay is healthy, it will be signaled to forward a Alamouti code, otherwise it will be asked to remain idle. Even though the scheme promises full diversity, it only works for single-relay and two-relay networks.

In [31], the space-time code designed for N_c co-located transmit antennas is used in the L-relay systems with $L > N_c$. Suppose that there are N_s relays which can successfully decode the received signal frame from the source, the diversity order that the distributed space-time coding is given by $\min(N_s, N_c)$. To accomplish the best expected diversity, N_c should be equal to the expectation of N_s. In this scheme, each relay is pre-assigned a unique $N_c \times 1$ signature vector. Each relay that has successfully decoded the information frame will multiply the N_c-dimensional space-time code with its signature vector, and then forwards the output vector to the destination. Low-complexity coherent, differential and noncoherent detection methods at the destination have been proposed and they have shown to achieve a diversity of $\min(N_s, N_c)$. Also, the design criteria for the signature vector so as to achieve the promised diversity have been proposed. Even though the space-time code for MIMO systems has been intelligently exploited to the distributed relay scenario with low-complexity detection at the destination, the full diversity L is still unachievable.

In [32], randomized space-time coding is applied to multi-relay systems. After receiving the signal from the source, each relay determines whether it can successfully decode the signal or not. If so, the relay $\mathbb{R}_i$ will traditionally map the decoded data frame to a L-dimension space-time codeword (a matrix with the rank of L), and will then forward one randomly-selected row vector of the codeword. However, two distinct relays may choose the same row vector and consequently, the spatial diversity is reduced. In [32], each successful relay randomly selects a few row vectors of the corresponding space-time codeword, and then forwards a linear-combination of these row vectors. It is proved that the diversity achieved is $\min(L, N)$, with the exception that the diversity is fractional if $N = L$. However, in this scheme, the successful relays need to send the destination their random codes, i.e., the indices of the selected row vectors such that MRC reception can be used at the destination.

2.4.2.2.2 Distributed AF relaying : In distributed AF relaying schemes, each relay amplifies the received signal subject to its power constraint and forwards it to destination, instead of attempting to decode the received signal as in the DF scheme. To coordinate the amplified signal frames of the L relays distributively so as to achieve the optimal performance has been a very important issue [33–36]. As a simplest and special case of space-time block codes, the Alamouti code [12] for two transmit antennas has been modified and applied to a single-relay system associated with the AF relaying scheme [35]. The equivalent SNR at the destination has been derived [35] and used to analyze the outage probability and average SER performance.

In [33], a distributed AF relaying scheme is proposed, in which the forwarded signal frames from the L relays form a distributed space-time codeword. To transmit a $L \times N$ codeword from the relays, the proposed scheme needs $L + 1$ time slots, which is much larger than the two time slots consumed by other distributed relaying schemes [11, 34]. The increase of L will significantly reduce the spectral efficiency. Moreover, the proposed distributed code does not achieve the full diversity. In [34], the linear dispersion code has been applied to construct the distributed space-time code and in [36], a distributed orthogonal space-time block code has been proposed. Both schemes can achieve the full cooperative diversity, which is L for the L-relay systems without the direct $\mathbb{S} - \mathbb{D}$ link, but the maximum spectral efficiency cannot be guaranteed.

2.4.2.3 Asynchronously distributed relaying

In [37], it has been proposed that each relay which can successfully decode the received signal frame from the source will be assigned a randomly delay chosen from an intentionally designed delay pool. By exploiting a decision feedback equalizer (DFE) [75, 76], which combines the signal from the source via a frequency non-selective fading channel and the signal from the relays via an equivalent frequency selective fading channel, the destination feedbacks the filter coefficients by optimizing the minimum mean square error (MMSE) of the detection. Even though the method can retain some diversity order, the full diversity order, which is $L + 1$, cannot be guaranteed. In [39], a distributed Alamouti space-time code based on orthogonal frequency division multiplexing (OFDM) has been designed to suppress the asynchronous impairment. In the special Alamouti-emulating code, each element of the 2×2 space-time code is an OFDM symbol, in which a cyclic prefix (CP) is deliberately designed to eliminate the synchronization error between the two relays. The OFDM modulator is implemented in the source, while the relay nodes only process the received signal linearly before forwarding. Full diversity is achieved only for the two-relay systems but not for other multi-relay systems. In [41], the OFDM method is combined with the linear dispersion coding scheme [34] at the asynchronous relay nodes to combat the asynchronous timing errors while conserving the full diversity order. In particular, a distributed space-time block code (STBC) derived from the layer structure of universal space-time codes has been proposed to fulfill the aim.

While the AF strategy has been used in the aforementioned methods, the DF-based distributed space-time codes have also been studied for asynchronous multi-relay systems to achieve full-diversity relaying [38, 40]. In [40], the authors systematically construct a family of distributed space-time trellis codes with BPSK modulation scheme basis on stack construction [77]. The distributed space-time trellis codes is also generalized to QAM and PSK modulation schemes by using unified construction [78]. However, the memory order of trellis coding construction for the relay nodes increases exponentially with the number of relays. In addition, the decoding complexity at the destination node increases exponentially with the memory order. To reduce the memory order and the decoding complexity, the shift-full-rank distributed space-time trellis code construction for asynchronous multi-relay systems has been proposed [38]. The minimum memory order of the shift-full-rank matrices is the same as the number of relay nodes.

Recently, the asynchronous multi-relay systems over frequency-selective fading channel has further been studied [42]. Based on the code construction strategy [38], a family of distributed space-time trellis codes has been constructed to achieve the full cooperative and multipath diversity of the relaying systems when the number of relay nodes is less than five.

2.4.2.4 Opportunistic relaying

As mentioned previously, the main challenges of distributed space-time coding is the synchronization among the relays forwarding the information frame. Even though some of the distributed space-time trellis codes [38, 42] can guarantee the full co-operative diversity, in order to avoid inter-frame interference, the frame forwarded by each relay nodes is padded by a preamble with length no less than the maximum asynchronous timing difference between enrolled relay nodes. This padding of a dumb-symbol preamble will reduce the spectral efficiency. In addition, for the asynchronous relaying system with a large number of relay nodes, the associated large frame length will lead to a high decoding complexity at the destination. In [43], a simple opportunistic relaying method to achieve the full cooperative diversity has been introduced. In the opportunistic relaying, only one "best" relay node is selected to forward the information frame while the other relay nodes remain idle, thus avoiding the synchronization issue which is critical to the success of the distributed relaying protocols.

The selected relay node can process the received signal with the AF scheme and DF scheme, giving rise to opportunistic AF (OAF) protocol and opportunistic DF (ODF) protocol, respectively. The performance of OAF has been studied in terms of asymptotic outage probability [79] and asymptotic average SER [80]. The outage probability of ODF has also been evaluated in [81]. In [59], a selection method with limited feedback from the destination is investigated with the ODF. The relay selection is obtained with a centralized strategy at the destination. Specifically, the selective relaying is implemented with the hybrid-ARQ scheme at the medium access control (MAC) layer and is designed to achieve the maximum diversity-multiplexing gain. In [60], assuming that the channel state information (CSI) is available at the source node, a few selection relaying protocols have been proposed.

Similarly to the notion of IAF and the protocols proposed in [59], we will propose two new opportunistic relaying protocols, and analyze the performance of several opportunistic relaying protocols in Chapter 4 and Chapter 5.

2.4.3 Multi-relay two-way networks

2.4.3.1 Two-way relaying with amplify-and-forward

The two-way relay system was first presented and studied in [82–84], and subsequently integrated with network coding [65]. For a two-way relay network with a single relay and the AF relaying scheme, both $\mathbb{S}_1$ and $\mathbb{S}_2$ broadcast their information frames to the unique relay in the first time slot. In the second time slot, the relay amplifies the received signal frame subject to its power constraint and broadcasts the amplified signal frame back to the sources. The received signal frame at the relay is the superposition of the channel-distorted frames from both sources plus Gaussian noise. The two-way AF relaying strategy has been extended to multi-relay two-way

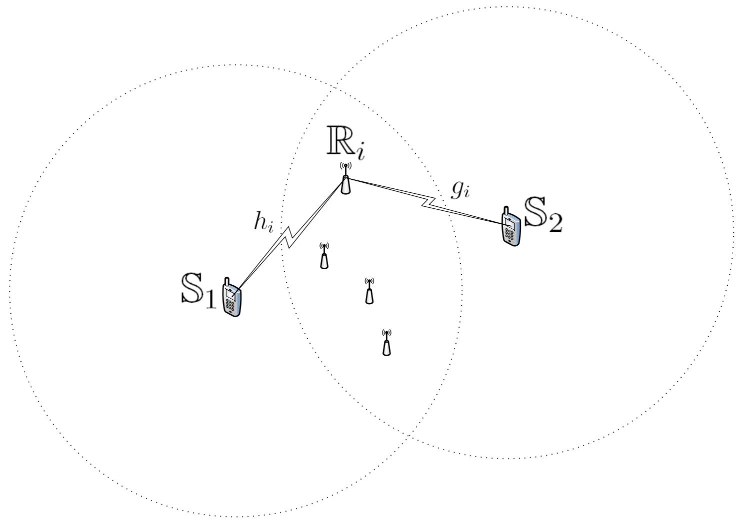

Figure 2.15: The system model of a multi-relay system with two sources and two-way communications.

networks, and integrated with distributed space-time codes to achieve the full diversity, which equals the number of available relays [66]. However the AF scheme will amplify the noise signals at each relay and broadcast the amplified noise back to the sources, which implies ineffective utilization of the relay power and performance degradation. The distributed-DF two-way relaying method reviewed in the following section will circumvent this drawback.

2.4.3.2 Two-way relaying with decode-and-forward

In [66], a distributed space-time coding (STC) with modular network coding for two-way relaying systems has been proposed and referred to as the "partial decode-and-forward II (PDF II)" scheme. To reflect the relaying strategy more precisely, in this thesis, we name such an relaying scheme as the "fully-distributed space-time two-way relaying (FDST-TR)" scheme. Consider the two-way relay network shown in Fig. 2.15, where two source nodes $\mathbb{S}_1$ and $\mathbb{S}_2$ exchange their information with the help of L relay nodes $\mathbb{R}_i$ $(i = 1, \cdots, L)$. We assume that all the relays are within the transmission ranges of both $\mathbb{S}_1$ and $\mathbb{S}_2$, but there is no direct link connecting $\mathbb{S}_1$

and $\mathbb{S}_2$. In the FDST-TR scheme, the two-way relaying is fulfilled in two time slots.

In the first time slot, the two sources broadcast their information frames to the common relays simultaneously. Then, each relay will decode the received signal frame using a generalized sphere decoder [85]. Afterwards, the relay will combine the two decoded signal frames from the two sources into one frame by using modular network coding. It will also determine if the decoded symbol vectors satisfy certain conditions. If so, the relay will further linearly transform the networked-coded signal vector and broadcast the resultant vector back to the two source nodes in the second time slot. Finally, $\mathbb{S}_1$ and $\mathbb{S}_2$ decode the sent symbols from its counterpart based on the received signal vectors sent from the relays.

It has been shown that the FDST-TR scheme can achieve the full diversity order if the number of symbols in a frame is no less than the number of relays L. In other words, when L becomes large, the frame length has to be increased accordingly. This will reduces the probability that the decoded symbol vectors at the relays satisfying the required conditions and hence degrades the system performance. Besides, whenever there is a new relay joining the active transmission, all other relays need to change their transformations on the networked-coded signal vector. Furthermore, the synchronization among all relays becomes more and more difficult when L is large. These disadvantages of FDST-TR can be avoided in our proposed opportunistic two-way relaying (O-TR) method, which will be introduced and analyzed in Chapter 6.

2.5 Summary

As an extension to the MIMO technique, the relaying technique has gained increasing attention recently. By using relays to assist the transmission of information frames, degradation due to channel fading can be mitigated and throughput can be enhanced. In this chapter, we have briefly reviewed a number of relaying protocols for use in single-relay networks, multi-relay networks and multi-relay two-way networks. We have also discuss the pros and cons of such protocols. In the next few chapters, we will present some new protocols and compare their performance with existing ones.

Chapter 3

Two New Relaying Protocols for Single-Relay Networks

In this chapter, we investigate a cooperative single-relay network. By exploiting a simple two-bit feedback message from the destination, we propose two incremental relaying protocols, namely incremental selection amplify-and-forward (ISAF) and joint incremental selection relaying (JISR) with an aim to balancing the load between the source and the relay. We also derive the asymptotic outage probabilities of the two new protocols and find them to be lower than that of the incremental amplify-and-forward (IAF) protocol, which has been identified as the best protocol so far. Moreover, the spectral efficiencies of ISAF and JISR match that of IAF. Simulation results have verified the asymptotic performance of the protocols and have shown that JISR outperforms ISAF and IAF over all signal-to-noise ratio values.

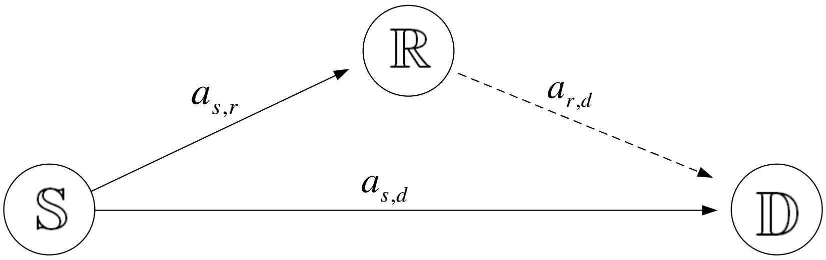

Figure 3.1: The system model of a user-cooperation system with one relay. $\mathbb{S}$ denotes the source, $\mathbb{R}$ denotes the relay and $\mathbb{D}$ denotes the destination. All terminals are equipped a single antenna.

3.1 System Model and Proposed Protocols

3.1.1 User-cooperation system

Consider the communication system shown in Fig. 3.1, where the source transmits information packets to the destination with the aid of the relay. All terminals are supposed to work in half-duplex model. Moreover, it is assumed the medium access control employed in the system is using time-division-multiple-access (TDMA) scheme. Thus, the destination cannot receive packets from the source and the relay simultaneously. In general, such a cooperative transmission is divided temporally into two time slots. In the first time slot, the source broadcasts an information packet to the relay and the destination, whereas in the second time slot, depending upon the protocol used, various scenarios may occur. For example, the relay amplifies the received analog signal and forwards it to the destination when the amplify-and-forward relaying (AF) protocol is implemented. For the decode-and-forward relaying (DF) protocol, the relay decodes the received packet, encodes it and sends the encoded packet to the destination; and for the selection DF protocol, either DF or direct transmission (DT) is chosen depending on the link quality between the source and the relay.

Let $a_{i,j}$ be the link coefficient between terminal i (source denoted by s or relay denoted by r) and terminal j (relay r or destination denoted by d). In the single-relay network, the channel is characterized by $a_{s,d}$, $a_{s,r}$ and $a_{r,d}$. All of them are modeled as zero-mean, independent, circularly symmetric, complex Gaussian random variables with variance $\sigma_{i,j}^2$. Thus, $|a_{i,j}|^2$ are exponential random variables with parameter $\sigma_{i,j}^{-2}$. Suppose that the channel experiences slow fading, i.e., $a_{i,j}$ is assumed to remain the same within one time frame, which contains two timeslots for the two transmission phases, but vary among time frames.

The baseband-equivalent, discrete-time model of the cooperative relaying channel is then modeled as follows. In the first time slot, the source broadcast an information packet, denoted by $\mathbf{x}_s = (x_s[1], ..., x_s[N/2])$, with power P. The received signals at the relay and the destination are then expressed, respectively, by

$$y_r[k] = a_{s,r}x_s[k] + n_{s,r}[k]; \quad k = 1, ..., N/2 \tag{3.1}$$

and

$$y_{d,1}[k] = a_{s,d}x_s[k] + n_{s,d}[k]; \quad k = 1, ..., N/2. \tag{3.2}$$

During the second time slot, depending on the protocol used, the received signal at the destination can be categorized into

$$y_{d,2}[k] \quad = \quad \begin{cases} a_{r,d}x_r[k] + n_{r,d}[k], & \text{for} \quad \text{DF, AF} \\ a_{s,d}x_s[k] + n_{s,d}[k], & \text{for} \quad \text{DT} \end{cases} \qquad k = N/2 + 1, ..., N \tag{3.3}$$

where $\mathbf{x}_r = (x_r[N/2+1], ..., x_r[N])$ represents the packet re-transmitted by the relay with power P, and $x_s[k] = x_s[k - N/2]$. Moreover, in the above equations, $n_{s,r}[k]$, $n_{s,d}[k]$ and $n_{r,d}[k]$ denote the noise samples and are modeled as zero-mean, independent, circularly symmetric complex Gaussian random sequences with variance N_0. At the end of second time slot, based on the received signal sequences $y_{d,1}[k]$ and

$y_{d,2}[k]$, the destination will have to decode the information packet.

In [10], the incremental amplify-and-forward (IAF) protocol has been proposed as an improvement over the AF protocol. The rationale of the protocol is that the relay repeating the source transmission will not be needed if the destination can successfully decode the information packet based solely on the received signal in the first time slot. In this situation, the protocol is exactly direct-transmission with only one transmission phase. But if the destination cannot decode the source information in first time slot, the AF protocol will be exploited to fulfill the re-transmission task. Compared with DF, AF and selection DF (SDF), the advantage of IAF is the improvement of the spectral efficiency with the cost of a limited feedback, “success” or “failure”, from the destination to the relay and the source. In the following, we will further exploit the feedback from the destination with an aim to enhancing the performance of the cooperative networks.

3.1.2 Incremental selection amplify-and-forward (ISAF) protocol

The first proposed protocol, ISAF protocol, assumes that at the end of the first time slot, the destination will broadcast one of three feedback messages, informing the source and the relay how successful the destination has decoded the information frame transmitted by the source. Details of feedback messages are described as follows.

1. SUCCESS: If the destination can decode the information frame without error during the first time slot, it will broadcast a “success” message to the source and the relay. Having received the feedback, the relay will not perform any transmission and the source will make use of the following time slot to send the next information frame.

2. HALF-SUCCESS: Suppose the destination cannot decode the frame successfully in the first time slot. However, it realizes that doubling the signal-to-noise ratio (SNR) will allow a successful decoding of the frame[1]. Then, it will broadcast a "half-success" message. Having received this feedback, the relay will not perform any transmission while the source will send the same information frame again in the second time slot.

3. FAILURE: Suppose the destination cannot decode the frame successfully in the first time slot. Moreover, it realizes that doubling the signal-to-noise ratio (SNR) will not allow a successful decoding of the frame. Then, it will broadcast a "failure" message. For this feedback, the relay will amplify-and-forward the information signal it receives from the source to the destination in the second time slot while the source will not perform any transmission.

The flow chart of ISAF is illustrated in Fig. 3.2.

3.1.3 Joint incremental selection relaying (JISR) protocol

In the ISAF protocol, the channel condition between the source and the relay, which is known at the relay side, has not been utilized at all. In the proposed joint incremental selection relaying (JISR) protocol, this piece of information will be made use of when determining the action to take during the second time slot. Like the ISAF protocol, the JISR protocol assumes that at the end of the first time slot, the destination will broadcast one of the three feedbacks, as described in ISAF, to the source and the relay. Moreover, same actions as in the ISAF protocol will be

[1]For each information frame, we select some of the information bits, say the last N bits, and append them to the information frame. Then, we compute the CRC bits of these selected information bits. Further, the CRC bits are repeated twice and are appended to the information frame, which is subsequently sent to the receiver. At the receiver, both the selected information bits and the CRC bits are received twice. Thus, the SNR of these bits are twice as those bits that have been sent only once. In consequence, if the CRC check of the selected information bits is passed, we can foresee that doubling the SNR will allow a successful decoding of the whole frame.

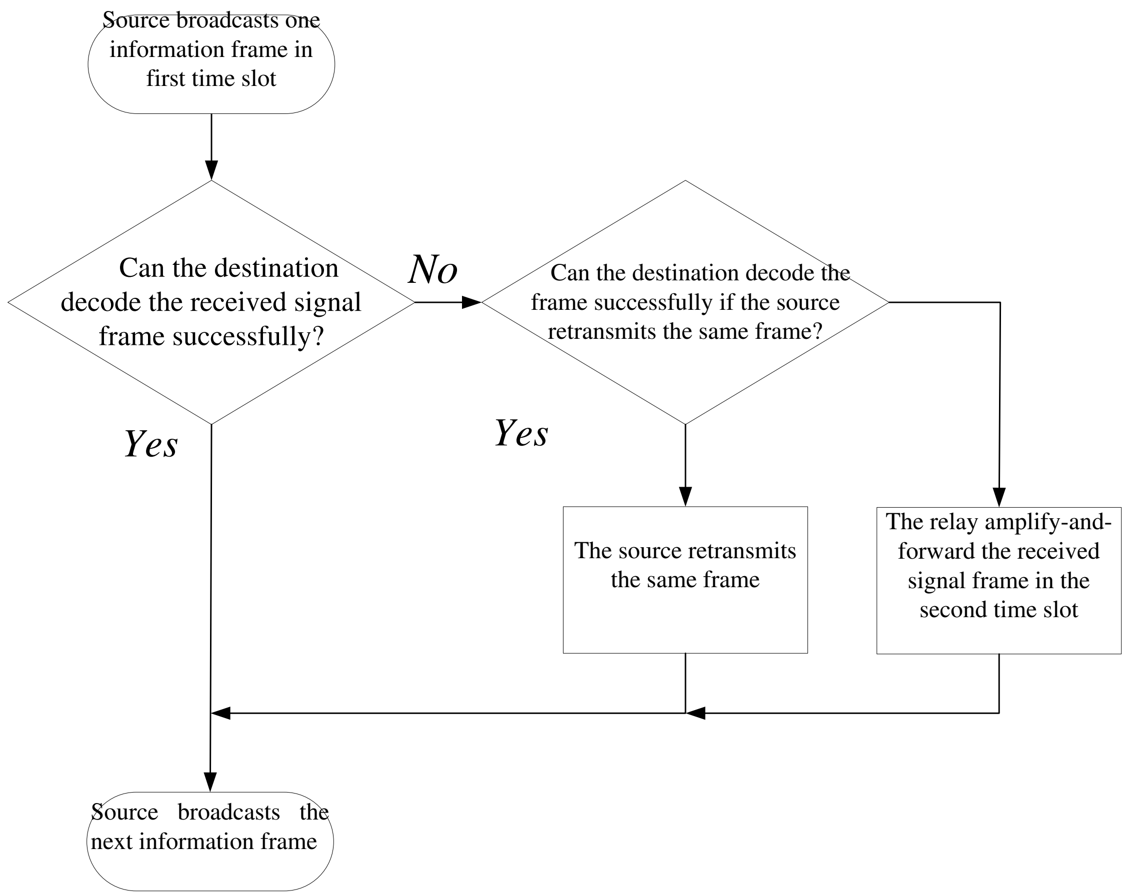

Figure 3.2: The flow chart of the ISAF relaying protocol.

taken by the source and the relay when the "success" or "half-success" feedback is received. But when the "failure" feedback is received, the source will not perform any transmission while the relay will take one of the following two actions. If the relay can successfully decode the information frame it has received from the source during the first time slot, it will encode the frame and forward it to the destination in the second time slot. But if the decoding is not successful, the relay will simply amplify-and-forward the information signal it receives from the source to the destination in the second time slot. The flow chart of JISR is illustrated in Fig. 3.3.

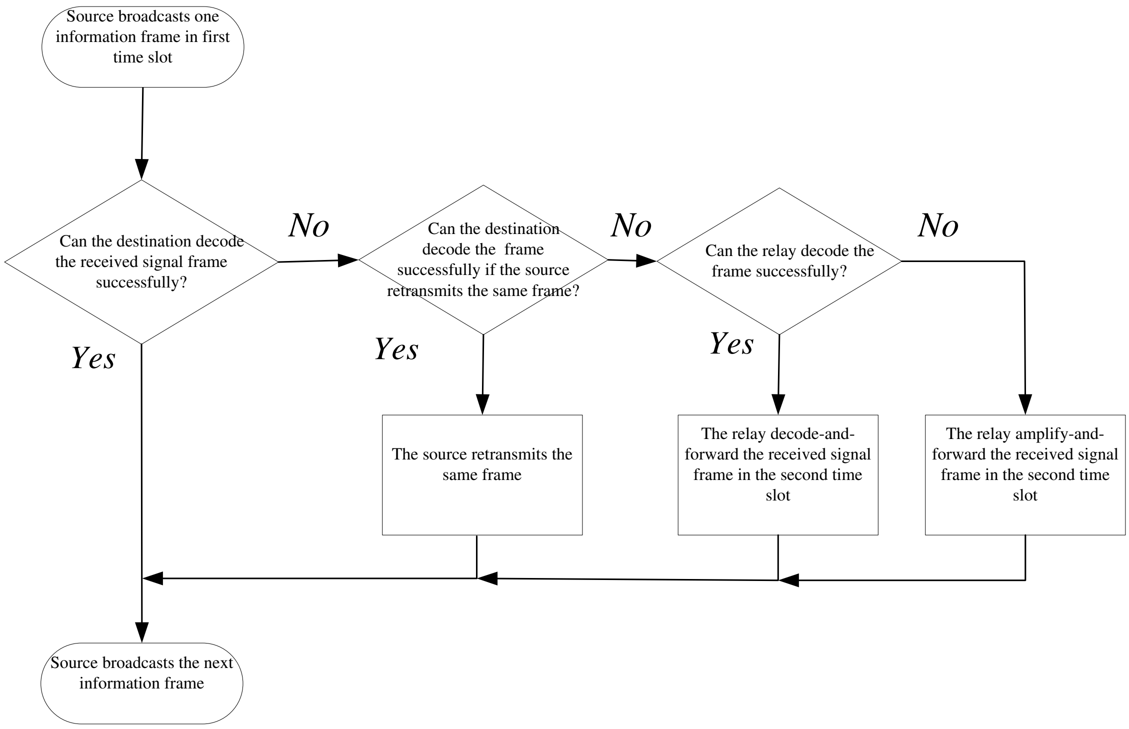

Figure 3.3: The flow chart of the JISR relaying protocol.

3.2 Outage Probability Analysis and Expected Spectral Efficiency

Denote the signal-to-noise ratio (SNR) by $\bar{\gamma}$ and define it as P/N_0. Then the instantaneous SNR of the link between terminal i and terminal j can be represented by $\bar{\gamma}|a_{i,j}|^2$. Moreover, we denote the spectral efficiency by $\mathtt{R}$ when the direct transmission by the source is successfully decoded at the destination during the first time slot and the second time slot is omitted. Thus the spectral efficiency becomes $\mathtt{R}/2$ when the source or the relay needs to transmit in the second time slot. In the following we will derive the asymptotic outage probabilities of the ISAF and JISR protocols from the information theoretic perspective.

3.2.1 Incremental selection amplify-and-forward (ISAF) protocol

For the ISAF protocol, the maximum average mutual information between the source and the destination equals

$$I_{\text{ISAF}} = \begin{cases} I_{\text{DT}}, & \text{if } |a_{s,d}|^2 \geq g(\bar{\gamma}) \\ I_{\text{DRT}}, & \text{if } g(\bar{\gamma}) > |a_{s,d}|^2 \geq \frac{1}{2}g(\bar{\gamma}) \\ I_{\text{AF}}, & \text{if } \frac{1}{2}g(\bar{\gamma}) > |a_{s,d}|^2 \end{cases} \tag{3.4}$$

where $g(\bar{\gamma}) = (2^{\mathtt{R}} - 1)/\bar{\gamma}$ and (refer to Chapter 2)

$$\begin{aligned} I_{\text{DT}} &= \log(1 + \bar{\gamma}|a_{s,d}|^2) & (3.5) \\ I_{\text{DRT}} &= \frac{1}{2}\log(1 + 2\bar{\gamma}|a_{s,d}|^2) & (3.6) \\ I_{\text{AF}} &= \frac{1}{2}\log(1 + \bar{\gamma}|a_{s,d}|^2 + f(\bar{\gamma}|a_{s,r}|^2, \bar{\gamma}|a_{r,d}|^2)) & (3.7) \\ f(x,y) &= (xy)/(x+y+1). & (3.8) \end{aligned}$$

Since the protocol operates at a spectral efficiency of $\mathtt{R}$ and $\mathtt{R}/2$, respectively, when the destination can and cannot decode the information successfully in the first time slot, the outage probability, i.e., the probability that the mutual information is less than the spectral efficiency, is readily shown equal to

$$\begin{aligned} P_{\text{out,ISAF}}(\bar{\gamma}, \mathtt{R}) &= \Pr(|a_{s,d}|^2 < g(\bar{\gamma})/2, I_{\text{AF}} < \mathtt{R}/2) \\ &= \Pr(|a_{s,d}|^2 < g(\bar{\gamma})/2, r_{\bar{\gamma}} < g(\bar{\gamma}) - |a_{s,d}|^2) & (3.9) \end{aligned}$$

where $r_{\bar{\gamma}} = f(\bar{\gamma}|a_{s,r}|^2, \bar{\gamma}|a_{r,d}|^2)/\bar{\gamma}$. Moreover, at high SNR region, (3.9) can be simplified into

$$\begin{aligned} P_{\text{out,ISAF}}(\bar{\gamma}, \mathtt{R}) &\sim \int_0^{g(\bar{\gamma})/2} (\sigma_{s,r}^{-2} + \sigma_{r,d}^{-2})(g(\bar{\gamma}) - u) p_U(u) du \\ &\sim \left(\frac{3}{8\sigma_{s,d}^2} \frac{\sigma_{s,r}^2 + \sigma_{r,d}^2}{\sigma_{s,r}^2 \sigma_{r,d}^2} \right) \left(\frac{2^{\mathtt{R}} - 1}{\bar{\gamma}} \right)^2 \end{aligned} \tag{3.10}$$

where the random variable (RV) $U = |a_{s,d}|^2$ is an exponential RV with parameter $\sigma_{s,d}^{-2}$. Note that the above expression is derived based on the results in [10] and in the Appendix.

3.2.2 Joint incremental selection relaying (JISR) protocol

Similar to the ISAF protocol, the mutual information can be readily shown equal to

$$I_{\text{JISR}} = \begin{cases} I_{\text{DT}}, & \text{if } |a_{s,d}|^2 \geq g(\bar{\gamma}) \\ I_{\text{DRT}}, & \text{if } g(\bar{\gamma}) > |a_{s,d}|^2 \geq \frac{1}{2} g(\bar{\gamma}) \\ I_{\text{DF}}, & \text{if } \frac{1}{2} g(\bar{\gamma}) > |a_{s,d}|^2 \ \& \ |a_{s,r}|^2 \geq g(\bar{\gamma}) \\ I_{\text{AF}}, & \text{if } \frac{1}{2} g(\bar{\gamma}) > |a_{s,d}|^2 \ \& \ g(\bar{\gamma}) > |a_{s,r}|^2 \end{cases} \tag{3.11}$$

where

$$I_{\text{DF}} = \frac{1}{2} \min\{\log(1 + \bar{\gamma}|a_{s,r}|^2), \log(1 + \bar{\gamma}|a_{s,d}|^2 + \bar{\gamma}|a_{r,d}|^2)\} \tag{3.12}$$

and all other terms have been defined in the previous section. Since an outage occurs when the mutual information is smaller than the spectral efficiency, the corresponding probability equals

$$P_{\text{out,JISR}}(\bar{\gamma}, \mathtt{R}) = \Pr(|a_{s,d}|^2 < g(\bar{\gamma})/2, I_{\text{DF}} < \mathtt{R}/2, |a_{s,r}|^2 \geq g(\bar{\gamma}))$$

$$
\begin{aligned}
&\quad + \Pr(|a_{s,d}|^2 < g(\bar{\gamma})/2, I_{\mathrm{AF}} < \mathtt{R}/2, |a_{s,r}|^2 < g(\bar{\gamma})) \\
&= \mathtt{P}_{\mathrm{JISR},1} + \mathtt{P}_{\mathrm{JISR},2} \qquad (3.13)
\end{aligned}
$$

where

$$
\mathtt{P}_{\mathrm{JISR},1} = \Pr(|a_{s,d}|^2 < g(\bar{\gamma})/2, I_{\mathrm{DF}} < \mathtt{R}/2, |a_{s,r}|^2 \geq g(\bar{\gamma})) \qquad (3.14)
$$

$$
\mathtt{P}_{\mathrm{JISR},2} = \Pr(|a_{s,d}|^2 < g(\bar{\gamma})/2, I_{\mathrm{AF}} < \mathtt{R}/2, |a_{s,r}|^2 < g(\bar{\gamma})). \qquad (3.15)
$$

Making use of the fact that

$$
\mathtt{P}_{\mathrm{JISR},1} \leq \Pr(|a_{s,d}|^2 < g(\bar{\gamma})/2, I_{\mathrm{AF}} < \mathtt{R}/2, |a_{s,r}|^2 \geq g(\bar{\gamma})), \qquad (3.16)
$$

and substituting it into (3.13), we can obtain

$$
P_{\mathrm{out,JISR}}(\bar{\gamma}, \mathtt{R}) \leq \Pr(|a_{s,d}|^2 < g(\bar{\gamma})/2, I_{\mathrm{AF}} < \mathtt{R}/2) = P_{\mathrm{out,ISAF}}(\bar{\gamma}, \mathtt{R}), \qquad (3.17)
$$

implying that JISR performs no worse than ISAF. Moreover, at high SNR region, $\mathtt{P}_{\mathrm{JISR},1}$ and $\mathtt{P}_{\mathrm{JISR},2}$ can be approximated, respectively, by

$$
\begin{aligned}
\mathtt{P}_{\mathrm{JISR},1} &= \Pr\left(|a_{s,d}|^2 < g(\bar{\gamma})/2, |a_{s,r}|^2 > g(\bar{\gamma}), |a_{s,d}|^2 + |a_{r,d}|^2 < g(\bar{\gamma})\right) \\
&= \exp\left(-\frac{g(\bar{\gamma})}{\sigma_{s,r}^2}\right) \int_0^{\frac{1}{2}g(\bar{\gamma})} \sigma_{r,d}^{-2}(g(\bar{\gamma}) - u) p_U(u) du \\
&\sim \left(\frac{3}{8\sigma_{s,d}^2 \sigma_{r,d}^2}\right) g^2(\bar{\gamma}) \qquad (3.18)
\end{aligned}
$$

and

$$
\begin{aligned}
\mathtt{P}_{\mathrm{JISR},2} &\geq \Pr(|a_{s,d}|^2 < g(\bar{\gamma})/2, |a_{s,r}|^2 < (g(\bar{\gamma}) - |a_{s,d}|^2), \\
&\qquad f(\bar{\gamma}|a_{s,r}|^2/\bar{\gamma}, \bar{\gamma}|a_{r,d}|^2) < g(\bar{\gamma}) - |a_{s,d}|^2) \\
&= \Pr(|a_{s,d}|^2 < g(\bar{\gamma})/2, |a_{s,r}|^2 < (g(\bar{\gamma}) - |a_{s,d}|^2)
\end{aligned}
$$

$$\sim \left(\frac{3}{8\sigma_{s,d}^2\sigma_{s,r}^2}\right) g^2(\bar{\gamma}) \tag{3.19}$$

where $U = |a_{s,d}|^2$ is exponentially distributed. Note that the above expressions are also derived based on the results in [10] and in the Appendix. Combining (3.18) and (3.19), it can be readily shown that at high SNR region, the asymptotic outage probability of the JISR protocol is lower-bounded by

$$\begin{aligned} & \left(\frac{3}{8\sigma_{s,d}^2\sigma_{r,d}^2}\right) g^2(\bar{\gamma}) + \left(\frac{3}{8\sigma_{s,d}^2\sigma_{s,r}^2}\right) g^2(\bar{\gamma}) \\ = & \left(\frac{3}{8\sigma_{s,d}^2}\frac{\sigma_{s,r}^2+\sigma_{r,d}^2}{\sigma_{s,r}^2\sigma_{r,d}^2}\right)\left(\frac{2^{\mathtt{R}}-1}{\bar{\gamma}}\right)^2. \end{aligned} \tag{3.20}$$

But the results from (3.17) and (3.10) further indicates that the asymptotic outage probability is upper-bounded by the same expression in (3.20). Thus we conclude that the asymptotic probability equals

$$P_{\text{out,JISR}}(\bar{\gamma},\mathtt{R}) \sim \left(\frac{3}{8\sigma_{s,d}^2}\frac{\sigma_{s,r}^2+\sigma_{r,d}^2}{\sigma_{s,r}^2\sigma_{r,d}^2}\right)\left(\frac{2^{\mathtt{R}}-1}{\bar{\gamma}}\right)^2. \tag{3.21}$$

3.2.3 Expected spectral efficiency

Same as the IAF protocol [10], both the ISAF protocol and the JISR protocol possess an average spectral efficiency of less than $\mathtt{R}$ but larger than $\mathtt{R}/2$. Moreover, the value of the average spectral efficiency, denoted by $\bar{\mathtt{R}}$, can be obtained as

$$\begin{aligned} \bar{\mathtt{R}} &= \mathtt{R}\cdot \Pr(|a_{s,d}|^2 \geq g(\bar{\gamma})) + \frac{\mathtt{R}}{2}\cdot \Pr(g(\bar{\gamma}) > |a_{s,d}|^2) \\ &= \frac{\mathtt{R}}{2}\left[1+\exp\left(-\frac{2^{\mathtt{R}}-1}{\bar{\gamma}\sigma_{s,d}^2}\right)\right]. \end{aligned} \tag{3.22}$$

Table 3.1: Asymptotic outage probabilities of IAF, ISAF and JISR protocols

Protocol	**Outage Probability** $P_{\text{out}}(\bar{\gamma}, \mathtt{R})$
IAF [10]	$\left(\frac{1}{2\sigma_{s,d}^2}\frac{\sigma_{s,r}^2+\sigma_{r,d}^2}{\sigma_{s,r}^2\sigma_{r,d}^2}\right)\left(\frac{2^{\mathtt{R}}-1}{\bar{\gamma}}\right)^2$
ISAF	$\left(\frac{3}{8\sigma_{s,d}^2}\frac{\sigma_{s,r}^2+\sigma_{r,d}^2}{\sigma_{s,r}^2\sigma_{r,d}^2}\right)\left(\frac{2^{\mathtt{R}}-1}{\bar{\gamma}}\right)^2$
JISR	$\left(\frac{3}{8\sigma_{s,d}^2}\frac{\sigma_{s,r}^2+\sigma_{r,d}^2}{\sigma_{s,r}^2\sigma_{r,d}^2}\right)\left(\frac{2^{\mathtt{R}}-1}{\bar{\gamma}}\right)^2$

3.3 Simulation Results

The asymptotic outage probabilities of the two proposed protocols, namely ISAF and JISR, together with that of IAF [10], are listed in Table 3.1. In the following discussions, we will adopt $(\bar{\gamma}, \mathtt{R}_{\mathtt{norm}})$ pairs to parameterize the cooperative systems, where the normalized spectral efficiency $\mathtt{R}_{\mathtt{norm}}$ is defined [10] as

$$\mathtt{R}_{\mathtt{norm}} = \frac{\bar{\mathtt{R}}}{\log(1+\bar{\gamma}\sigma_{s,d}^2)}. \tag{3.23}$$

3.3.1 Symmetric systems

First, we investigate the system with identical fading characteristics between any two of the terminals, i.e., $\sigma_{s,d}^2 = \sigma_{s,r}^2 = \sigma_{r,d}^2$. Without loss of generality, we set $\sigma_{s,d}^2 = 1$. Fig. 3.4 plots the analytical asymptotic outage probabilities for different protocols when the normalized spectral efficiency $\mathtt{R}_{\mathtt{norm}}$ equals 0.1. The results for SDF was obtained based on (2.39) [10]. The figure indicates that ISAF and JISR, which have the same asymptotic performance (as shown in Table 3.1), achieve the best theoretical performance among the different protocols. At a outage probability of 10^{-4}, ISAF and JISR have about 1.0 dB and 7.5 dB advantages over IAF and SDF [10], respectively. Note that SDF gives the worst performance when all protocols are assumed to provide the same normalized spectral efficiency.

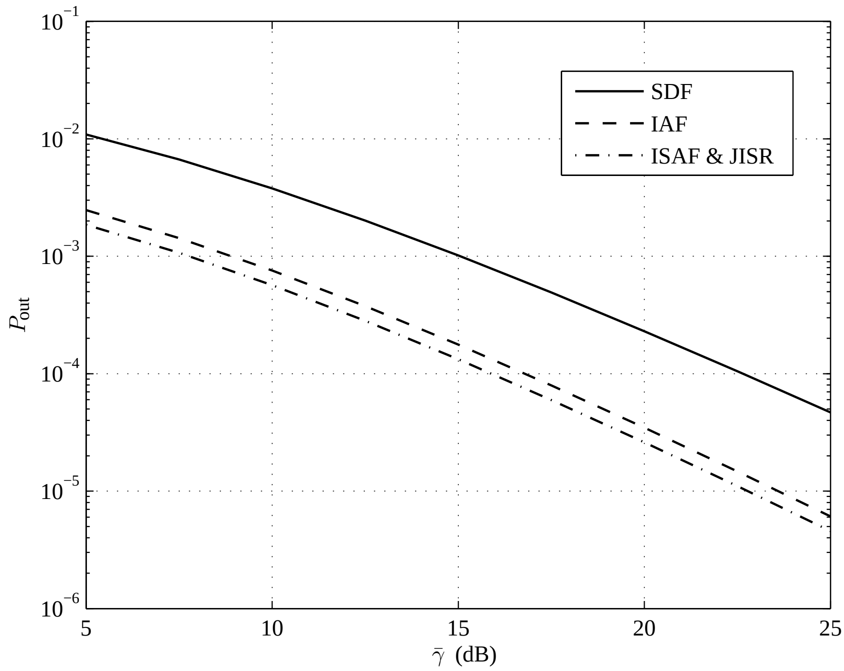

Figure 3.4: Asymptotic outage probabilities versus $\bar{\gamma}$ for a cooperative network with three terminals. Normalized spectral efficiency $\mathtt{R_{norm}} = 0.1$. $\sigma^2_{s,d} = \sigma^2_{s,r} = \sigma^2_{r,d} = 1$.

3.3.2 Asymmetric systems

Next, we examine the case when $\sigma^2_{s,r} > \sigma^2_{r,d}$, i.e., the fading of the source-relay link is not as severe as that of the relay-destination link. Fig. 3.5 shows the outage probabilities of IAF, ISAF and JISR protocols for the system with $\mathtt{R_{norm}} = 0.1$, $\sigma^2_{s,d} = 0.1$, $\sigma^2_{s,r} = 10\sigma^2_{s,d}$ and $\sigma^2_{r,d} = 1.25\sigma^2_{s,d}$. We can observe that the simulation results of both ISAF and JISR match the theoretical asymptotic results at high SNR ($\bar{\gamma}$) regime. This verifies the accuracy of the theoretical outage probabilities of both protocols. In addition, we find from the simulation results that JISR has a much better outage probability performance than ISAF and IAF at low SNR regime ($\bar{\gamma}$ less than 15 dB). Furthermore, ISAF outperforms IAF for all SNR values under consideration. It is also interesting to note that the simulation results of JISR match the asymptotic predictions at both the high SNR regime and the low SNR regime.

Finally, we investigate the system with $\sigma^2_{s,r} < \sigma^2_{r,d}$, and the outage probabilities

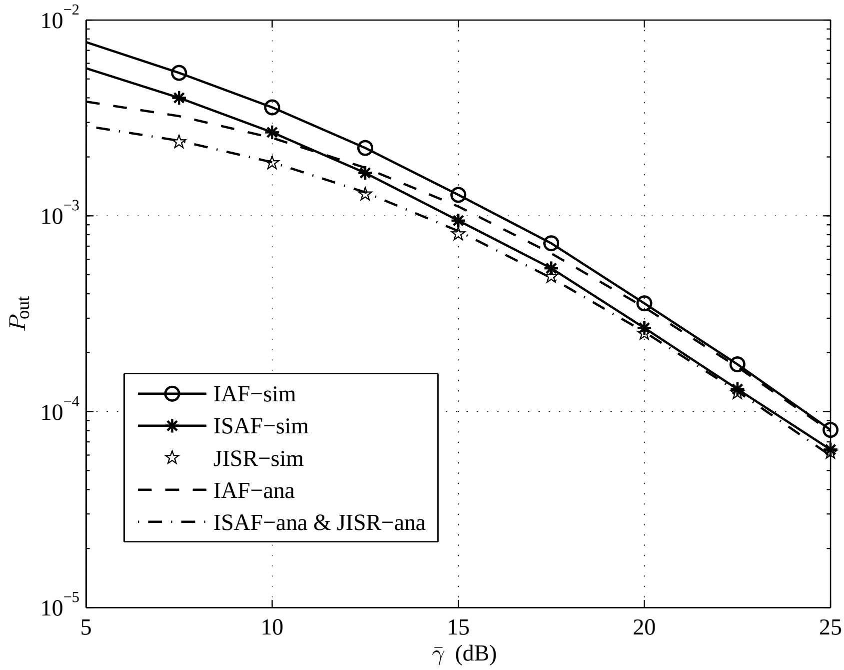

Figure 3.5: Asymptotic and simulated outage probabilities of the IAF, ISAF and JISR protocols versus SNR ($\bar{\gamma}$). $\mathtt{R_{norm}} = 0.1$. $\sigma^2_{s,d} = 0.1$, $\sigma^2_{s,r} = 1$ and $\sigma^2_{r,d} = 0.125$. sim: simulated outage probability; ana: asymptotic outage probability.

are plotted in Fig. 3.6. Similar observations as reported in the previous case are found. In particular, JISR still achieves the lowest outage probability over all SNR values.

Note that we have only considered the systems when $\sigma^2_{s,r} \geq \sigma^2_{s,d}$ and $\sigma^2_{r,d} \geq \sigma^2_{s,d}$. In fact, we are making use of a path loss model in which $\sigma^2_{i,j} \propto d^{-\kappa}_{i,j}$, where $d_{i,j}$ denotes the distance between the terminal i and the terminal j, and κ represents the path-loss exponent [86, 87]. Hence, $\sigma^2_{s,r} \geq \sigma^2_{s,d}$ and $\sigma^2_{r,d} \geq \sigma^2_{s,d}$ imply that $d_{s,r} \leq d_{s,d}$ and $d_{r,d} \leq d_{s,d}$, respectively. In other words, the constraints require the relay to be located in a region somewhere between the source and the destination. In practice, only a relay placed in this region can effectively aid the transmission of the source.

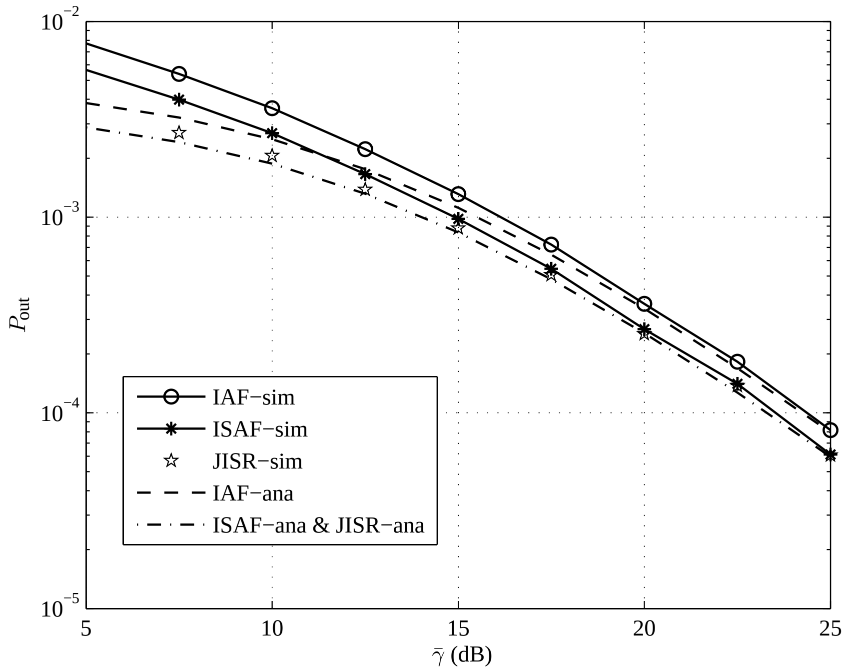

Figure 3.6: Asymptotic and simulated outage probabilities of the IAF, ISAF and JISR protocols versus SNR ($\bar{\gamma}$). $\mathtt{R_{norm}} = 0.1$. $\sigma^2_{s,d} = 0.1$, $\sigma^2_{s,r} = 0.125$ and $\sigma^2_{r,d} = 1$. sim: simulated outage probability; ana: asymptotic outage probability.

3.4 Summary

In this chapter, we have proposed two new relaying protocols for three-terminal systems, namely the incremental selection amplify-and-forward (ISAF) protocol and the joint incremental selection relaying (JISR) protocol. Theoretical asymptotic outage probability analyses have indicated that both ISAF and JISR are superior to incremental amplify-and-forward (IAF) for large SNR cases, and that JISR is no worse than ISAF over all SNR values. Moreover, the asymptotic outage probabilities have been verified by simulation results. The simulations results also show that ISAF is slightly better than IAF, and JISR is much better than ISAF at low SNR regime. Finally, the asymptotic outage probability of the JISR protocol is found to agree well with the simulation results even at low SNR values.

In contrast to IAF that requires a 1-bit feedback from the destination, both

JISR and ISAF need a 2-bit feedback. Yet, even after coding used to protect the feedback information has been considered, the overall spectral efficiencies of the systems employing IAF, JISR or ISAF are going to be very similar. On the other hand, gains of JISR and ISAF over IAF are observed at both the high SNR regime (gain of around 1 dB) and the low SNR region (gain of 2 to 5 dB). Hence, there is still a net advantage of ISAF and JISR over IAF.

In the next chapter, we will study multi-relay networks and evaluate their detailed performance when opportunistic relaying protocols with maxmin selection are used. We will further extend our ISAF and JISR protocols to opportunistic relaying and compare their performance with existing protocols.

Appendix 3.A

Let X be an exponential RV with parameter λ_X. Denote its probability density function by $p_X(x)$. For any function $g(t)$ that is continuous at $t = t_0$ and satisfies $g(t) \to 0$ as $t \to t_0$, we have

$$\lim_{t \to t_0} \frac{1}{g^2(t)} \int_0^{g(t)} x p_X(x) dx = \frac{\lambda_X}{2}. \tag{3.24}$$

The above result is readily proven by using the formula (cf. 3.351.1) in [73] and the Taylor series $\exp(-x) = 1 - x + \frac{1}{2}x^2 + \mathcal{O}(x^3)$ with $x \to 0$.

Chapter 4

Opportunistic Relaying Protocols with Maxmin Selection Criterion

In the previous chapter, we have proposed two new protocols, namely incremental selection amplify-and-forward (ISAF) and joint incremental selection relaying (JISR), for use in single-relay networks. In this chapter, we will examine in detail a cooperative network with multiple relays. In particular, we will investigate protocols that incorporate the opportunistic relaying technique.

In the opportunistic relaying mechanisms, one "best" relay among the multiple relays is selected during a predefined transmission period and only that chosen relay may forward packets to the destination while the other relays are kept idle. The "best" relay can be selected with a distributed algorithm [44, 45] that maximizes (i) the minimum of the source-relay channel gain and the relay-destination channel gain; or (ii) the harmonic mean of source-relay channel gain and the relay-destination channel gain [44]. Alternatively, the selection algorithm can be implemented at the destination if all channel gains are known to the destination. In such cases, the relay that contributes most to the received SNR will be chosen [88]. Having selected the "best" relay, various protocols, including the opportunistic decode-and-forward (ODF) protocol, opportunistic amplify-and-forward (OAF) protocol [44] and selection-AF protocol [88] have been proposed and studied. The aforementioned protocols have one point in common, i.e., each packet transmission will involve two or more phases — direct transmission(s) from the source and re-transmission(s) from the relay. When the signal-to-noise ratio (SNR) is large, however, the destination may be able to decode the message based only on the signal from the source. In such cases, a simple feedback from the destination can remove the re-transmission phase, thus improving the spectral efficiency. For example, the incremental transmission relay selection (ITRS) protocol proposed in [59] will eliminate the relay-retransmission phase if the destination can successfully decode the transmitted packets during the source-broadcasting phase.

In the following sections, we will extend the IAF protocol to opportunistic relaying, forming the opportunistic IAF (OIAF) protocol. Further, we will extend our ISAF and JISR protocols to opportunistic relaying, forming the opportunistic ISAF and the opportunistic JISR, respectively. Then, we attempt to study the opportunistic relaying protocols from the information-theoretic perspective. We further derive the asymptotic outage probabilities of all the aforementioned protocols. Finally, we compare the analytical asymptotic outage probabilities with the simulation results.

4.1 Opportunistic Relaying Protocols

We consider a wireless communication system with a source ($\mathbb{S}$), a destination ($\mathbb{D}$) and L relays ($\mathbb{R}_i; i = 1, 2, \ldots, L$), as in Fig. 4.1. The role of the source is to send data packets to the destination. To improve the success rate of the data transmissions, the relays may aid forwarding the data frames to the destination. To simplify the study, we assume that all terminals work in half-duplex mode. Moreover, time-division-multiple-access (TDMA) is used at the medium-access-control layer. As a consequence, the destination will not be able to receive frames from both the source and the relay at the same time.

When the opportunistic relaying technique is used, a "best" relay will be selected for each frame transmission based on some predefined criterion. Such a cooperative transmission is normally divided temporally into two time slots with equivalent durations. During the first time slot, the source broadcasts an information frame to the relays and the destination (direct transmission, DT), whereas in the second time slot, different transmissions may occur depending on the protocols. In the following, we will describe six different opportunistic protocols, namely opportunistic DF (ODF), opportunistic AF (OAF), opportunistic selection DF (OSDF), opportunistic incremental AF (OIAF), opportunistic incremental selection AF (OISAF) and opportunistic joint incremental selection relaying (OJISR). The first two protocols, ODF and OAF, have been investigated in [43] and will be briefly reviewed here. The third and fourth ones, OSDF and OIAF, are the extensions of SDF and IAF to opportunistic relaying, whereas the last two protocols, OISAF and OJISR, are extensions of our proposed ISAF and JISR protocols.

4.1.1 No feedback from destination

We first present the ODF, OAF and OSDF relaying protocols, which assume that no feedback is provided by the destination after the first time slot.

4.1.1.1 Opportunistic decode-and-forward (ODF)

The selected relay[1] decodes the received frame, encodes it and sends the encoded frame to the destination in the second time slot.

[1] "Selected relay" and "best relay" are used interchangeably in this thesis.

4.1.1.2 Opportunistic amplify-and-forward (OAF)

The selected relay amplifies the received analog signal from the source and forwards it to the destination in the second time slot.

4.1.1.3 Opportunistic selection DF (OSDF)

In the OSDF protocol, the link conditions between the source and selected relay are assumed to be known at the source as well as the selected relay. Thus, to send some information to the destination, in the second time slot, both the source and the selected relay know whether the source should perform direct re-transmission (DRT) of the same frame or the selected relay should forward the received signal using DF to the destination [10, 89].

4.1.2 With feedback from destination

4.1.2.4 Opportunistic incremental AF (OIAF)

In this protocol, the source will perform a DT first. Depending on the destination being or not being able to decode the information frame correctly, the destination will broadcast a simple message — success or failure[2] — to the source and the relays. It is further assumed that this feedback message will be encoded using low-rate coding such that it will be correctly decoded by the source and the relays. Therefore, if the information sent using DT cannot be correctly received by the destination, the selected relay will amplify-and-forward what it has received from the source to the destination. Otherwise, the selected relay does nothing and the source will be able to make use of the time slot to transmit new information frame to the destination based on DT. Since there are occasions that the information needs

[2] In practice, the "success" and "failure" flag indications can be realized by a cyclic redundancy check (CRC).

only to be sent once, time slots are saved, resulting a better spectral efficiency.

4.1.2.5 Opportunistic incremental selection AF (OISAF)

In the first proposed protocol, namely opportunistic incremental selection amplify-and-forward (OISAF) protocol, we assume that at the end of the first time slot, depending on how successful the destination has decoded the information frame transmitted by the source, the destination will broadcast one of the following three feedbacks to the source and the best relay using low-rate encoding.

1. SUCCESS: If the destination can decode the information frame successfully, it will broadcast a “success” message. Then, the best relay will not transmit or forward any information frame and the source will start sending the next information frame.

2. SUCCESS-IF-REPEAT: If the destination cannot decode the whole frame but finds that doubling the signal-to-noise ratio (SNR) will allow a successful decoding of the frame, it will broadcast a “success-if-repeat” message. For this feedback, the best relay will not transmit or forward any information frame while the source will send the same information frame again in the second time slot.

3. FAILURE: If the destination cannot decode the frame and finds that doubling the SNR will not allow a successful decoding of the frame neither, it will broadcast a “failure” message. Having received this feedback, the best relay will amplify-and-forward the information signal it receives from the source to the destination in the second time slot. However, the source will not perform any work.

For the "success-if-repeat" cases, the source will repeat sending the same information frame to the destination. Having received the same frame twice under the same channel conditions, the destination will have a much better SNR (doubled or increased by 3 dB), ensuring that the whole frame can be decoded correctly. With such a differentiation, it is guaranteed that all the "success-if-repeat" packets will be decoded correctly at the end of the second time slot.

4.1.2.6 Opportunistic Joint Incremental Selection Relaying (OJISR) Protocol

In OISAF, the channel condition between the source and the best relay has not been taken into consideration when determining the action to take during the second time slot. Since this extra piece of information is already available at the best relay, further enhancement in system performance should be attained when it is utilized. In the proposed opportunistic joint incremental selection relaying (OJISR) protocol, it is also assumed that at the end of the first time slot, the destination will broadcast one of the three feedbacks, as described in the previous section, to the source and the best relay. Compared with OISAF, OJISR has implemented two different actions, depending on the source-best-relay channel condition, when the "failure" feedback is received. Specifically, when the source and the best relay receive a "failure" message, the source will not perform any work. The best relay, however, will attempt to decode the information frame it has received from the source during the first time slot. If the frame is successfully decoded, the relay will encode the frame and forward it to the destination in the second time slot. Otherwise, the best relay will simply amplify-and-forward the information signal it receives from the source to the destination in the second time slot.

4.2 Performance Analysis

4.2.1 System model

Referring to Fig. 4.1, we define

- $a_{s,i}$ as the channel gain between the source and the ith relay ($i = 1, 2, \ldots, L$);
- $a_{i,d}$ as the channel gain between the ith relay ($i = 1, 2, \ldots, L$) and the destination;
- $a_{s,d}$ as the channel gain between the source and the destination;
- $a_{s,r}$ as the channel gain between the source and the "best" relay;
- $a_{r,d}$ as the channel gain between the "best" relay and the destination.

Moreover, the channel coefficients $a_{s,i}$, $a_{i,d}$ and $a_{s,d}$, collectively denoted by $a_{k,l}$, are modeled as zero-mean independent circularly symmetric complex Gaussian random variables with variance $\sigma^2_{k,l}$, i.e., $\mathcal{CN}(0, \sigma^2_{i,j})$. Furthermore, we assume that $a_{k,l}$ keeps constant over one time frame, which consists of two time slots to support two transmission phases, but varies among time frames.

The baseband-equivalent, discrete-time model of the opportunistic relaying channel can then be modeled as follows. In the first time slot, the source performs a direct transmission (DT). Then, the received signals at the selected relay and the destination are expressed, respectively, by

$$y_r[j] = a_{s,r}x_s[j] + n_{s,r}[j]; \quad j = 1, ..., N \tag{4.1}$$

and

$$y_{d,1}[j] = a_{s,d}x_s[j] + n_{s,d}[j]; \quad j = 1, ..., N \qquad \text{(Direct Transmission)} \tag{4.2}$$

where $\mathbf{x}_s = (x_s[1], ..., x_s[N])$ denotes the source-transmitted frame with power P. In the second time slot, the destination received signal is given by

$$y_{d,2}[j] \;=\; \begin{cases} a_{r,d}x_r[j] + n_{r,d}[j], & \text{for} \quad \mathrm{ODF, OAF} \\ a_{s,d}x_s[j] + n_{s,d}[j], & \text{for} \quad \mathrm{DRT} \end{cases} \qquad j = N+1, ..., 2N \tag{4.3}$$

where $\mathbf{x}_r = (x_r[N+1], ..., x_r[j])$ represents the relay-transmitted frame with power P[3], and $x_s[j] = x_s[j-N]$. In (4.2) and (4.3), $n_{s,r}[j]$, $n_{s,d}[j]$ and $n_{r,d}[j]$ are modeled as zero-mean, independent, circularly symmetric complex Gaussian random sequences with variance N_0. Subsequently, the destination will decode the information frame based on the received signal sequences $y_{d,1}[j]$ and $y_{d,2}[j]$.

For simplicity of analysis, we assume that the channel characteristics between the source and each of the relays are identical, i.e., $\sigma^2_{s,1} = \sigma^2_{s,2} = \cdots = \sigma^2_{s,L} \triangleq \sigma^2_{s,r}$. Similarly, the channel characteristics between each of the relays and the destination are assumed to be the same, i.e., $\sigma^2_{1,d} = \sigma^2_{2,d} = \cdots = \sigma^2_{L,d} \triangleq \sigma^2_{r,d}$. Let $\bar{\gamma} := P/N_0$, the instantaneous signal-to-noise ratio of the link between terminal k and the terminal l is then characterized by $\bar{\gamma}|a_{k,l}|^2$. Note that another important parameter characterizing the relaying channel is the spectral efficiency $\mathtt{R}$ [10].

4.2.2 Maxmin selection criterion

In all opportunistic relaying protocols, for each frame transmission, the system chooses one opportunistic relay among the L available relay candidates by a distributed algorithm. Only the selected relay can forward frame transmitted by the source to the destination while the other relays are kept idle. In our study, we select the "best" relay with an aim to maximizing the minimum of the source-relay channel gain and the relay-destination channel gain. First, for the ith relay ($i = 1, 2, \ldots, L$),

[3] In the case of OAF, the relay gain equals $\sqrt{P/(|a_{s,r}|^2 P + N_0)}$ [10].

we select the smaller value between the square of source-relay channel gain and the square of relay-destination channel gain, i.e., $\min(|a_{s,i}|^2, |a_{i,d}|^2)$. Then, among these L values $(\min(|a_{s,1}|^2, |a_{1,d}|^2), \ldots, \min(|a_{s,i}|^2, |a_{i,d}|^2), \ldots, \min(|a_{s,L}|^2, |a_{L,d}|^2))$, we select the largest one, i.e., $\max(\min(|a_{s,1}|^2, |a_{1,d}|^2), \ldots, \min(|a_{s,L}|^2, |a_{L,d}|^2))$, and the corresponding relay will be the "best" relay [4]. Since $a_{s,r}$ represents the channel gain between the source and the "best" relay and $a_{r,d}$ denotes the channel gain between the "best" relay and the destination, we have

$$\min(|a_{s,r}|^2, |a_{r,d}|^2) = \max\left(\min(|a_{s,1}|^2, |a_{1,d}|^2), \ldots, \min(|a_{s,L}|^2, |a_{L,d}|^2)\right). \quad (4.4)$$

Based on (4.4), we can write

$$\min(|a_{s,r}|^2, |a_{r,d}|^2) \geq \min(|a_{s,i}|^2, |a_{i,d}|^2) \quad \forall \quad i \in \{1, 2, \ldots, L\}. \quad (4.5)$$

Note that the "best" relay may correspond to different physical relays for different frame transmissions. Moreover, although the channel gains $a_{s,i}$ and $a_{i,d}$ for the same relay $i \in \{1, 2, \ldots, L\}$ are independent, the channel gains $a_{s,r}$ and $a_{r,d}$ for the "best" relay (which varies for different frame transmissions) are not independent[5]. The gains $a_{s,r}$ and $a_{r,d}$ are related in the sense that both $|a_{s,r}|^2$ and $|a_{r,d}|^2$ have to be larger than either the magnitude square of the source-relay channel gain and/or the magnitude square of the relay-destination channel gain of all other relays, as can be seen in (4.5). This selection strategy is called *maxmin* criterion. Though the algorithm has to be run once for every new frame transmission, we assume that the time consumed by (i) the opportunistic relay selection algorithm; (ii) the decoding and encoding process of the relay; and (iii) the feedback of the destination

[4]In the distributed algorithm [43], the ith relay set a timer T_i, which is proportional to $1/\min(|a_{s,i}|^2, |a_{i,d}|^2)$. All relays start their timers simultaneously. The one which runs out of its timer will signal other relays, claiming it is the best relay. Alternatively, the "best" relay could be selected in a centralized algorithm.

[5]In the single-relay cooperative networks [10], $a_{s,r}$ and $a_{r,d}$ are independent because there is only one relay.

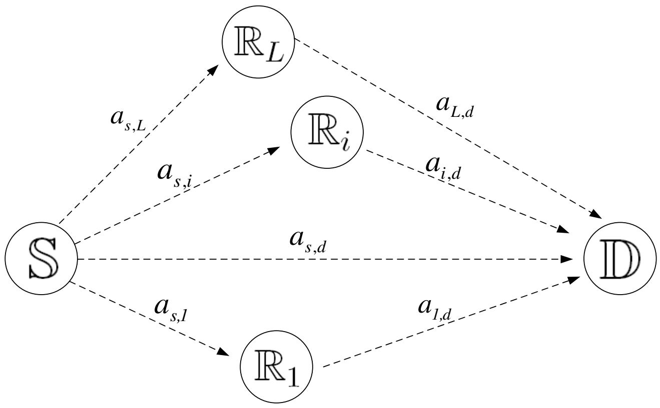

Figure 4.1: User-cooperation system with L relays. All terminals, including the source and the destination and the relays, are equipped with a single antenna.

is negligible and will not reduce the spectral efficiency [43, 44].

Moreover, allocating the power to source and relay based on the channel condition will achieve more reliable transmission [89]. However, the transmitter side must obtain the instantaneous channel state information prior to the transmission. This process will both increase the transmission strategy complexity and reduce the spectral efficiency. To keep the feedback process simple and to facilitate the ease of implementation, we assume that the fading coefficients are not passed to the transmitters. Based on the above assumption, assigning power equally between the source and the relay is the optimal approach, by which we will derive the asymptotical outage probabilities of the protocols.

Before we derive the outage probabilities, we present two important theorems, the proofs of which are shown in the Appendix.

Theorem 4.1. *For any function $g(t)$ that is continuous at $t = t_0$ and satisfies $g(t) \to 0$ as $t \to t_0$, then as $t \to t_0$*

$$\Pr(|a_{s,r}|^2 < g(t)) \sim \sigma_{s,r}^{-2}(\sigma_{s,r}^{-2} + \sigma_{r,d}^{-2})^{L-1} g^L(t) \tag{4.6}$$

$$\Pr(|a_{r,d}|^2 < g(t)) \sim \sigma_{r,d}^{-2}(\sigma_{s,r}^{-2} + \sigma_{r,d}^{-2})^{L-1} g^L(t). \tag{4.7}$$

Theorem 4.2. *Define* $r_\epsilon = \epsilon f(|a_{s,r}|^2/\epsilon, |a_{r,d}|^2/\epsilon)$ *where* $\epsilon > 0$. *For any positive function* $h(\epsilon)$ *continuous at* $\epsilon = 0$ *and* $\lim_{\epsilon\to 0} \epsilon/h(\epsilon) = d < \infty$, *then*

$$\lim_{\epsilon\to 0} \frac{1}{h^L(\epsilon)} \Pr(r_\epsilon < h(\epsilon)) = (\sigma_{s,r}^{-2} + \sigma_{r,d}^{-2})^L. \tag{4.8}$$

4.2.3 Asymptotic outage probability analysis

We first derive the asymptotic outage probabilities of these opportunistic relaying protocols.

4.2.3.1 Opportunistic decode-and-forward (ODF)

Given a certain channel realization, denote the maximum mutual information per channel use for the ODF protocol by I_{ODF}, which can be expressed by [10, 43]

$$I_{\mathrm{ODF}} = \frac{1}{2} \min\{\log(1 + \bar{\gamma}|a_{s,r}|^2), \log(1 + \bar{\gamma}|a_{s,d}|^2 + \bar{\gamma}|a_{r,d}|^2)\}. \tag{4.9}$$

Since the spectral efficiency equals $\mathtt{R}/2$ when the relay is exploited, the outage probability is computed asymptotically as

$$\begin{aligned} P_{\mathrm{out,ODF}}(\bar{\gamma}, \mathtt{R}) &= \Pr(I_{\mathrm{ODF}} < \mathtt{R}/2) \\ &\sim \Pr(|a_{s,r}|^2 < g(\bar{\gamma})) + \Pr(|a_{s,r}|^2 > g(\bar{\gamma})) \times \Pr(|a_{s,d}|^2 + |a_{r,d}|^2 < g(\bar{\gamma})) \\ &\sim \sigma_{s,r}^{-2}(\sigma_{s,r}^{-2} + \sigma_{r,d}^{-2})^{L-1} g^L(\bar{\gamma}) \end{aligned} \tag{4.10}$$

where

$$g(\bar{\gamma}) = (2^{\mathtt{R}} - 1)/\bar{\gamma} \tag{4.11}$$

and $f_1(\bar{\gamma}) \sim f_2(\bar{\gamma})$ indicates that $\lim_{\gamma\to\infty} \frac{f_1(\bar{\gamma})}{f_2(\bar{\gamma})} = 1$ [10]. Moreover, the last step in (4.10) is arrived at by applying Theorem 4.1 together with Corollaries 4.1 & 4.2 in the Appendix.

4.2.3.2 Opportunistic amplify-and-forward (OAF)

The maximum mutual information per channel use for OAF equals [10, 44]

$$I_{\mathrm{OAF}} = \frac{1}{2}\log(1+\bar{\gamma}|a_{s,d}|^2 + f(\bar{\gamma}|a_{s,r}|^2, \bar{\gamma}|a_{r,d}|^2)) \tag{4.12}$$

where $f(x, y) = (xy)/(x + y + 1)$. Therefore, the asymptotic outage probability can be obtained from

$$\begin{aligned} P_{\mathrm{out,OAF}}(\bar{\gamma}, \mathtt{R}) &= \Pr(I_{\mathrm{OAF}} < \mathtt{R}/2) \\ &= \Pr\left(|a_{s,d}|^2 + \frac{1}{\bar{\gamma}} f(\bar{\gamma}|a_{s,r}|^2, \bar{\gamma}|a_{r,d}|^2) < g(\bar{\gamma})\right) \\ &\sim \int_0^{g(\bar{\gamma})} (\sigma_{s,r}^{-2} + \sigma_{r,d}^{-2})^L (g(\bar{\gamma}) - x)^L \sigma_{s,d}^{-2} \exp(-\sigma_{s,d}^{-2} x) dx \\ &\sim \sigma_{s,d}^{-2} (\sigma_{s,r}^{-2} + \sigma_{r,d}^{-2})^L \frac{g^{L+1}(\bar{\gamma})}{L+1} \end{aligned} \tag{4.13}$$

where the RV $X = |a_{s,d}|^2$. Moreover, Theorem 4.2 has been exploited to achieve the result.

4.2.3.3 Opportunistic selection DF (OSDF)

The maximum mutual information for the OSDF protocol can be readily shown equal to [10]

$$I_{\mathrm{OSDF}} = \begin{cases} \frac{1}{2}\log(1+\bar{\gamma}(|a_{s,d}|^2 + |a_{r,d}|^2)), & \text{if} \quad |a_{s,r}|^2 \geq g(\bar{\gamma}) \\ I_{\mathrm{DRT}}, & \text{if} \quad |a_{s,r}|^2 < g(\bar{\gamma}) \end{cases} \tag{4.14}$$

where $I_{\mathrm{DRT}} = \frac{1}{2}\log(1+2\bar{\gamma}|a_{s,d}|^2)$. Therefore, the asymptotic outage probability, i.e., the probability of $I_{\mathrm{OSDF}} < \mathtt{R}/2$, equals

$$\begin{aligned}
P_{\mathrm{out,OSDF}}(\bar{\gamma},\mathtt{R}) &= \Pr(I_{\mathrm{OSDF}} < \mathtt{R}/2) \\
&= \Pr(|a_{s,r}|^2 \geq g(\bar{\gamma})) \times \Pr(|a_{s,d}|^2 + |a_{r,d}|^2 < g(\bar{\gamma})) \\
&\quad + \Pr(|a_{s,r}|^2 < g(\bar{\gamma})) \times \Pr(2|a_{s,d}|^2 < g(\bar{\gamma})) \\
&\sim \left(\frac{\sigma_{s,r}^{-2}}{2} + \frac{\sigma_{r,d}^{-2}}{L+1}\right)\sigma_{s,d}^{-2}(\sigma_{s,r}^{-2}+\sigma_{r,d}^{-2})^{L-1} g^{L+1}(\bar{\gamma}),
\end{aligned} \tag{4.15}$$

which has been derived using Theorem 4.1, Fact 4.1, Corollary 4.1 and Corollary 4.2 in the Appendix.

4.2.3.4 Opportunistic incremental AF (OIAF)

The maximum mutual information for the OIAF protocol can be readily shown equal to [10]

$$I_{\mathrm{OIAF}} = \begin{cases} I_{\mathrm{DT}}, & \text{if} \quad |a_{s,d}|^2 \geq g(\bar{\gamma}) \\ I_{\mathrm{OAF}}, & \text{if} \quad |a_{s,d}|^2 < g(\bar{\gamma}) \end{cases} \tag{4.16}$$

where $I_{\mathrm{DT}} = \log(1+\bar{\gamma}|a_{s,d}|^2)$. Note that when $|a_{s,d}|^2 \geq g(\bar{\gamma})$, no outage occurs because the frame can be successfully decoded in the first time slot. As a consequence, the second time slot is not mandatory in OIAF. As for the outage probability, it will be the same as that for the OAF protocol [10], i.e.,

$$P_{\mathrm{out,OIAF}}(\bar{\gamma},\mathtt{R}) = P_{\mathrm{out,OAF}}(\bar{\gamma},\mathtt{R}) \sim \sigma_{s,d}^{-2}(\sigma_{s,r}^{-2}+\sigma_{r,d}^{-2})^{L}\frac{g^{L+1}(\bar{\gamma})}{L+1}. \tag{4.17}$$

Note that for the same outage probability, OIAF provides a better spectral efficiency than OAF as the second time slot will not be needed whenever the frame has been decoded successfully in the first time slot. Conversely, for the same spectral efficiency, OIAF will have a lower outage than OAF. More discussions will be presented in Section 4.2.4.

4.2.3.5 Opportunistic incremental selection AF (OISAF)

The maximum mutual information is given by

$$I_{\text{OISAF}} = \begin{cases} I_{\text{DT}}, & \text{if} \quad |a_{s,d}|^2 \geq g(\bar{\gamma}) \\ I_{\text{DRT}}, & \text{if} \quad g(\bar{\gamma}) > |a_{s,d}|^2 \geq \frac{1}{2}g(\bar{\gamma}) \\ I_{\text{OAF}}, & \text{if} \quad \frac{1}{2}g(\bar{\gamma}) > |a_{s,d}|^2. \end{cases} \tag{4.18}$$

The frame will be decoded successfully at the destination as long as $|a_{s,d}|^2 \geq \frac{1}{2}g(\bar{\gamma})$. An outage event occurs only when $|a_{s,d}|^2 < \frac{1}{2}g(\bar{\gamma})$ and $I_{\text{OISAF}}(= I_{\text{OAF}})$ is less than the spectral efficiency $\mathtt{R}/2$. Hence, the asymptotic outage probability can be shown equal to

$$\begin{aligned} P_{\text{out,OISAF}}(\bar{\gamma}, \mathtt{R}) &= \Pr(|a_{s,d}|^2 < g(\bar{\gamma})/2, I_{\text{OAF}} < \mathtt{R}/2) \\ &= \Pr(|a_{s,d}|^2 < g(\bar{\gamma})/2, r_{\bar{\gamma}} < g(\bar{\gamma}) - |a_{s,d}|^2) \\ &= \int_0^{\frac{1}{2}g(\bar{\gamma})} (r_{\bar{\gamma}} < g(\bar{\gamma}) - x) p_X(x) dx \\ &\sim \int_0^{\frac{1}{2}g(\bar{\gamma})} (\sigma_{s,r}^{-2} + \sigma_{r,d}^{-2})^L (g(\bar{\gamma}) - x)^L p_X(x) dx \\ &\sim \frac{2^{L+1} - 1}{2^{L+1}(L+1)} \sigma_{s,d}^{-2} (\sigma_{s,r}^{-2} + \sigma_{r,d}^{-2})^L g^{L+1}(\bar{\gamma}) \end{aligned} \tag{4.19}$$

where $r_{\bar{\gamma}} = \frac{1}{\bar{\gamma}} f(\bar{\gamma}|a_{s,r}|^2, \bar{\gamma}|a_{r,d}|^2)$ and the RV $X = |a_{s,d}|^2$. Note that Theorem 4.2 has been used to derive the final result.

4.2.3.6 Opportunistic joint incremental selection relaying (OJISR)

The mutual information for the OJISR protocol is expressed by

$$I_{\mathrm{OJISR}} = \begin{cases} I_{\mathrm{DT}}, & \text{if} \quad |a_{s,d}|^2 \geq g(\bar{\gamma}) \\ I_{\mathrm{DRT}}, & \text{if} \quad g(\bar{\gamma}) > |a_{s,d}|^2 \geq \frac{1}{2}g(\bar{\gamma}) \\ I_{\mathrm{ODF}}, & \text{if} \quad \frac{1}{2}g(\bar{\gamma}) > |a_{s,d}|^2, |a_{s,r}|^2 \geq g(\bar{\gamma}) \\ I_{\mathrm{OAF}}, & \text{if} \quad \frac{1}{2}g(\bar{\gamma}) > |a_{s,d}|^2, g(\bar{\gamma}) > |a_{s,r}|^2. \end{cases} \tag{4.20}$$

When the OJISR protocol is adopted, the transmission fails under two scenarios. The first one is $I_{\mathrm{OJISR}}(= I_{\mathrm{ODF}})$ less than $\mathtt{R}/2$ when $\frac{1}{2}g(\bar{\gamma}) > |a_{s,d}|^2$ and $|a_{s,r}|^2 \geq g(\bar{\gamma})$. The other occasion is $I_{\mathrm{OJISR}}(= I_{\mathrm{OAF}})$ smaller than $\mathtt{R}/2$ when $\frac{1}{2}g(\bar{\gamma}) > |a_{s,d}|^2$ and $g(\bar{\gamma}) > |a_{s,r}|^2$. In consequence, the outage probability equals

$$\begin{aligned} P_{\mathrm{out,OJISR}}(\bar{\gamma}, \mathtt{R}) &= \underbrace{\Pr(|a_{s,d}|^2 < g(\bar{\gamma})/2, I_{\mathrm{ODF}} < \mathtt{R}/2, |a_{s,r}|^2 \geq g(\bar{\gamma}))}_{\mathrm{P}_{\mathrm{OJISR},1}} \\ &\quad + \underbrace{\Pr(|a_{s,d}|^2 < g(\bar{\gamma})/2, I_{\mathrm{OAF}} < \mathtt{R}/2, |a_{s,r}|^2 < g(\bar{\gamma}))}_{\mathrm{P}_{\mathrm{OJISR},2}}. \end{aligned} \tag{4.21}$$

Using the fact that $\mathrm{P}_{\mathrm{OJISR},1} \leq \Pr(|a_{s,d}|^2 < g(\bar{\gamma})/2, I_{\mathrm{OAF}} < \mathtt{R}/2, |a_{s,r}|^2 \geq g(\bar{\gamma}))$ and comparing (4.19) and (4.21), we can easily conclude that

$$P_{\mathrm{out,OJISR}}(\bar{\gamma}, \mathtt{R}) \leq P_{\mathrm{out,OISAF}}(\bar{\gamma}, \mathtt{R}). \tag{4.22}$$

In other words, OJISR always performs no worse than OISAF. Moreover, using Theorem 4.1, Corollary 4.2 and Corollary 4.3 in the Appendix, $\mathrm{P}_{\mathrm{OJISR},1}$ and $\mathrm{P}_{\mathrm{OJISR},2}$ can be derived as follows.

$$\mathrm{P}_{\mathrm{OJISR},1} = \Pr(|a_{s,d}|^2 < g(\bar{\gamma})/2, |a_{s,r}|^2 \geq g(\bar{\gamma}), |a_{s,d}|^2 + |a_{r,d}|^2 < g(\bar{\gamma}))$$

$$
\begin{aligned}
&\sim \int_0^{g(\bar{\gamma})/2} \sigma_{r,d}^{-2}(\sigma_{s,r}^{-2}+\sigma_{r,d}^{-2})^{L-1}(g(\bar{\gamma})-x)^L p_X(x)dx \\
&\sim \frac{2^{L+1}-1}{2^{L+1}(L+1)}\sigma_{s,d}^{-2}\sigma_{r,d}^{-2}(\sigma_{s,r}^{-2}+\sigma_{r,d}^{-2})^{L-1}g^{L+1}(\bar{\gamma}) \qquad (4.23)
\end{aligned}
$$

where $X = |a_{s,d}|^2$.

$$
\begin{aligned}
\mathrm{P}_{\mathrm{OJISR},2} &\geq \Pr(|a_{s,d}|^2 < g(\bar{\gamma})/2, |a_{s,r}|^2 < g(\bar{\gamma}) - |a_{s,d}|^2, \\
&\qquad f(\bar{\gamma}|a_{s,r}|^2, \bar{\gamma}|a_{r,d}|^2)/\bar{\gamma} < g(\bar{\gamma}) - |a_{s,d}|^2) \\
&= \Pr(|a_{s,d}|^2 < g(\bar{\gamma})/2, |a_{s,r}|^2 < g(\bar{\gamma}) - |a_{s,d}|^2) \\
&\sim \frac{2^{L+1}-1}{2^{L+1}(L+1)}\sigma_{s,d}^{-2}\sigma_{s,r}^{-2}(\sigma_{s,r}^{-2}+\sigma_{r,d}^{-2})^{L-1}g^{L+1}(\bar{\gamma}) \qquad (4.24)
\end{aligned}
$$

Finally, combining (4.19) and (4.21)–(4.24), the asymptotic outage probability of the OJISR is obtained as

$$
P_{\mathrm{out,OJISR}}(\bar{\gamma}, \mathtt{R}) \sim \frac{2^{L+1}-1}{2^{L+1}(L+1)}\sigma_{s,d}^{-2}(\sigma_{s,r}^{-2}+\sigma_{r,d}^{-2})^{L}\left(\frac{2^{\mathtt{R}}-1}{\bar{\gamma}}\right)^{L+1}. \qquad (4.25)
$$

4.2.4 Expected spectral efficiency

In the previous section, we have derived the outage probabilities of different opportunistic relaying protocols. In particular, it has been shown that the OAF and OIAF protocols produce identical outage probabilities. But in fact, as will be explained in the following, OIAF outperforms OAF under the same set of conditions.

Consider the scenario when the channel between the source and the destination is good enough for the data frame to be decoded successfully in the first time slot. For the OAF protocol, the selected relay will perform the AF action in the second time slot, even though the signal being forwarded will become redundant as far as the destination is concerned. But for the OIAF protocol, under the same situation, the transmission during the second time slot will be canceled. Instead, the time slot will be spent on transmitting the next frame in the buffer at the source. As can be observed, OIAF apparently has twice the spectral efficiency as OAF. Specifically, the spectral efficiency of OIAF is $\mathtt{R}$ while that of OAF is $\mathtt{R}/2$. Note also that such cases will not contribute to the outage probability, as the packets have been decoded successfully.

On the other hand, when the destination fails to decode the signal received from the source during the first time slot, both the OAF and OIAF protocols will take the same action, i.e., amplify-and-forward the received signal. Depending on the channel conditions, the destination may or may not be able to decode the frame correctly even after receiving the forwarded signal from the selected relay. Under such conditions, both protocols will produce the same outage probability and achieve the same spectral efficiency ($\mathtt{R}/2$). Define the expected spectral efficiency of the protocols as the ensemble average of the spectral efficiency. It is clear that the expected spectral efficiency of OIAF is higher than that of OAF, which means OIAF has a better performance than OAF even though they have the same outage probability. Conversely, if the expected spectral efficiencies for OAF and OIAF are given and equal, the outage probability of OIAF is readily shown lower than that of OAF.

Let $\bar{\mathtt{R}}$ denote the expected spectral efficiency of the protocols. Since all ODF, OAF and OSDF protocols transmit in both the first time slot and the second time slot in all time frames, the expected spectral efficiency are identical and are equal to $\mathtt{R}/2$, i.e.,

$$\bar{\mathtt{R}}_{\mathrm{ODF}} = \bar{\mathtt{R}}_{\mathrm{OAF}} = \bar{\mathtt{R}}_{\mathrm{OSDF}} = \mathtt{R}/2. \tag{4.26}$$

For the OIAF protocol, the spectral efficiency equals $\mathtt{R}$ and $\mathtt{R}/2$ when $|a_{s,d}|^2 \geq g(\bar{\gamma})$ and $g(\bar{\gamma}) > |a_{s,d}|^2$, respectively. Therefore, the expected spectral efficiency of OIAF is given by

$$\begin{aligned}\bar{\mathtt{R}}_{\text{OIAF}} &= \mathtt{R}\cdot\Pr(|a_{s,d}|^2 \geq g(\bar{\gamma})) + \frac{\mathtt{R}}{2}\cdot\Pr(g(\bar{\gamma}) > |a_{s,d}|^2)\\ &= \frac{\mathtt{R}}{2}\left[1+\exp\left(-\frac{2^{\mathtt{R}}-1}{\bar{\gamma}\sigma_{s,d}^2}\right)\right]. \qquad (4.27)\end{aligned}$$

Finally, using a similar argument, it can be easily shown that the expected spectral efficiencies of the OISAF and OJISR protocols are the same as that of the OIAF protocol, i.e.,

$$\bar{\mathtt{R}}_{\text{OISAF}} = \bar{\mathtt{R}}_{\text{OJISR}} = \bar{\mathtt{R}}_{\text{OIAF}}. \qquad (4.28)$$

4.2.5 Diversity-multiplexing tradeoff

In the previous two sections, we have derived the outage probabilities and the expected spectral efficiencies of various opportunistic relaying protocols. In this section, we will continue with our analysis by examining the diversity-multiplexing tradeoff of the aforementioned protocols. The diversity-multiplexing tradeoff mainly relates the effect of the diversity gain on the multiplexing gain, and vice versa. While the diversity gain and the multiplexing gain were originally used to characterize the MIMO systems [19], they have been employed recently to measure performance of cooperative relaying systems [10, 90]. The multiplexing gain, denoted by m, is defined as the ratio of the expected spectral efficiency and $\log\bar{\gamma}$ at the high SNR region, i.e.,

$$m := \lim_{\bar{\gamma}\to\infty}\frac{\bar{\mathtt{R}}}{\log\bar{\gamma}}. \qquad (4.29)$$

Moreover, for a given multiplexing gain m, the diversity gain, denoted by $d(m)$, is defined as the absolute value of the slope of the outage-probability-versus-$\bar{\gamma}$ curve plotted in a log-log scale and at the high SNR region, i.e.,

$$d(m) = -\lim_{\bar{\gamma}\to\infty} \frac{\log \mathrm{P}^{\mathtt{out}}(\bar{\gamma}, m)}{\log \bar{\gamma}}. \tag{4.30}$$

4.2.5.1 ODF

We have shown from (4.10) that at high $\bar{\gamma}$, $P_{\text{out,ODF}} \propto g^L(\bar{\gamma})$. This indicates that ODF can only achieve a maximum diversity gain of L, but not $L+1$. In addition, substituting (4.11), (4.26) and (4.29) into (4.10), we can obtain

$$P_{\text{out,ODF}} \sim \sigma_{s,r}^{-2}(\sigma_{s,r}^{-2} + \sigma_{r,d}^{-2})^{L-1} \left(\frac{2^{2m \log \bar{\gamma}} - 1}{\bar{\gamma}} \right)^L . \tag{4.31}$$

Using the fact that $2^{2m \log \bar{\gamma}} \gg 1$ for all $m > 0$ and $\bar{\gamma} \to \infty$, we substitute (4.31) into (4.30) to obtain the diversity-multiplexing tradeoff for ODF as

$$d_{\text{ODF}}(m) = L(1 - 2m), \quad \text{for} \quad m > 0. \tag{4.32}$$

4.2.5.2 OAF and OSDF

Based on a similar analysis, it is readily shown that the diversity-multiplexing tradeoff expressions for OAF and OSDF are equivalent and are given by

$$d_{\text{OAF}}(m) = d_{\text{OSDF}}(m) = (L+1)(1 - 2m), \quad \text{for} \quad m > 0. \tag{4.33}$$

4.2.5.3 OIAF, OISAF and OJISR

For the OIAF, OISAF and OJISR protocols, since their expected spectral efficiency $\bar{\mathtt{R}} = \mathtt{R}$ as $\bar{\gamma} \to \infty$, their tradeoff expressions can be easily shown to be equivalent and are described by

$$d_{\mathrm{OIAF}}(m) = d_{\mathrm{OISAF}}(m) = d_{\mathrm{OJISR}}(m) = (L+1)(1-m), \quad \text{for} \quad m > 0. \tag{4.34}$$

4.3 Simulation Results

In Table 4.1, we summarize the outage probabilities, expected spectral efficiencies and diversity-multiplexing tradeoff expressions of all the protocols under investigation. Moreover, in the following discussions, we will adopt the $(\bar{\gamma}, \mathtt{R}_{\mathtt{norm}})$ pairs, instead of $(\bar{\gamma}, \bar{\mathtt{R}})$ or $(\bar{\gamma}, \mathtt{R})$, to parameterize various systems. The symbol $\mathtt{R}_{\mathtt{norm}}$ represents the normalized spectral efficiency and is defined as

$$\mathtt{R}_{\mathtt{norm}} = \frac{\bar{\mathtt{R}}}{\log(1+\bar{\gamma}\sigma_{s,d}^2)}. \tag{4.35}$$

There are two main reasons for defining and using the same $\mathtt{R}_{\mathtt{norm}}$ for all protocols. First, for fixed $\bar{\gamma}$ and $\sigma_{s,d}^2$, the expected spectral efficiency $\bar{\mathtt{R}}$ will be the same for all protocols, allowing a fair comparison of the resulting outage probabilities. Second, the normalized spectral efficiency is in fact equivalent to the multiplexing gain at high SNR region because

$$m = \lim_{\bar{\gamma}\to\infty} \frac{\bar{\mathtt{R}}}{\log\bar{\gamma}} = \lim_{\bar{\gamma}\to\infty} \frac{\bar{\mathtt{R}}}{\log(1+\bar{\gamma}\sigma_{s,d}^2)} = \mathtt{R}_{\mathtt{norm}}. \tag{4.36}$$

Therefore, using the same $\mathtt{R}_{\mathtt{norm}}$ for all protocols implies that all protocols achieves the same multiplexing gain.

4.3.1 Single-relay networks

First, it should be noted that when there is only one relay in the system, i.e., $L = 1$, the ODF, OAF, OSDF and OIAF protocols degenerate to the DF, AF, SDF and IAF protocols, respectively. Consequently, it is readily shown that by substituting $L = 1$ into the asymptotic outage probability expressions of the ODF, OAF, OSDF, and OIAF protocols, as listed in Table 4.1, we can obtain the same outage probability expressions of the DF, AF, SDF and IAF protocols found in [10]. Note also that the asymptotic outage probabilities of OAF and OSDF are equal when $L = 1$ (but OAF produces a lower outage probability than OSDF when $L \geq 2$).

Next, we examine a bit more on the protocols which require feedback from the destination. Fig. 4.2 shows the outage probabilities of the OIAF, OISAF and OJISR protocols for a single-relay system with $\mathtt{R_{norm}} = 0.2$ and $\sigma^2_{s,d} = 0.1$. Cases where the fading of the source-relay link is more and less severe than the relay-destination link, i.e., $\sigma^2_{s,r} \lessgtr \sigma^2_{r,d}$, have both been studied. We can observe that the simulation results of both OJISR and OISAF match the theoretical asymptotic results when $\bar{\gamma}$ is large. This verifies the accuracy of the asymptotic outage probability predictions of both protocols. In addition, we find from the simulation results that OJISR has a much better outage probability performance than OISAF and OIAF at low $\bar{\gamma}$ regime (roughly, when $\bar{\gamma}$ less than 15 dB). Also, OISAF attains the same $\bar{\gamma}$ improvement over OIAF for all $\bar{\gamma}$ values under consideration.

Note that, here, we have only considered scenarios in which $\sigma^2_{s,d}$ is the smallest among $\sigma^2_{s,r}$, $\sigma^2_{r,d}$ and $\sigma^2_{s,d}$. By deliberately setting $\sigma^2_{s,d}$ smaller than both $\sigma^2_{s,r}$ and $\sigma^2_{r,d}$, we are putting the relays somewhere between the source and the destination. In reality, only relays located in this region can effectively aid the transmission of the source packets.

Table 4.1: Asymptotic outage probabilities, expected spectral efficiencies and diversity-multiplexing tradeoffs of various protocols

Protocols	Asymptotic outage probability $P_{\text{out}}(\bar{\gamma}, \mathtt{R})$	Expected spectral efficiency $\bar{\mathtt{R}}$	Diversity-multiplexing tradeoff
ODF	$\sigma_{s,r}^{-2}(\sigma_{s,r}^{-2} + \sigma_{r,d}^{-2})^{L-1}(\frac{2^{\mathtt{R}}-1}{\bar{\gamma}})^{L}$	$\mathtt{R}/2$	$L(1-2m)$
OAF	$\frac{1}{L+1}\sigma_{s,d}^{-2}(\sigma_{s,r}^{-2} + \sigma_{r,d}^{-2})^{L}(\frac{2^{\mathtt{R}}-1}{\bar{\gamma}})^{L+1}$	$\mathtt{R}/2$	$(L+1)(1-2m)$
OSDF	$(\frac{\sigma_{s,r}^{-2}}{2} + \frac{\sigma_{r,d}^{-2}}{L+1})\sigma_{s,d}^{-2}(\sigma_{s,r}^{-2} + \sigma_{r,d}^{-2})^{L-1}(\frac{2^{\mathtt{R}}-1}{\bar{\gamma}})^{L+1}$	$\mathtt{R}/2$	$(L+1)(1-2m)$
OIAF	$\frac{1}{L+1}\sigma_{s,d}^{-2}(\sigma_{s,r}^{-2} + \sigma_{r,d}^{-2})^{L}(\frac{2^{\mathtt{R}}-1}{\bar{\gamma}})^{L+1}$	$\frac{\mathtt{R}}{2}[1 + \exp(-\frac{2^{\mathtt{R}}-1}{\bar{\gamma}\sigma_{s,d}^{2}})]$	$(L+1)(1-m)$
OISAF	$\frac{2^{L+1}-1}{2^{L+1}(L+1)}\sigma_{s,d}^{-2}(\sigma_{s,r}^{-2} + \sigma_{r,d}^{-2})^{L}(\frac{2^{\mathtt{R}}-1}{\bar{\gamma}})^{L+1}$	$\frac{\mathtt{R}}{2}[1 + \exp(-\frac{2^{\mathtt{R}}-1}{\bar{\gamma}\sigma_{s,d}^{2}})]$	$(L+1)(1-m)$
OJISR	$\frac{2^{L+1}-1}{2^{L+1}(L+1)}\sigma_{s,d}^{-2}(\sigma_{s,r}^{-2} + \sigma_{r,d}^{-2})^{L}(\frac{2^{\mathtt{R}}-1}{\bar{\gamma}})^{L+1}$	$\frac{\mathtt{R}}{2}[1 + \exp(-\frac{2^{\mathtt{R}}-1}{\bar{\gamma}\sigma_{s,d}^{2}})]$	$(L+1)(1-m)$

4.3.2 Multiple-relay networks

When $L \geq 2$, it can be found from Table 4.1 that OAF produces the lowest outage probability among the protocols not requiring any feedback from the destination, i.e., ODF, OAF and OSDF. Hence, we compare only the outage performance of OAF, OIAF, OISAF and OJISR protocols in the following. The channel parameters used are $\sigma^2_{s,d} = 0.025$, $\sigma^2_{s,r} = 1.25\sigma^2_{s,d}$ and $\sigma^2_{r,d} = 2.5\sigma^2_{s,d}$.

Figure 4.3 plots the outage probabilities of the OAF, OIAF, OISAF and OJISR protocols as $\bar{\gamma}$ increases. The normalized spectral efficiency equals 0.4, i.e., $\mathtt{R}_{\mathtt{norm}} = 0.4$, and there are two relays in the network ($L = 2$). Firstly, we compare the simulated outage probabilities with the asymptotic ones. It can be observed that the simulated outage probabilities for OAF, OIAF, OISAF and OJISR protocols converge to the corresponding asymptotic outage probabilities as $\bar{\gamma}$ increases, verifying the accuracy of the analytical outage expressions derived in Section 4.2.3. Moreover, the simulated and analytical outage probabilities of the OJISR protocol are very close even at low $\bar{\gamma}$ values (5 dB). Secondly, we compare the simulated outage performance of the four protocols. The results in Fig. 4.3 indicate that the OAF protocol, compared with the other three protocols, produces a much higher outage probability for all $\bar{\gamma}$ values. In contrast, OJISR produces the lowest outage probability, but its superiority over OISAF and OIAF diminishes as $\bar{\gamma}$ increases. Finally, OISAF always outperforms OIAF but with a small margin over all $\bar{\gamma}$ values under consideration.

Next, we investigate the network performance as the normalized spectral efficiency $\mathtt{R}_{\mathtt{norm}}$ varies. The number of relays remains at 2 ($L = 2$) while the $\bar{\gamma}$ is now fixed at 15 dB and 30 dB separately. We can see from Fig. 4.4 that the outage increases with $\mathtt{R}_{\mathtt{norm}}$. When both the $\bar{\gamma}$ and $\sigma^2_{s,d}$ are fixed, increasing $\mathtt{R}_{\mathtt{norm}}$ is equivalent to increasing the expected spectral efficiency $\bar{\mathtt{R}}$ (see (4.35)). Consequently, $\mathtt{R}$ will

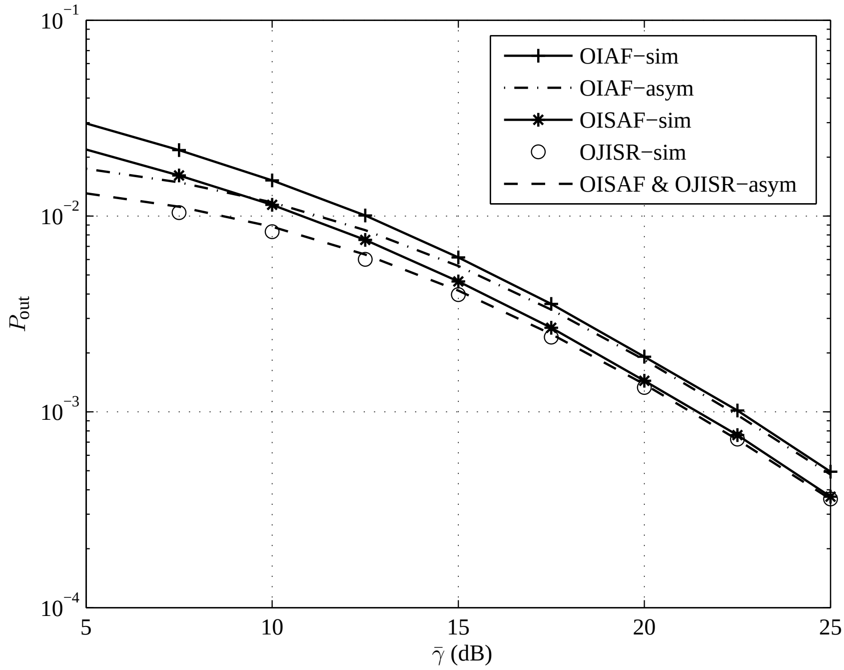

(a)

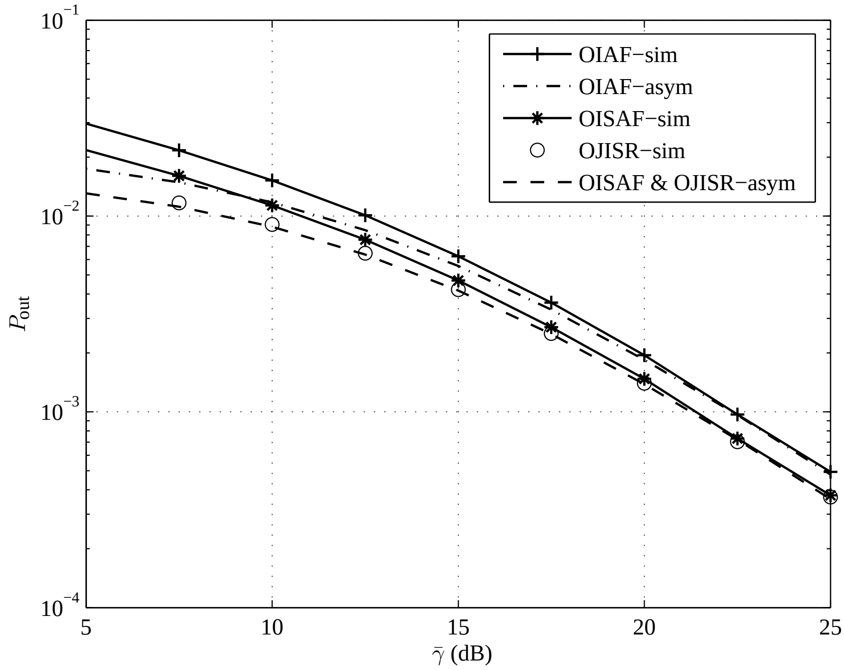

(b)

Figure 4.2: Outage probability as a function of $\bar{\gamma}$ for a cooperative network with a single relay (i.e., $L = 1$). Normalized spectral efficiency $\mathtt{R_{norm}} = 0.2$. $\sigma_{s,d}^2 = 0.1$. (a) $\sigma_{s,r}^2 = 0.125$ and $\sigma_{r,d}^2 = 1$; (b) $\sigma_{s,r}^2 = 1$ and $\sigma_{r,d}^2 = 0.125$. sim: simulated outage probability; asym: asymptotic outage probability.

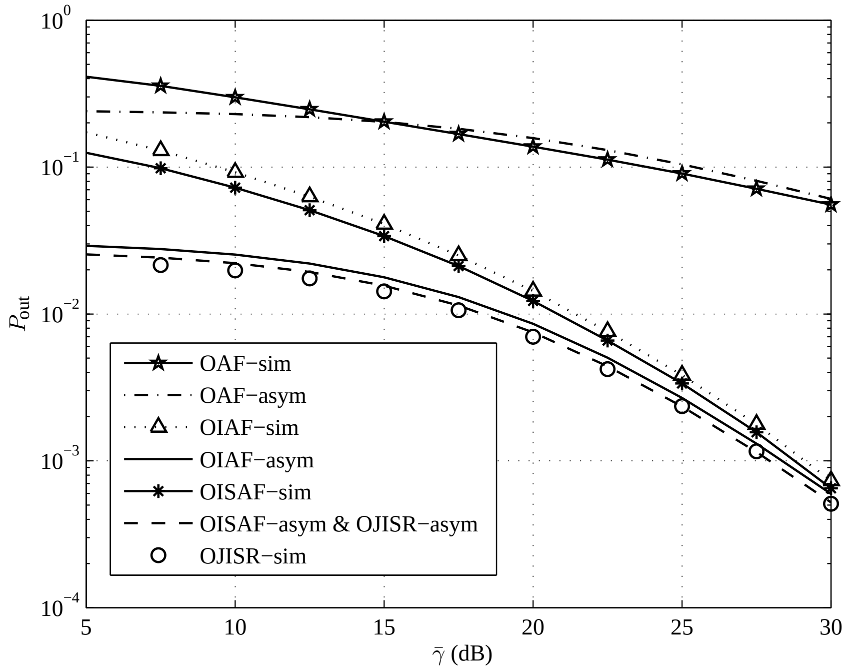

Figure 4.3: Asymptotic and simulated outage probabilities of the OAF, OIAF, OISAF and OJISR relaying protocols versus $\bar{\gamma}$. $\mathtt{R_{norm}} = 0.4$ and $L = 2$. $\sigma_{s,d}^2 = 0.025$, $\sigma_{s,r}^2 = 1.25\sigma_{s,d}^2$, $\sigma_{r,d}^2 = 2.5\sigma_{s,d}^2$. sim: simulated outage probability; asym: asymptotic outage probability.

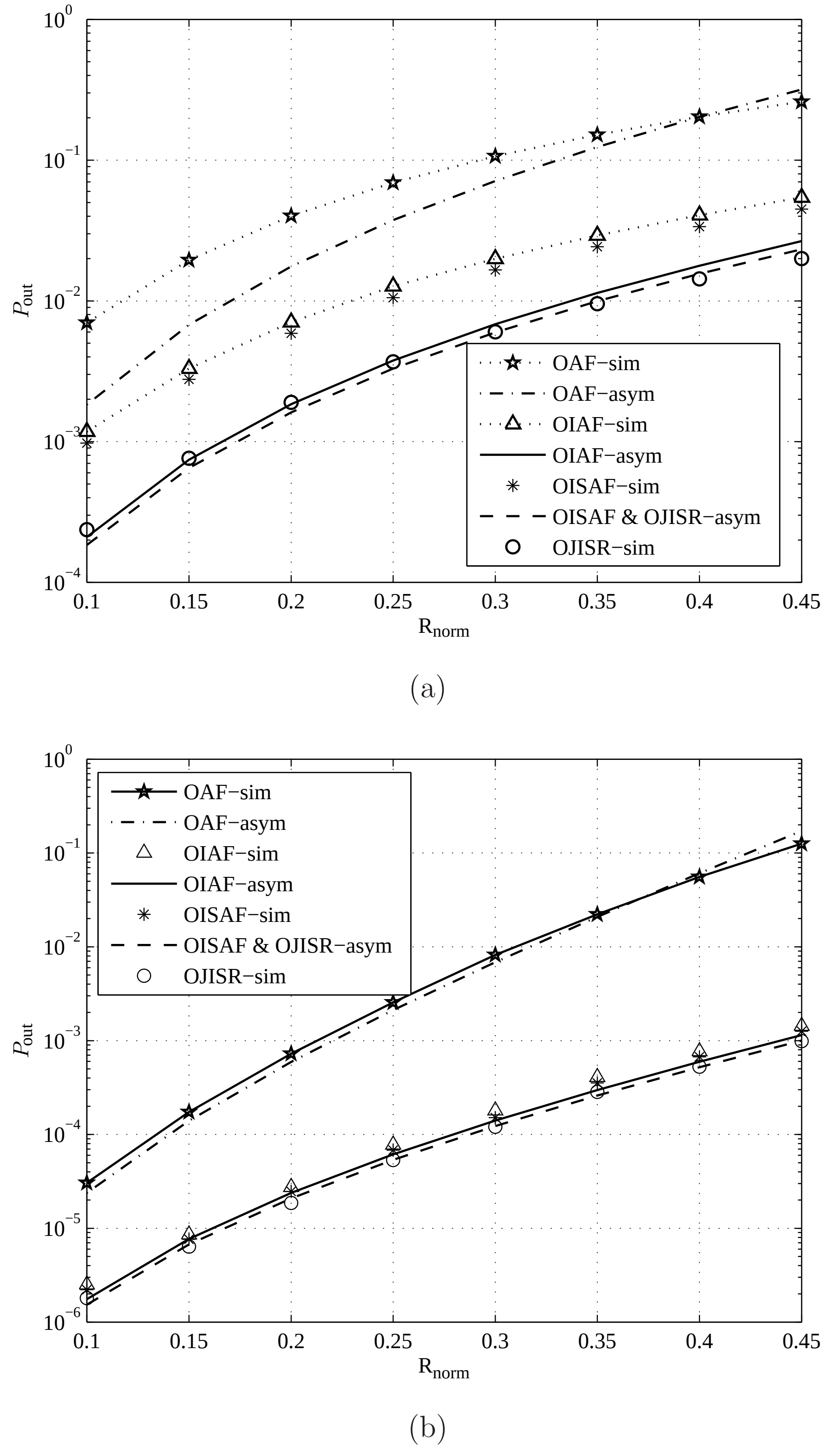

Figure 4.4: Asymptotic and simulated outage probabilities of the OAF, OIAF, OISAF and OJISR relaying protocols versus $\mathtt{R_{norm}}$. $L = 2$, $\sigma_{s,d}^2 = 0.025$, $\sigma_{s,r}^2 = 1.25\sigma_{s,d}^2$, $\sigma_{r,d}^2 = 2.5\sigma_{s,d}^2$. sim: simulated outage probability; asym: asymptotic outage probability. (a) $\bar{\gamma} = 15$ dB; (b) $\bar{\gamma} = 30$ dB.

be increased and the outage performance will need to be sacrificed (see Table 4.1). We also observe that, like in Fig. 4.3, the relative outage performance of the protocols remains in the same order, i.e., OJISR outperforms OISAF, which outperforms OIAF, and OAF is the worst. Figure 4.4(a) further shows that with $\bar{\gamma} = 15$ dB, only the simulated outage results of OJISR match well with the analytical asymptotic outage probabilities. For OAF, OIAF and OISAF, the simulated outage probabilities become closer to the corresponding analytical asymptotic outage probabilities as $\mathtt{R}_{\mathtt{norm}}$ increases from 0.1 to 0.45. When $\bar{\gamma}$ is increased to 30 dB, however, we can observe from Fig. 4.4(b) that the simulation results of OAF, OIAF, OISAF and OJISR are all in good agreement with their corresponding analytical asymptotic outage probabilities. The results again verify that when $\bar{\gamma}$ is large, the analytical asymptotic outage probabilities can provide accurate estimation of the actual performance of the OAF, OIAF, OISAF and OJISR protocols even for a wide range $\mathtt{R}_{\mathtt{norm}}$ values.

Then, we fix $\bar{\gamma} = 25$ dB and $\mathtt{R}_{\mathtt{norm}} = 0.4$, and examine the outage performance as the number of relays L changes. Figure 4.5 shows that the outage diminishes with L. As expected, when there are more relays to choose from, the chance of getting a good (relaying) channel is higher, resulting a lower outage probability. Also the relative outage performance of the protocols is exactly the same as that observed in the aforementioned results, i.e., $P_{\text{out,OJISR}} \leq P_{\text{out,OISAF}} \leq P_{\text{out,OIAF}} < P_{\text{out,OAF}}$. Further, the analytical asymptotic outage probabilities provide a very close match with the actual outage performance for the OJISR protocol, but not the other protocols. Note that the analytical asymptotic outage probability curve for OIAF converges to that for the OISAF & OJISR protocol as L increases, which can be readily predicted based on the expressions listed in Table 4.1.

Finally, we plot the diversity-multiplexing tradeoffs for the opportunistic relaying protocols in Fig. 4.6. As shown in Section 4.2.5, OAF and OSDF have

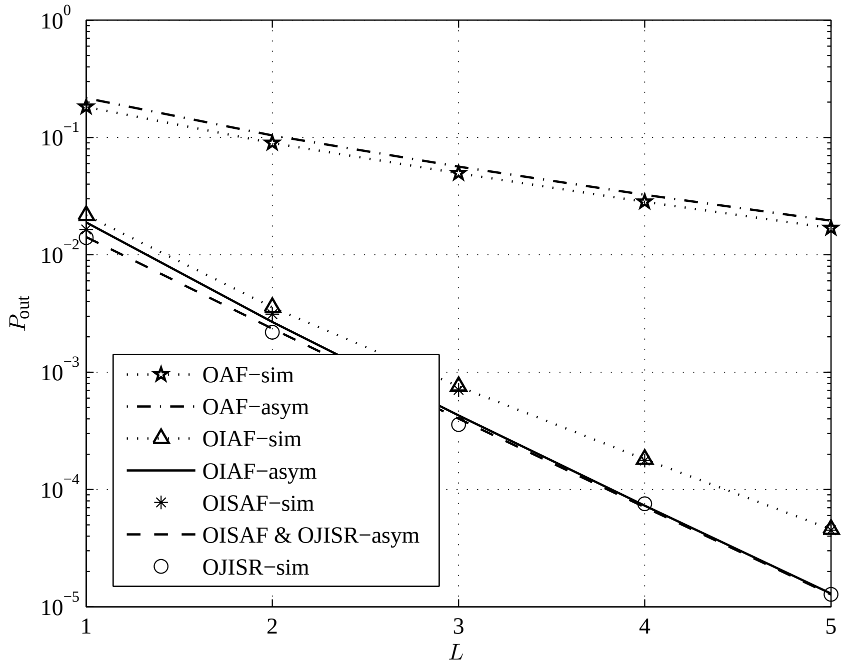

Figure 4.5: Asymptotic and simulated outage probabilities of the OAF, OIAF, OISAF and OJISR relaying protocols versus L. $\bar{\gamma} = 25$ dB and $\mathtt{R_{norm}} = 0.4$. $\sigma^2_{s,d} = 0.025$, $\sigma^2_{s,r} = 1.25\sigma^2_{s,d}$, $\sigma^2_{r,d} = 2.5\sigma^2_{s,d}$. sim: simulated outage probability; asym: asymptotic outage probability.

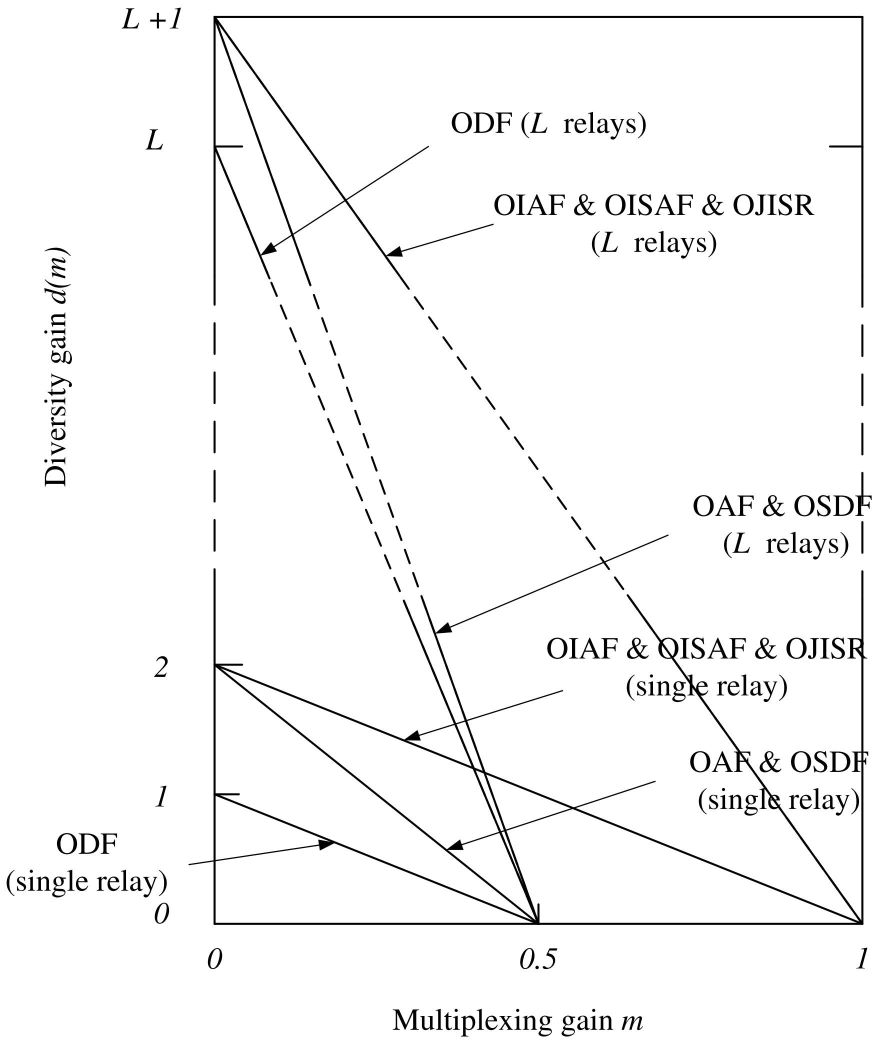

Figure 4.6: Diversity-multiplexing tradeoff of different relaying protocols.

the same diversity-multiplexing tradeoff expression and the tradeoff expression for OIAF, OISAF and OJISR protocols are identical. The results in Fig. 4.6 indicate that except ODF which can only achieve a maximum diversity gain of L, all other opportunistic relaying protocols can achieve a maximum diversity gain of $L+1$. In addition, due to the fact that the same frame is transmitted temporally twice, the ODF, OAF and OSDF protocols can only achieve a maximum multiplexing gain of 0.5. Note also that though the tradeoff performance of OIAF, OISAF and OJISR are equal, the actual outage performance of the OIAF, OISAF and OJISR protocols are not the same, depending on the values of $\mathtt{R_{norm}}$ and $\bar{\gamma}$. As shown in the previous results, in general, OJISR will outperform OISAF which in turn outperforms OIAF, i.e., $P_{\text{out,OJISR}} \leq P_{\text{out,OISAF}} \leq P_{\text{out,OIAF}}$.

4.4 Summary

In this chapter, we have examined a cooperative communication network with multiple relays in detail. Our main contributions can be categorized into three parts. First, based on a simple feedback with three states — success, half-success and failure — from the destination, we have extended the incremental selection amplify-and-forward (ISAF) and joint incremental selection relaying protocols (JISR) for use in opportunistic relaying, forming the opportunistic ISAF (OISAF) and opportunistic JISR (OJISR), respectively. We have shown that they outperform all other existing protocols (opportunistic decode-and-forward (ODF), opportunistic amplify-and-forward (OAF), opportunistic selection DF (OSDF) and opportunistic incremental AF (OIAF)). In particular, OJISR outperform others with a large margin at low SNR region. Second, we have derived the analytical expressions for the asymptotic outage probabilities of six different protocols — ODF, OAF, OSDF, OIAF, OISAF and OJISR. Such results can greatly facilitate researchers analysing and comparing performance of different protocols in future. Third, we have compared the analytical outage probabilities with the simulation results. We conclude that when SNR is large, the analytical asymptotic outage probabilities can provide accurate estimation of the actual performance of the OAF, OIAF, OISAF and OJISR protocols. Further, the simulated and analytical outage probabilities of the OJISR protocol are very close even at low SNR values (5 dB). Finally, when comparing the outage probabilities, OJISR outperforms OISAF, which outperforms OIAF, and OAF is the worst.

In the next chapter, we will continue our study on CSI-assisted OAF systems using the maxmin selection.

Appendix 4.A

Fact 4.1. *Let X be a RV with exponential distribution and parameter λ_X. Denote the cumulative distribution function (cdf) of X by $F_X(x)$. For any function $g(t)$ that is continuous at $t = t_0$ and satisfies $g(t) \to 0$ as $t \to t_0$, then [10]*

$$\lim_{t \to t_0} \frac{1}{g(t)} F_X(g(t)) = \lambda_X. \tag{4.37}$$

Fact 4.2. *Let $\epsilon > 0$ and $r_\epsilon = \epsilon f(v/\epsilon, w/\epsilon)$, where v and w are independent exponential RVs with parameters λ_v and λ_w, respectively. Let $h(\epsilon)$ be any positive function continuous at $\epsilon = 0$ and $\lim_{\epsilon \to 0} \epsilon / h(\epsilon) = d < \infty$. Then [10]*

$$\lim_{\epsilon \to 0} \frac{1}{h(\epsilon)} \Pr(r_\epsilon < h(\epsilon)) = \lambda_v + \lambda_w. \tag{4.38}$$

Lemma 4.1. *Let X be an exponential RV with parameter λ_X. Denote the pdf of X by $f_X(x)$. Given a function $g(t)$ that is continuous at $t = t_0$ and satisfies $g(t) \to 0$*

as $t \to t_0$. Then, for any positive integer L,

$$\lim_{t\to t_0} \frac{1}{g^{L+1}(t)} \int_0^{g(t)} x^L f_X(x)dx = \frac{1}{(L+1)}\lambda_X. \tag{4.39}$$

Proof. $\int_0^{g(t)} x^L f_X(x)dx \sim \lambda_X \int_0^{g(t)} x^L(1-\lambda_X x)dx \sim \frac{\lambda_X}{L+1} g^{L+1}(t)$. $\square$

In the following, we show the proofs of Theorem 4.1 and Theorem 4.2 stated in Section 4.

Proof of Theorem 4.1. Based on the characteristics of exponential RVs, it is readily shown that $\min(|a_{s,i}|^2, |a_{i,d}|^2)$ $(i = 1, 2, \ldots, L)$ are independent, identical exponential RVs with parameter $(\sigma_{s,r}^{-2} + \sigma_{r,d}^{-2})$. Suppose that at one realization the kth relay is chosen as the "best" relay, i.e., $a_{s,r} = a_{s,k}$ and $a_{r,d} = a_{k,d}$. Let the RV $V = \max\{\min(|a_{s,i}|^2, |a_{i,d}|^2) : i = 1, ..., L; i \neq k\}$. Then,

$$\begin{aligned} \Pr(V < g(t)) &= \Pr\left(\cap_{i\neq k}^{L}(\min(|a_{s,i}|^2, |a_{i,d}|^2) < g(t))\right) \\ &\sim (\sigma_{s,r}^{-2} + \sigma_{r,d}^{-2})^{L-1} g^{L-1}(t). \end{aligned} \tag{4.40}$$

Denote the event $|a_{s,k}|^2 = \min\{|a_{s,k}|^2, |a_{k,d}|^2\}$ by $E_{k,1}$, the probability of which is readily shown equal to $\Pr(|a_{s,k}|^2 > V, |a_{s,k}|^2 < |a_{k,d}|^2)$. Therefore the asymptotic probability of $|a_{s,r}|^2 < g(t)$ given $E_{k,1}$ is obtained by

$$\begin{aligned} \Pr(|a_{s,r}|^2 < g(t), E_{k,1}) &= \Pr(g(t) > |a_{s,k}|^2 > V, |a_{s,k}|^2 < |a_{k,d}|^2) \\ &\sim \int_0^{g(t)} (\sigma_{s,r}^{-2} + \sigma_{r,d}^{-2})^{L-1} x^{L-1} \exp(-\sigma_{r,d}^{-2} x) f_X(x)dx \\ &\sim \sigma_{s,r}^{-2}(\sigma_{s,r}^{-2} + \sigma_{r,d}^{-2})^{L-1} \frac{1}{L} g^L(t) \end{aligned} \tag{4.41}$$

where $X = |a_{s,k}|^2$. Denote the event $|a_{k,d}|^2 = \min\{|a_{s,k}|^2, |a_{k,d}|^2\}$ by $E_{k,2}$, the probability of which equals $\Pr(|a_{k,d}|^2 > V, |a_{s,k}|^2 > |a_{k,d}|^2)$. Then,

$$\begin{aligned}
\Pr(|a_{s,r}|^2 < g(t), E_{k,2}) &= \Pr(g(t) > |a_{s,k}|^2 > |a_{k,d}|^2, |a_{k,d}|^2 > V) \\
&= \int_0^{g(t)} \left(\int_0^x (\sigma_{s,r}^{-2} + \sigma_{r,d}^{-2})^{L-1} y^{L-1} f_Y(y) dy \right) f_X(x) dx \\
&\sim \mathcal{O}(g^{L+1}(t)) \qquad (4.42)
\end{aligned}$$

where $Y = |a_{k,d}|^2$. Finally, the probability of $|a_{s,r}|^2 < g(t)$ is given by

$$\begin{aligned}
\Pr(|a_{s,r}|^2 < g(t)) &= \sum_{k=1}^{L} \left[\Pr(|a_{s,r}|^2 < g(t), E_{k,1}) + \Pr(|a_{s,r}|^2 < g(t), E_{k,2}) \right] \\
&\sim \sigma_{s,r}^{-2} (\sigma_{s,r}^{-2} + \sigma_{r,d}^{-2})^{L-1} g^L(t). \qquad (4.43)
\end{aligned}$$

Note that the asymptotic probability of $|a_{r,d}|^2 < g(t)$ could be calculated with a similar method. □

Corollary 4.1. *Let U be an exponential RV with parameter λ_u. Suppose $a_{s,r}$ is the channel gain of the source-best-relay link and $a_{r,d}$ is the channel gain of the best-relay-destination link. For any function $g(t)$ that is continuous at $t = t_0$ and satisfies $g(t) \to 0$ as $t \to t_0$, then*

$$\lim_{t \to t_0} \frac{1}{g^{L+1}(t)} \Pr(|a_{r,d}|^2 + U < g(t)) = (\sigma_{s,r}^{-2} + \sigma_{r,d}^{-2})^{L-1} \sigma_{r,d}^{-2} \frac{\lambda_u}{L+1}. \qquad (4.44)$$

Proof. From Theorem 4.1, we have

$$\begin{aligned}
\Pr(|a_{r,d}|^2 + U < g(t)) &= \int_0^{g(t)} \Pr(|a_{r,d}|^2 < g(t) - u) p_U(u) du \\
&\sim \sigma_{r,d}^{-2} (\sigma_{s,r}^{-2} + \sigma_{r,d}^{-2})^{L-1} \int_0^{g(t)} (g(t) - u)^L \lambda_u \exp(-\lambda_u u) du.
\end{aligned}$$

Using the fact that $\exp(-\lambda_u u) = 1 - \lambda_u u$ as $u \to 0$, we can rewrite the integral part of the above equation as follows

$$\int_0^{g(t)} (g(t)-u)^L \lambda_u (1-\lambda_u u)du = \frac{\lambda_u}{L+1} g^{L+1}(t) - \frac{\lambda_u^2}{(L+1)(L+2)} g^{L+2}(t),$$

in which the second term is negligible compared to the first one as $g(t) \to 0$. Thus, the Corollary is proved. □

Corollary 4.2. *Suppose $a_{s,r}$ is the channel gain of the source-best-relay link and $a_{r,d}$ is the channel gain of the best-relay-destination link. Let $g(t)$ be any function that is continuous at $t = t_0$ and satisfies $g(t) \to 0$ as $t \to t_0$. Given $0 \le \alpha < g(t)$, then*

$$\Pr(|a_{s,r}|^2 > g(t), |a_{r,d}|^2 + \alpha < g(t)) \sim \Pr(|a_{s,r}|^2 > g(t)) \times \Pr(|a_{r,d}|^2 + \alpha < g(t)) \quad (4.45)$$

Proof. The LHS of (4.45) can be rewritten as

$$\begin{aligned} & \Pr(|a_{s,r}|^2 > g(t), |a_{r,d}|^2 + \alpha < g(t)) \\ = & \sum_{k=1}^{L} \Pr(|a_{s,k}|^2 > g(t), |a_{k,d}|^2 + \alpha < g(t), |a_{k,d}|^2 > V) \\ \sim & \sum_{k=1}^{L} \int_0^{g(t)-\alpha} (\sigma_{s,r}^{-2} + \sigma_{r,d}^{-2})^{L-1} y^{L-1} \exp(-\sigma_{s,r}^{-2} g(t)) f_Y(y) dy \\ \sim & \sigma_{r,d}^{-2} (\sigma_{s,r}^{-2} + \sigma_{r,d}^{-2})^{L-1} (g(t)-\alpha)^L \end{aligned} \quad (4.46)$$

where X, Y and V are variables defined in the proof of Theorem 4.1. Further, based on Theorem 4.1, the RHS of (4.45) equals

$$\Pr(|a_{s,r}|^2 > g(t)) \times \Pr(|a_{r,d}|^2 + \alpha < g(t)) \sim \sigma_{r,d}^{-2} (\sigma_{s,r}^{-2} + \sigma_{r,d}^{-2})^{L-1} (g(t)-\alpha)^L \quad (4.47)$$

and thus the corollary is proved. □

Proof of Theorem 4.2. We apply a similar strategy as in [10] and try to derive the upper and lower bounds of $\Pr(r_\epsilon < h(\epsilon))$. To obtain the lower bound, we let $v = |a_{s,r}|^2$ and $w = |a_{r,d}|^2$. Then,

$$\begin{aligned}\Pr(r_\epsilon < h(\epsilon)) &= \Pr(1/v + 1/w + \epsilon/vw > 1/h(\epsilon)) \\ &> \Pr(1/v + 1/w > 1/h(\epsilon)) \\ &\geq \Pr(\max\{1/v, 1/w\} > 1/h(\epsilon)) \\ &= \Pr(\min\{v, w\} < h(\epsilon)) \\ &\sim (\sigma_{s,r}^{-2} + \sigma_{r,d}^{-2})^L h^L(\epsilon)\end{aligned}$$

in which the final step is derived using the same technique as in the proof of Theorem 1. To find the upper bound, we set two constants α and β with the conditions $1 \gg \alpha > 0$ and $\beta \gg 1$. Then,

$$\begin{aligned}&\Pr(r_\epsilon < h(\epsilon)) \\ \leq\ & \Pr(v < (1+\alpha)h(\epsilon)) + \Pr\left((1+\alpha)h(\epsilon) \leq v \leq \beta h(\epsilon), w < \frac{1+\epsilon/v}{1/h(\epsilon) - 1/v}\right) \\ &+ \Pr\left(\beta h(\epsilon) < v, w < \frac{1+\epsilon/v}{1/h(\epsilon) - 1/v}\right) \\ \sim\ & \sigma_{s,r}^{-2}(\sigma_{s,r}^{-2} + \sigma_{r,d}^{-2})^{L-1}(1+\alpha)^L h^L(\epsilon) \\ &+ \mathcal{O}(h^{L+1}(\epsilon)) + \sigma_{r,d}^{-2}(\sigma_{s,r}^{-2} + \sigma_{r,d}^{-2})^{L-1}\left(\frac{1+\epsilon/\beta h(\epsilon)}{1-1/\beta}\right)^L h^L(\epsilon)\end{aligned}$$

in which the last step is deduced by using the same methods as in Theorem 1 and Corollary 2. Since α and β are arbitrary, we take the limits $\alpha \to 0$ and $\beta \to \infty$ and the above upper bound is readily shown equal to the lower bound. Thus, the asymptotic probability equals to the bounds and the theorem is proved. □

Corollary 4.3. *Let $\epsilon > 0$ and $r_\epsilon = \epsilon f(v/\epsilon, w/\epsilon)$ where $v = |a_{s,r}|^2$ and $w = |a_{r,d}|^2$. Let $h(\epsilon)$ be any positive function continuous at $\epsilon = 0$ and $\lim_{\epsilon\to 0} \epsilon/h(\epsilon) = d < \infty$. Then,*

$$\lim_{\epsilon\to 0} \frac{1}{h^L(\epsilon)} \Pr(r_\epsilon < h(\epsilon), v < h(\epsilon)) = \sigma_{s,r}^{-2}(\sigma_{s,r}^{-2} + \sigma_{r,d}^{-2})^{L-1}. \tag{4.48}$$

Proof. Since $v < h(\epsilon) \Rightarrow r_\epsilon < h(\epsilon)$, $\Pr(r_\epsilon < h(\epsilon), v < h(\epsilon)) = \Pr\left(v < h(\epsilon)\right)$. Finally, we can apply (4.43) to complete the proof. $\square$

Chapter 5

Performance Analysis of Opportunistic Amplify-and-Forward Protocol with Maxmin Selection Criterion

Recall that, depending on how the relay amplifies the received signals, the amplify-and-forward (AF) protocol can be further categorized into channel-state-information-assisted (CSI-assisted) AF [10] and fixed-gain AF [71]. Particularly, it is called a fixed-gain AF protocol if the relay amplifies the received signal with a constant gain, which is a function of the expectation of the power of received signals. Since the received signal power at the relay is time-varying due to channel fading, the transmission power of the relay node is not constant for the fixed-gain AF relaying. In contrast, when operating in the CSI-assisted AF mode, the relay amplifies the received signal with a time-varying gain which is a function of the received signal power. Under such a mode of operation, the role of the time-varying gain function is to maintain a constant transmission power of the relay node.

Both the decode-and-forward (DF) and AF protocols have been studied for single-relay cooperative networks over various fading channels. The performance of single-relay DF networks have been extensively evaluated in terms of asymptotic outage probability [10], exact outage probability [23] and exact symbol error rate [20, 91]. In contrast, the analytic outage performance expression of single-relay CSI-assisted AF networks is difficult, if not impossible, to obtain because of the existence of the $(\bar{\gamma}^2 xy)/(\bar{\gamma}x + \bar{\gamma}y + 1)$ term, in which $\bar{\gamma}$ represents the SNR without fading distortion, and x and y are the powers of two independent channel fading coefficients, which are generally modeled as random variables (RVs) with Rayleigh, or Nakagami-m distributions. Some studies have approximated $(\bar{\gamma}^2 xy)/(\bar{\gamma}x + \bar{\gamma}y + 1)$ by $(\bar{\gamma}^2 xy)/(\bar{\gamma}x + \bar{\gamma}y)$ when evaluating the outage performance [68, 69] and the asymptotic outage performance [10, 79] of single-relay CSI-assisted AF networks.

When there are multiple relays available, opportunistic relaying is an efficient and simple relaying protocol as described in Chap. 4. In opportunistic relaying protocols, a distributed algorithm is run among the relays to determine which relay should be active. More specifically, at the transmission of each information frame (e.g., a codeword or a block of multiple codewords), the relay with the highest metric is selected as the opportunistic relay and participates in the relaying process while the other relays keep idle. The asymptotic outage performance has been studied for opportunistic DF (ODF) networks [43], and for opportunistic AF (OAF) networks [46, 49, 79, 92]. Moreover, the exact outage performance of ODF networks has been derived [93]. For the opportunistic network employing fixed-gain AF, the explicit expression of the outage probability has been found [46]. Yet, to the best of our knowledge, the exact analytical performance of opportunistic CSI-assisted AF networks using a maximal-ratio-combining (MRC) receiver at the destination has not been reported.

In this chapter, we focus on the performance analysis of the CSI-assisted OAF systems using an MRC receiver at the destination and employing the maxmin selection. We derive the upper and lower bounds of the outage probability, the ergodic achievable rate, and the average symbol error rate when the relaying systems employ M-PSK modulation. We then run Monte Carlo simulations to verify these derived bounds.

5.1 System Model

Consider a cooperative communication system with L (≥ 1) relays. Assume that the channel-state-information-assisted opportunistic amplify-and-forward (CSI-assisted OAF) relaying protocol is employed and that an MRC receiver is used at the destination. As shown in Fig. 4.1, let $a_{i,j} \sim \mathcal{CN}(0, \sigma_{i,j}^2)$ be the channel gain between Node i and Node j, and it is assumed that $a_{i,j}$'s are independent of one another. We also assume that the channel characteristics between the source and each of the relays are identical, i.e., $\sigma_{s,1}^2 = \sigma_{s,2}^2 = \cdots = \sigma_{s,L}^2 \triangleq \sigma_{s,r}^2$. Similarly, the channel characteristics between each of the relays and the destination are assumed to be the same, i.e., $\sigma_{1,d}^2 = \sigma_{2,d}^2 = \cdots = \sigma_{L,d}^2 \triangleq \sigma_{r,d}^2$. With the maxmin best-relay selection criterion, the opportunistic relay r will be chosen if $r = \mathrm{argmax}_l\{\min(|a_{s,l}|^2, |a_{l,d}|^2)\}$. Also, the selection algorithm is distributed and runs once for every transmission unit. In the following analysis, unless otherwise stated, $a_{s,r}$ and $a_{r,d}$ represent the corresponding source-best-relay gain and best-relay-destination gain, respectively.

Let the transmission powers of both the source and the opportunistic relay be P, and define $\bar{\gamma} := P/N_0$, where N_0 denotes the noise power spectral density at the receiving sides of the L relays and at the destination node. The instantaneous mutual information for the CSI-assisted OAF protocol, denoted by I_{OAF}, is given by

$$I_{\mathrm{OAF}} = \frac{1}{2}\log(1 + \bar{\gamma}|a_{s,d}|^2 + f(\bar{\gamma}|a_{s,r}|^2, \bar{\gamma}|a_{r,d}|^2)), \tag{5.1}$$

where $f(x,y) = (xy)/(x+y+1)$. To further facilitate our analysis, we define the following symbols: $\eta_1 = \sigma_{s,d}^{-2}$, $\eta_2 = \sigma_{s,r}^{-2}$, $\eta_3 = \sigma_{r,d}^{-2}$, $\lambda = \eta_2 + \eta_3$. Moreover, we use $\binom{n}{i} = \frac{n!}{(n-i)!i!}$ to represent the binomial coefficient. For simplicity of notation, OAF refers to CSI-assisted OAF in the following analysis, unless mentioned otherwise.

5.2 Performance Bounds of OAF

We study the performance of OAF in terms of outage probability, ergodic achievable rate and average SER under the M-ary phase-shift-key (M-PSK) modulation scheme.

5.2.1 Outage probability

When the relaying channel suffers slow (quasi-static) fading, in which the time duration of each transmission is much less than the channel coherence time [4], given the required transmission rate $\mathtt{R}$ during single time slot, an outage occurs if $I_{\text{OAF}} < \mathtt{R}/2$. To evaluate the outage probability of the OAF protocol, we use the following theorem.

Theorem 5.1. *Define the RV $T = f(\bar{\gamma}|a_{s,r}|^2, \bar{\gamma}|a_{r,d}|^2)$. Then the cdf of T, i.e., $F_T(t)$, is bounded as follows*

$$\begin{aligned} F_T(t) \;\leq\; & L\left[e^{-\lambda\frac{t}{\bar{\gamma}}} - \frac{2\sqrt{t^2+t}\sqrt{\eta_2\eta_3}}{\bar{\gamma}}e^{-\frac{\lambda t}{\bar{\gamma}}}K_1\left(\frac{2\sqrt{t^2+t}\sqrt{\eta_2\eta_3}}{\bar{\gamma}}\right)\right] \\ & \qquad\qquad \times (1-e^{-\lambda\frac{2t}{\bar{\gamma}}})^{L-1} + (1-e^{-\lambda\frac{t}{\bar{\gamma}}})^L \\ & + L\left[\frac{2t\sqrt{\eta_2\eta_3}}{\bar{\gamma}}e^{-\frac{\lambda t}{\bar{\gamma}}}K_1(\frac{2t\sqrt{\eta_2\eta_3}}{\bar{\gamma}}) - \frac{2\sqrt{t^2+t}\sqrt{\eta_2\eta_3}}{\bar{\gamma}}e^{-\frac{\lambda t}{\bar{\gamma}}}K_1(\frac{2\sqrt{t^2+t}\sqrt{\eta_2\eta_3}}{\bar{\gamma}})\right] \\ & \qquad\qquad \times \left[(1-e^{-\lambda\frac{(\sqrt{1/t+1}-1)^{-1}}{\bar{\gamma}}})^{L-1} - (1-e^{-\lambda\frac{2t}{\bar{\gamma}}})^{L-1}\right] \end{aligned} \tag{5.2}$$

$$\begin{aligned} F_T(t) \;\geq\; & L\left[e^{-\lambda\frac{t}{\bar{\gamma}}} - \frac{2\sqrt{t^2+t}\sqrt{\eta_2\eta_3}}{\bar{\gamma}}e^{-\frac{\lambda t}{\bar{\gamma}}}K_1\left(\frac{2\sqrt{t^2+t}\sqrt{\eta_2\eta_3}}{\bar{\gamma}}\right)\right](1-e^{-\lambda\frac{t}{\bar{\gamma}}})^{L-1} \\ & \qquad\qquad + (1-e^{-\lambda\frac{t}{\bar{\gamma}}})^L \end{aligned} \tag{5.3}$$

with $K_1(\cdot)$ *being the first order* modified Bessel function *of the second kind [73].*

Proof. The detailed proof is presented in Appendix 5.A. $\square$

Using (5.1), the outage probability, i.e., $\Pr(I_{\mathrm{OAF}} < \mathtt{R}/2)$, can be expressed as

$$\mathrm{E}[\Pr(T < 2^{\mathtt{R}} - 1 - \bar{\gamma}X | X = x)] \tag{5.4}$$

where $\mathrm{E}[\cdot]$ denotes the expectation and $X = |a_{s,d}|^2$. Hence,

$$\Pr(I_{\mathrm{OAF}} < \mathtt{R}/2) = \int_0^{\frac{2^{\mathtt{R}}-1}{\bar{\gamma}}} F_T(2^{\mathtt{R}} - 1 - \bar{\gamma}x) f_X(x) \mathrm{d}x \tag{5.5}$$

where $f_X(x)$ represents the pdf of X. Applying (5.2) to the above equation, we obtain the upper bound of $\Pr(I_{\mathrm{OAF}} < \mathtt{R}/2)$ as

$$\begin{aligned} P_{\mathrm{out,OAF,upper}} &= L \sum_{i=0}^{L-1} (-1)^i \binom{L-1}{i} \Bigg[\zeta((2i+1)\lambda) + \frac{\eta_1}{\bar{\gamma}} \exp(-\eta_1 \frac{2^{\mathtt{R}} - 1}{\bar{\gamma}}) \times \\ & \int_0^{2^{\mathtt{R}}-1} \Bigg[\frac{2y\sqrt{\eta_2\eta_3}}{\bar{\gamma}} K_1(\frac{2y\sqrt{\eta_2\eta_3}}{\bar{\gamma}})(e^{-\frac{\lambda}{\bar{\gamma}}(i(\sqrt{1/y+1}-1)^{-1}+y)} - e^{-\frac{\lambda}{\bar{\gamma}}(y(2i+1))}) \\ & - \frac{2\sqrt{y^2+y}\sqrt{\eta_2\eta_3}}{\bar{\gamma}} K_1\left(\frac{2\sqrt{y^2+y}\sqrt{\eta_2\eta_3}}{\bar{\gamma}}\right) e^{-\frac{\lambda}{\bar{\gamma}}(i(\sqrt{1/y+1}-1)^{-1}+y)} \Bigg] e^{\frac{\eta_1}{\bar{\gamma}}y} \mathrm{d}y \Bigg] \\ & + \sum_{i=0}^{L} (-1)^i \binom{L}{i} \zeta(i\lambda) \end{aligned} \tag{5.6}$$

where

$$\begin{aligned} \zeta(\kappa) &= \int_0^{\frac{2^{\mathtt{R}}-1}{\bar{\gamma}}} \exp\left(-\kappa \frac{2^{\mathtt{R}} - 1 - \bar{\gamma}x}{\bar{\gamma}}\right) f_X(x) dx \\ &= \begin{cases} \frac{\eta_1(2^{\mathtt{R}}-1)}{\bar{\gamma}} \exp(-\frac{\eta_1(2^{\mathtt{R}}-1)}{\bar{\gamma}}) & \text{for} \quad \kappa = \eta_1 \\ \frac{\eta_1}{\kappa-\eta_1} [\exp(-\frac{\eta_1(2^{\mathtt{R}}-1)}{\bar{\gamma}}) - \exp(-\frac{\kappa}{\bar{\gamma}}(2^{\mathtt{R}} - 1))] & \text{for} \quad \kappa \neq \eta_1. \end{cases} \end{aligned} \tag{5.7}$$

Furthermore, based on (5.3), the lower bound of $\Pr(I_{\mathrm{OAF}} < \mathtt{R}/2)$ is obtained as

$$\begin{aligned} P_{\mathrm{out,OAF,lower}} &= L\sum_{i=0}^{L-1}(-1)^i\binom{L-1}{i}\Bigg[\zeta((i+1)\lambda)-\frac{\eta_1}{\bar\gamma}\exp(-\eta_1\frac{2^{\mathtt{R}}-1}{\bar\gamma})\times \\ &\quad \int_0^{2^{\mathtt{R}}-1}\frac{2\sqrt{y^2+y}\sqrt{\eta_2\eta_3}}{\bar\gamma}K_1\left(\frac{2\sqrt{y^2+y}\sqrt{\eta_2\eta_3}}{\bar\gamma}\right)e^{-\frac{\lambda}{\bar\gamma}(i+1)y}e^{\frac{\eta_1}{\bar\gamma}y}\mathrm{d}y\Bigg] \\ &\quad +\sum_{i=0}^{L}(-1)^i\binom{L}{i}\zeta(i\lambda) \end{aligned} \tag{5.8}$$

As x goes to zero, it can be proved that $1-xK_1(x)$ converges to zero faster than $1-\exp(-x)$. Moreover, we have

$$\begin{aligned} &\frac{2t\sqrt{\eta_2\eta_3}}{\bar\gamma}K_1(\frac{2t\sqrt{\eta_2\eta_3}}{\bar\gamma})-\frac{2\sqrt{t^2+t}\sqrt{\eta_2\eta_3}}{\bar\gamma}K_1(\frac{2\sqrt{t^2+t}\sqrt{\eta_2\eta_3}}{\bar\gamma}) \\ &\qquad < 1-\frac{2\sqrt{t^2+t}\sqrt{\eta_2\eta_3}}{\bar\gamma}K_1(\frac{2\sqrt{t^2+t}\sqrt{\eta_2\eta_3}}{\bar\gamma}). \end{aligned} \tag{5.9}$$

Using the above two properties, we can readily show that the bounds of $F_T(t)$, given by (5.2) and (5.3), are both dominated by the term $(1-e^{-\lambda\frac{t}{\bar\gamma}})^L$ when $\bar\gamma$ is large. In consequence, both the outage-probability bounds (5.6) and (5.8) are determined by $\sum_{i=0}^{L}(-1)^i\binom{L}{i}\zeta(i\lambda)$. Finally, it can be easily proved that $\sum_{i=0}^{L}(-1)^i\binom{L}{i}\zeta(i\lambda)$ asymptotically equals $\eta_1\lambda^L\frac{g^{L+1}(\bar\gamma)}{L+1}$ as $\bar\gamma$ increases. Since both bounds converge to $\eta_1\lambda^L\frac{g^{L+1}(\bar\gamma)}{L+1}$, the outage probability will also converge to the same value, i.e.,

$$P_{\mathrm{out,OAF}} \sim \eta_1\lambda^L\frac{g^{L+1}(\bar\gamma)}{L+1}, \tag{5.10}$$

producing in the same result as given in [79].

In the analysis of the single-relay AF networks, $f(\bar\gamma|a_{s,r}|^2,\bar\gamma|a_{r,d}|^2)$ has been approximated by $(\bar\gamma|a_{s,r}|^2\cdot\bar\gamma|a_{r,d}|^2)/(\bar\gamma|a_{s,r}|^2+\bar\gamma|a_{r,d}|^2)$ in [68,69]. The approximation is tight when $\bar\gamma$ is large. In the following, we employ the approximation to study the outage performance of the opportunistic relaying system.

Theorem 5.2. *Define the RV* $\widetilde{T}=(\bar\gamma|a_{s,r}|^2\cdot\bar\gamma|a_{r,d}|^2)/(\bar\gamma|a_{s,r}|^2+\bar\gamma|a_{r,d}|^2)$*. Then the* *cdf of $\widetilde{T}$, i.e., $F_{\widetilde{T}}(\widetilde{t})$ is bounded by*

$$F_{\widetilde{T}}(\widetilde{t}) \leq L(e^{-\lambda\frac{\tilde{t}}{\bar{\gamma}}} - \frac{2\tilde{t}\sqrt{\eta_2\eta_3}}{\bar{\gamma}}e^{-\frac{\lambda\tilde{t}}{\bar{\gamma}}}K_1(\frac{2\tilde{t}\sqrt{\eta_2\eta_3}}{\bar{\gamma}})) \times (1-e^{-\lambda\frac{2\tilde{t}}{\bar{\gamma}}})^{L-1} + (1-e^{-\lambda\frac{\tilde{t}}{\bar{\gamma}}})^L \tag{5.11}$$

$$F_{\widetilde{T}}(\widetilde{t}) \geq L(e^{-\lambda\frac{\tilde{t}}{\bar{\gamma}}} - \frac{2\tilde{t}\sqrt{\eta_2\eta_3}}{\bar{\gamma}}e^{-\frac{\lambda\tilde{t}}{\bar{\gamma}}}K_1(\frac{2\tilde{t}\sqrt{\eta_2\eta_3}}{\bar{\gamma}})) \times (1-e^{-\lambda\frac{\tilde{t}}{\bar{\gamma}}})^{L-1} + (1-e^{-\lambda\frac{\tilde{t}}{\bar{\gamma}}})^L. \tag{5.12}$$

Proof. Appendix 5.B outlines the proof. □

Consequently, using the same technique that derives (5.6) and (5.8), the bounds of the approximated outage probability ($\tilde{P}_{\text{out,OAF}} = \mathrm{E}[\Pr(\widetilde{T} < 2^{\mathtt{R}} - 1 - \bar{\gamma}X|X=x)]$) can be shown equal to

$$\tilde{P}_{\text{out,OAF,upper}} = L\sum_{i=0}^{L-1}(-1)^i\binom{L-1}{i}\Bigg[\zeta((2i+1)\lambda) - \frac{\eta_1}{\bar{\gamma}}\exp(-\eta_1\frac{2^{\mathtt{R}}-1}{\bar{\gamma}})\times \int_0^{2^{\mathtt{R}}-1}\frac{2\tilde{y}\sqrt{\eta_2\eta_3}}{\bar{\gamma}}K_1\left(\frac{2\tilde{y}\sqrt{\eta_2\eta_3}}{\bar{\gamma}}\right)e^{-\frac{\lambda}{\bar{\gamma}}(2i+1)\tilde{y}}e^{\frac{\eta_1}{\bar{\gamma}}\tilde{y}}\mathrm{d}\tilde{y}\Bigg] + \sum_{i=0}^{L}(-1)^i\binom{L}{i}\zeta(i\lambda) \tag{5.13}$$

$$\tilde{P}_{\text{out,OAF,lower}} = L\sum_{i=0}^{L-1}(-1)^i\binom{L-1}{i}\Bigg[\zeta((i+1)\lambda) - \frac{\eta_1}{\bar{\gamma}}\exp(-\eta_1\frac{2^{\mathtt{R}}-1}{\bar{\gamma}})\times \int_0^{2^{\mathtt{R}}-1}\frac{2\tilde{y}\sqrt{\eta_2\eta_3}}{\bar{\gamma}}K_1\left(\frac{2\tilde{y}\sqrt{\eta_2\eta_3}}{\bar{\gamma}}\right)e^{-\frac{\lambda}{\bar{\gamma}}(i+1)\tilde{y}}e^{\frac{\eta_1}{\bar{\gamma}}\tilde{y}}\mathrm{d}\tilde{y}\Bigg] + \sum_{i=0}^{L}(-1)^i\binom{L}{i}\zeta(i\lambda). \tag{5.14}$$

Similar to the previous case, it can be readily shown that the bounds of $F_{\widetilde{T}}(\widetilde{t})$ given by (5.11) and (5.12) are both dominated by the term $(1-e^{-\lambda\frac{\tilde{t}}{\rho}})^L$ when $\bar{\gamma}$ is large. Consequently, the bounds in (5.13) and (5.14) are determined by $\sum_{i=0}^{L}(-1)^i\binom{L}{i}\zeta(i\lambda)$, which asymptotically equals $\eta_1\lambda^L\frac{g^{L+1}(\bar{\gamma})}{L+1}$ as $\bar{\gamma}$ increases. Thus, $\tilde{\mathrm{P}}^{\text{out}}_{\text{OAF}}$ converges to the same expression shown in (5.10), i.e.,

$$\tilde{\mathrm{P}}^{\text{out}}_{\text{OAF}} \sim \eta_1\lambda^L\frac{g^{L+1}(\bar{\gamma})}{L+1}. \tag{5.15}$$

5.2.2 Ergodic achievable rate

When the opportunistic relay channel suffers block/fast fading, in which the time duration of each transmission is much larger than the channel coherence time, the ergodic achievable rate, defined as the expectation of the mutual information per channel use, is a more appropriate channel measure [4].

Let the RVs

$$\begin{aligned} X &= |a_{s,d}|^2 && (5.16) \\ Y &= \log(1+\bar{\gamma}|a_{s,d}|^2 + f(\bar{\gamma}|a_{s,r}|^2, \bar{\gamma}|a_{r,d}|^2)) \\ &= \log(1+\bar{\gamma}X+T). && (5.17) \end{aligned}$$

Then the ergodic achievable rate of the OAF protocol, denoted by R_{OAF}, is given by $R_{\mathrm{OAF}} = \frac{1}{2}\mathrm{E}[Y]$. The conditional expectation of Y given $X = x$ is therefore

$$\begin{aligned} \mathrm{E}[Y|x] &= \int_0^\infty [1-\Pr(Y<y|X=x)]\mathrm{d}y \\ &= \log_2(1+\bar{\gamma}x) + \int_{\log_2(1+\bar{\gamma}x)}^\infty [1-\Pr(Y<y|X=x)]\mathrm{d}y. && (5.18) \end{aligned}$$

Since $\Pr(Y<y|X=x) = F_T(2^y-1-\bar{\gamma}x)$, we have

$$\mathrm{E}[Y|x] = \log_2(1+\bar{\gamma}x) + \int_{\log_2(1+\bar{\gamma}x)}^\infty [1-F_T(2^y-1-\bar{\gamma}x)]\mathrm{d}y. \quad (5.19)$$

Further, averaging $\mathrm{E}[Y|x]$ over x with $f_X(x) = \eta_1\exp(-\eta_1 x)$, we obtain the expectation of Y as

$$\mathrm{E}[Y] = \int_0^\infty \mathrm{E}[Y|x]f_X(x)\mathrm{d}x = \frac{1}{\ln 2}\xi(\eta_1) + \int_0^\infty \int_{\log_2(1+\bar{\gamma}x)}^\infty [1-F_T(2^y-1-\bar{\gamma}x)]\mathrm{d}y f_X(x)\mathrm{d}x, \quad (5.20)$$

where

$$\xi(\eta_1) = \int_0^\infty f_X(x)\ln(1+\bar{\gamma}x)\mathrm{d}x = \exp(\frac{\eta_1}{\bar{\gamma}})\mathrm{Ei}(\frac{\eta_1}{\bar{\gamma}}) \tag{5.21}$$

is derived from the fact (cf. [73, (4.337.2)])

$$\int_0^\infty \exp(-\mu x)\ln(1+\beta x)\mathrm{d}x = \frac{1}{\mu}\exp(\frac{\mu}{\beta})\mathrm{Ei}(\frac{\mu}{\beta}) \tag{5.22}$$

where $\mathrm{Ei}(x) = \int_x^\infty \exp(-t)t^{-1}\mathrm{d}t$ is the *Exponential integral function.*

Applying (5.2) and (5.3) to (5.20), the lower and upper bounds of the ergodic achievable rate can be derived as

$$\begin{aligned} R_{\mathrm{OAF,lower}} &= \frac{1}{2\ln 2}\xi(\eta_1) - \frac{1}{2}L\sum_{i=0}^{L-1}(-1)^i\binom{L-1}{i}\Bigg[\varphi((2i+1)\lambda) + \frac{\eta_1}{\bar{\gamma}\ln 2}\times \\ &\int_0^\infty \Bigg[\frac{2y\sqrt{\eta_2\eta_3}}{\bar{\gamma}}K_1(\frac{2y\sqrt{\eta_2\eta_3}}{\bar{\gamma}})(e^{-\frac{\lambda}{\bar{\gamma}}(i(\sqrt{1/y+1}-1)^{-1}+y)} - e^{-\frac{\lambda}{\bar{\gamma}}(y(2i+1))}) \\ &\quad -\frac{2\sqrt{y^2+y}\sqrt{\eta_2\eta_3}}{\bar{\gamma}}K_1\left(\frac{2\sqrt{y^2+y}\sqrt{\eta_2\eta_3}}{\bar{\gamma}}\right)e^{-\frac{\lambda}{\bar{\gamma}}(i(\sqrt{1/y+1}-1)^{-1}+y)}\Bigg] \\ &\quad \times e^{\eta_1\frac{y+1}{\bar{\gamma}}}\mathrm{Ei}\left(\eta_1\frac{y+1}{\bar{\gamma}}\right)\mathrm{d}y\Bigg] - \frac{1}{2}\sum_{i=1}^{L}(-1)^i\binom{L}{i}\varphi(i\lambda) \end{aligned} \tag{5.23}$$

$$\begin{aligned} R_{\mathrm{OAF,upper}} &= \frac{1}{2\ln 2}\xi(\eta_1) - \frac{1}{2}L\sum_{i=0}^{L-1}(-1)^i\binom{L-1}{i}\Bigg[\varphi((i+1)\lambda) - \frac{\eta_1}{\bar{\gamma}\ln 2}\times \\ &\int_0^\infty \Bigg[\frac{2\sqrt{y^2+y}\sqrt{\eta_2\eta_3}}{\bar{\gamma}}K_1\left(\frac{2\sqrt{y^2+y}\sqrt{\eta_2\eta_3}}{\bar{\gamma}}\right)e^{-\frac{\lambda}{\bar{\gamma}}((i+1)y)}\Bigg] \\ &\quad \times e^{\eta_1\frac{y+1}{\bar{\gamma}}}\mathrm{Ei}\left(\eta_1\frac{y+1}{\bar{\gamma}}\right)\mathrm{d}y\Bigg] - \frac{1}{2}\sum_{i=1}^{L}(-1)^i\binom{L}{i}\varphi(i\lambda), \end{aligned} \tag{5.24}$$

where

$$\begin{aligned} \varphi(\kappa) &= \int_0^\infty\int_0^\infty \exp(-\kappa(1+\bar{\gamma}x)\frac{2^y-1}{\bar{\gamma}})\mathrm{d}y f_X(x)\mathrm{d}x \\ &= \begin{cases} \frac{1-\frac{\eta_1}{\bar{\gamma}}\xi(\eta_1)}{\ln 2}, & \text{for} \quad \kappa = \eta_1 \\ \frac{\eta_1}{(\kappa-\eta_1)\ln 2}\xi(\eta_1) + \frac{\eta_1}{(\eta_1-\kappa)\ln 2}\xi(\kappa), & \text{o.w.} \end{cases} \end{aligned} \tag{5.25}$$

is derived from the fact $\int_0^\infty \frac{\exp(-\mu x)}{x+\beta}\mathrm{d}x = \exp(\mu\beta)\mathrm{Ei}(\mu\beta)$ (cf. [73, (3.352.4)]).

5.2.3 Average symbol error probability

Assume that the OAF protocol uses M-PSK modulation. The symbol error rate (SER) for general M-PSK systems over AWGN channel can be accurately approximated by[74, p.231]

$$P_{\text{ser}} \approx 2Q(\sqrt{2A_M\mathrm{SNR}}) \tag{5.26}$$

where SNR is the signal-to-noise ratio per symbol, $Q(\cdot)$ is the Q-function ([74, p.84]) and $A_M = \sin^2\frac{\pi}{M}$. Based on (5.26), the average SER of the OAF protocol can be readily shown equal to

$$P_{\text{ser,OAF}} = \frac{2}{\pi}\int_0^{\pi/2} \frac{\eta_1}{\frac{\bar{\gamma}A_M}{\sin^2\theta}+\eta_1}\mathrm{E}\left[\exp(-\frac{A_M}{\sin^2\theta}f(\bar{\gamma}|a_{s,r}|^2, \bar{\gamma}|a_{r,d}|^2))\right]\mathrm{d}\theta. \tag{5.27}$$

Applying $T = f(\bar{\gamma}|a_{s,r}|^2, \bar{\gamma}|a_{r,d}|^2))$ and (6), we obtain

$$\begin{aligned}
&\mathrm{E}\left[\exp(-\frac{A_M}{\sin^2\theta}T)\right] = \frac{A_M}{\sin^2\theta}\int_0^\infty \exp(-\frac{A_M}{\sin^2\theta}t)F_T(t)\mathrm{d}t \\
\geq\ & \frac{A_M}{\sin^2\theta}\left[L\sum_{i=0}^{L-1}(-1)^i\binom{L-1}{i}\left(\frac{1}{\frac{A_M}{\sin^2\theta}+\lambda(i+1)/\bar{\gamma}}\right.\right. \\
&\left. - \int_0^\infty \exp(-\frac{A_M}{\sin^2\theta}t)\frac{2\sqrt{t^2+t}\sqrt{\eta_2\eta_3}}{\bar{\gamma}}e^{-\frac{(i+1)\lambda t}{\bar{\gamma}}}K_1(\frac{2\sqrt{t^2+t}\sqrt{\eta_2\eta_3}}{\bar{\gamma}})\mathrm{d}t\right) \\
&\left. + \sum_{i=0}^{L}(-1)^i\binom{L}{i}\frac{1}{\frac{A_M}{\sin^2\theta}+\lambda i/\bar{\gamma}}\right].
\end{aligned} \tag{5.28}$$

Substituting (5.28) into (5.27), the lower bound of the average SER can be found as

$$\begin{aligned}
P_{\text{ser,OAF,lower}} &= \frac{2L}{\pi}\sum_{i=0}^{L-1}(-1)^i\binom{L-1}{i}\left(\Lambda_1(A_M, \eta_1/\bar{\gamma}, \lambda(i+1)/\bar{\gamma}) - \frac{\pi}{2}\sqrt{\frac{A_M\eta_1^2}{\bar{\gamma}(\bar{\gamma}A_M+\eta_1)}}\right. \\
&\left.\times\int_0^\infty \exp(\frac{\eta_1 t}{\rho})\mathrm{erfc}(\sqrt{\frac{(\bar{\gamma}A_M+\eta_1)t}{\bar{\gamma}}})\frac{2\sqrt{t^2+t}\sqrt{\eta_2\eta_3}}{\bar{\gamma}}e^{-\frac{(i+1)\lambda t}{\bar{\gamma}}}K_1(\frac{2\sqrt{t^2+t}\sqrt{\eta_2\eta_3}}{\bar{\gamma}})\mathrm{d}t\right)
\end{aligned}$$

$$+\frac{2}{\pi}\sum_{i=0}^{L}(-1)^i\binom{L}{i}\Lambda_1(A_M,\eta_1/\bar{\gamma},\lambda i/\bar{\gamma}). \tag{5.29}$$

In arriving at (5.29), we have applied

$$\int_0^{\pi/2}\tfrac{1}{a+b\sin^2\theta}\exp(-\tfrac{c}{\sin^2\theta})\mathrm{d}\theta=\tfrac{\pi}{2\sqrt{a(a+b)}}\exp(\tfrac{bc}{a})\mathrm{erfc}(\sqrt{\tfrac{(a+b)c}{a}}) \tag{5.30}$$

derived from [73, (3.363.1) and (3.361.2)]; and

$$\begin{aligned}\Lambda_1(B,x,y)&=\int_0^{\pi/2}\left(\frac{x}{\frac{B}{\sin^2\theta}+x}\right)\left(\frac{B}{\sin^2\theta}\right)\left(\frac{1}{\frac{B}{\sin^2\theta}+y}\right)\mathrm{d}\theta\\&=\begin{cases}\frac{\pi}{4}\sqrt{\frac{B/x}{(1+B/x)^3}}, & \text{for}\quad x=y\\ \frac{\pi}{2}\left(\sqrt{\frac{B/y}{1+B/y}}-\sqrt{\frac{B/x}{1+B/x}}\right)\frac{x}{x-y}, & \text{for}\quad x\neq y\end{cases}\end{aligned} \tag{5.31}$$

derived from $\int_0^{\pi/2}\sin^2 t/(\sin^2 t+c)\mathrm{d}t=\pi(1-\sqrt{c/(1+c)})/2$ [74, (5A.9)].

Using a similar technique and based on (5.8), the upper bound of the average SER can be shown equal to

$$\begin{aligned}P_{\mathrm{ser,OAF,upper}} &= \frac{2L}{\pi}\sum_{i=0}^{L-1}(-1)^i\binom{L-1}{i}\Bigg(\Lambda_1(A_M,\eta_1/\bar{\gamma},\lambda(i+1)/\bar{\gamma})+\frac{\pi}{2}\sqrt{\frac{A_M\eta_1^2}{\bar{\gamma}(\bar{\gamma}A_M+\eta_1)}}\\&\times\int_0^{\infty}\exp(\frac{\eta_1 t}{\rho})\mathrm{erfc}(\sqrt{\frac{(\bar{\gamma}A_M+\eta_1)t}{\bar{\gamma}}})\Bigg[\frac{2t\sqrt{\eta_2\eta_3}}{\bar{\gamma}}K_1(\frac{2t\sqrt{\eta_2\eta_3}}{\bar{\gamma}})\\&\times(e^{-\frac{\lambda}{\bar{\gamma}}(i(\sqrt{1/t+1}-1)^{-1}+t)}-e^{-\frac{\lambda}{\bar{\gamma}}(t(2i+1))})\\&-\frac{2\sqrt{t^2+t}\sqrt{\eta_2\eta_3}}{\bar{\gamma}}K_1(\frac{2\sqrt{t^2+t}\sqrt{\eta_2\eta_3}}{\bar{\gamma}})e^{-\frac{\lambda}{\bar{\gamma}}(i(\sqrt{1/t+1}-1)^{-1}+t)}\Bigg]\mathrm{d}t\Bigg)\\&+\frac{2}{\pi}\sum_{i=0}^{L}(-1)^i\binom{L}{i}\Lambda_1(A_M,\eta_1/\bar{\gamma},\lambda i/\bar{\gamma}).\end{aligned} \tag{5.32}$$

As explained in Sect. 5.2.1, the bounds of $F_T(t)$ are both dominated by the term $(1-e^{-\lambda\frac{t}{\bar{\gamma}}})^L$ when $\bar{\gamma}$ is large. Using such a property, it can be shown further that the average SER bounds given by (5.29) and (5.32) are both dominated by $\frac{2}{\pi}\sum_{i=0}^{L}(-1)^i\binom{L}{i}\Lambda_1(A_M,\eta_1/\bar{\gamma},\lambda i/\bar{\gamma})$, which equals $\frac{\eta_1}{\lambda(L+1)}(\frac{\lambda}{2A_M\bar{\gamma}})^{L+1}\prod_{i=0}^{L}(2i+1)$ asymptotically as $\bar{\gamma}$ increases. Therefore, the asymptotic performance of the average SER

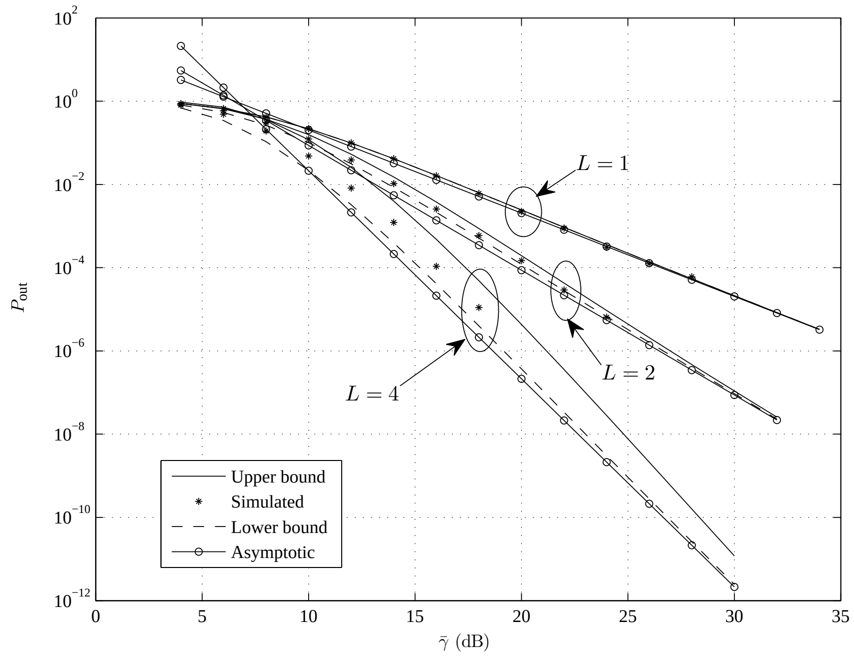

Figure 5.1: Comparison of the simulation results, the asymptotic results, and the upper and lower bounds for the outage performance of a CSI-assisted OAF system with $\mathtt{R} = 0.4$, $\eta_1 = 20$, $\eta_2 = 0.2\eta_1$, $\eta_3 = 0.8\eta_1$ and $L = 1, 2, 4$.

is given by

$$\bar{P}_{\text{OAF}}^{\texttt{SER}} \sim \frac{\eta_1}{\lambda(L+1)} \left(\frac{\lambda}{2A_M \bar{\gamma}} \right)^{L+1} \prod_{i=0}^{L} (2i+1). \tag{5.33}$$

5.3 Simulation Results

First, we study a CSI-assisted OAF system employing an MRC receiver at the destination with the parameters $\mathtt{R} = 0.4$, $\eta_1 = 20$, $\eta_2 = 0.2\eta_1$, $\eta_3 = 0.8\eta_1$ and $L = 1, 2, 4$. Figure 5.1 plots the simulated outage probability, the asymptotic curve calculated from (5.10), and the upper and lower bounds calculated using (5.6) and (5.8), respectively. The results clearly show that the analytical upper and lower bounds can accurately predict the range of the simulated outage probabilities. We also observe that the range becomes wider as L increases from 1 to 2, and then to

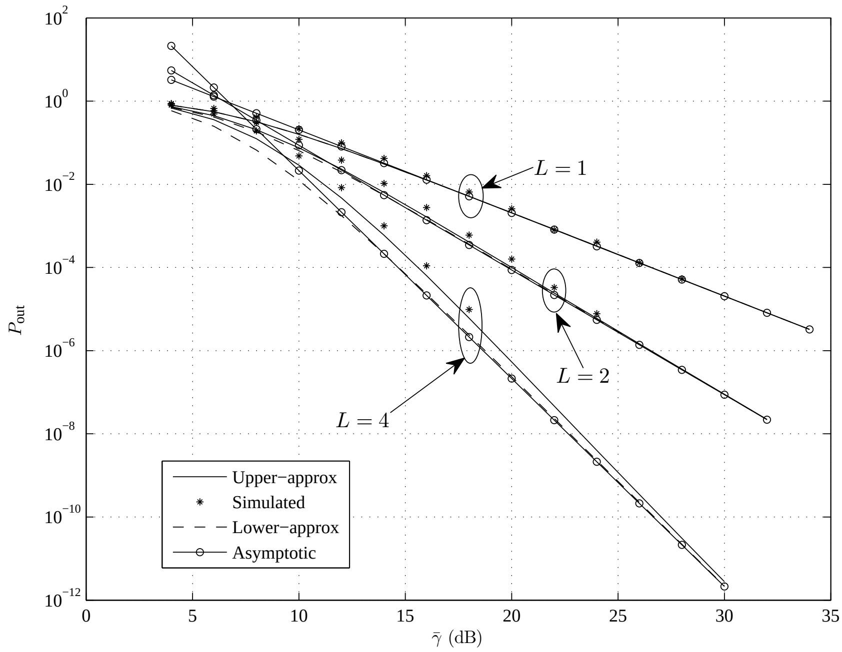

Figure 5.2: Comparison of the simulation results, the asymptotic results, and the upper and lower bounds obtained by approximating $f(\bar{\gamma}a_{s,r}, \bar{\gamma}a_{r,d})$ by $(\bar{\gamma}a_{s,r} \cdot \bar{\gamma}a_{r,d})/(\bar{\gamma}a_{s,r} + \bar{\gamma}a_{r,d})$ for the outage probability of a CSI-assisted OAF system with $\mathtt{R} = 0.4$, $\eta_1 = 20$, $\eta_2 = 0.2\eta_1$, $\eta_3 = 0.8\eta_1$ and $L = 1, 2, 4$.

4. Moreover, the upper bound and the lower bound for each individual case merge with the asymptotic curve as SNR increases. The observation is in line with our derivation in Sect. 5.2.1 that the diversity gain of the OAF protocol equals $L + 1$. In Fig. 5.2, we compare the simulated outage performance with the approximated upper and lower bounds given by (5.13) and (5.14), in which $f(\bar{\gamma}|a_{s,r}|^2, \bar{\gamma}|a_{r,d}|^2)$ is approximated by $(\bar{\gamma}|a_{s,r}|^2 \cdot \bar{\gamma}|a_{r,d}|^2)/(\bar{\gamma}|a_{s,r}|^2 + \bar{\gamma}|a_{r,d}|^2)$. For the case $L = 1$, the approximated upper bound and the approximated lower bounds are identical (as can be seen from (5.13) and (5.14), or equivalently (5.11) and (5.12)) and hence the curves overlap exactly in the figure. Moreover, the simulated results are mostly close to the approximated bounds. But for the cases $L = 2$ and $L = 4$, it is obvious that the simulated results are larger than the approximated upper bounds. In other words, the approximated bounds under-estimate the outage probability.

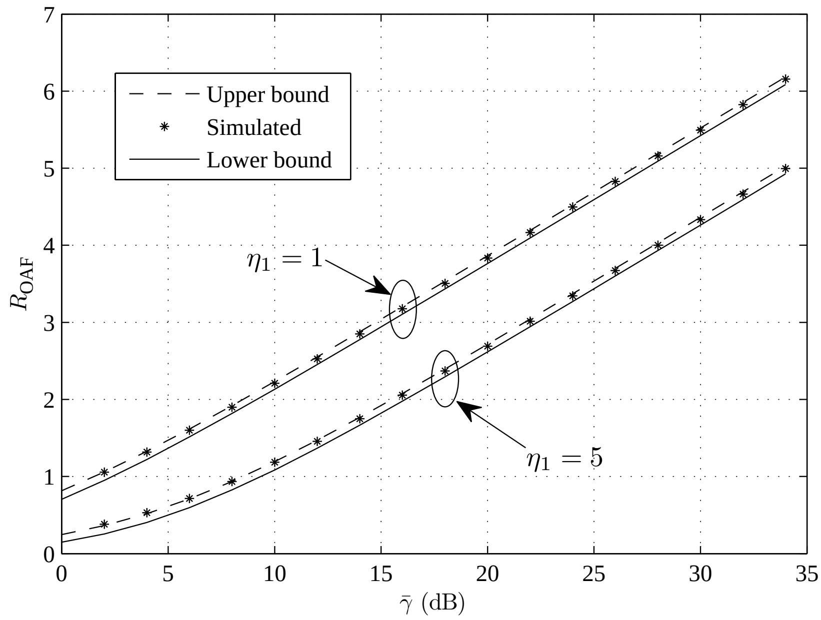

Figure 5.3: Comparison of the simulation results, the upper and lower bounds for the ergodic achievable rate of a CSI-assisted OAF system with $L = 4$, $\eta_1 = 1, 5$, $\eta_2 = 0.2\eta_1$, and $\eta_3 = 0.9\eta_1$.

Fig. 5.3 plots the ergodic achievable rate for the OAF protocol with parameters $L = 4$, $\eta_1 = 1$ and 5, $\eta_2 = 0.2\eta_1$ and $\eta_3 = 0.9\eta_1$. The curves show that the upper bound and the lower bound, given by (5.24) and (5.23), respectively, are very close. Even so, they can contain the simulated results. We also note that the ergodic achievable rate decreases as η_1 increases from 1 to 5. When η_1 is larger, it implies more severe fading, resulting in a lower ergodic achievable rate.

Finally, we examine the average SER for the opportunistic relaying systems using M-ary PSK modulation scheme. In Fig. 5.4, we plot the simulated results as well as the bounds (given by (5.32) and (5.29)) and the asymptotic results (given by (5.33)) for the system employing 4-ary PSK with $L = 2, 4$, $\eta_1 = 10$, $\eta_2 = 0.4\eta_1$ and $\eta_3 = 0.9\eta_1$. We can observe that the simulated results are well contained within the upper bound and the lower bound.

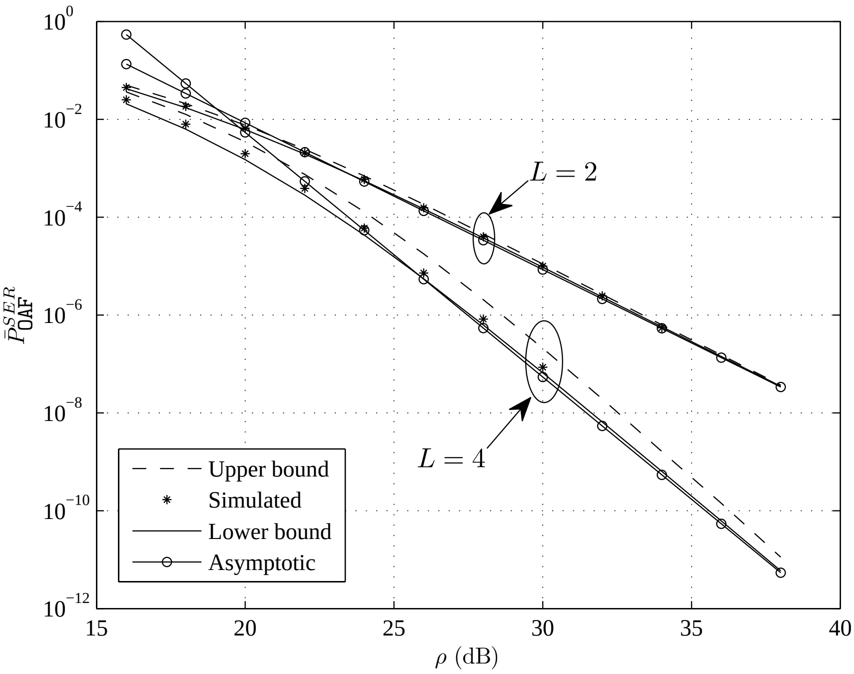

Figure 5.4: Comparison of the simulation results and the lower bound for the average SER performance of a CSI-assisted OAF system employing 4-ary PSK modulation with $L = 2, 4$, $\eta_1 = 10$, $\eta_2 = 0.4\eta_1$, and $\eta_3 = 0.9\eta_1$.

5.4 Summary

In this chapter, we have studied an opportunistic cooperative communication system that employs CSI-assisted AF relaying protocols and an MRC receiver at the destination. We have derived expressions for the upper and lower bounds for the outage probability, ergodic achievable rate and average SER of M-PSK, which are further verified by simulated results. The technique developed here can be extended to analyze multiple-relay systems under dissimilar fading, and also to the case when the energy fairness among the relays are taken into consideration [92]. In the next chapter, we will investigate two-way relaying systems.

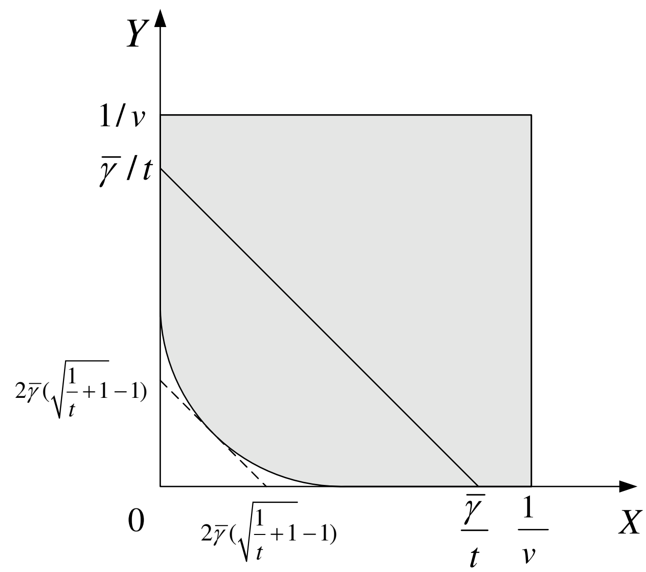

Figure 5.5: The grey region represents the integral area for $T = f(\bar{\gamma}|a_{s,r}|^2, \bar{\gamma}|a_{r,d}|^2)$ when $0 < v < \frac{t}{\bar{\gamma}}$.

Appendix 5.A

Recall $|a_{s,i}|^2$ and $|a_{i,d}|^2$ are independent exponential RVs. It is clear that $\min(|a_{s,i}|^2, |a_{i,d}|^2)$ for $(i = 1, 2, \ldots, L)$ are independent, identical exponential RVs with parameter $(\sigma_{s,r}^{-2} + \sigma_{r,d}^{-2})$. Suppose that the lth relay is chosen as the "best" relay, i.e., $a_{s,r} = a_{s,l}$ and $a_{r,d} = a_{l,d}$. Consider the "second best" relay and let the RV $V = \max\{\min(|a_{s,i}|^2, |a_{i,d}|^2) : i = 1, ..., L; i \neq l\}$. Then, for any $v > 0$

$$F_V(v) = \Pr(V < v) = \Pr\left(\cap_{i\neq l}^{L}[\min(|a_{s,i}|^2, |a_{i,d}|^2) < v]\right) = (1 - \exp(-\lambda v))^{L-1}. \tag{5.34}$$

Let $X = \frac{1}{|a_{s,l}|^2}$ and $Y = \frac{1}{|a_{l,d}|^2}$. Then the conditional cdf of T is given by

$$F_T(t|l, V = v) = \Pr(X + Y + \frac{1}{\bar{\gamma}}XY > \frac{\bar{\gamma}}{t}, X < V^{-1}, Y < V^{-1}). \tag{5.35}$$

When $0 < v < \frac{t}{\bar{\gamma}}$, as in Fig. 5.5, we have

$$F_T(t|l,v) = e^{-\lambda v} - \frac{2\sqrt{t^2+t}\sqrt{\eta_2\eta_3}}{\bar{\gamma}} e^{-\frac{\lambda t}{\bar{\gamma}}} K_1(\frac{2\sqrt{t^2+t}\sqrt{\eta_2\eta_3}}{\bar{\gamma}}) \tag{5.36}$$

After integrating over $0 < v < \frac{t}{\bar{\gamma}}$, we get

$$\begin{aligned} F_T(t|l, 0 < v < \frac{t}{\bar{\gamma}}) &= [e^{-\lambda \frac{t}{\bar{\gamma}}} - \frac{2\sqrt{t^2+t}\sqrt{\eta_2\eta_3}}{\bar{\gamma}} e^{-\frac{\lambda t}{\bar{\gamma}}} K_1(\frac{2\sqrt{t^2+t}\sqrt{\eta_2\eta_3}}{\bar{\gamma}})](1-e^{-\lambda\frac{t}{\bar{\gamma}}})^{L-1} \\ &\quad + \frac{1}{L}(1-e^{-\lambda\frac{t}{\bar{\gamma}}})^L. \end{aligned} \tag{5.37}$$

Similarly, when $\frac{t}{\bar{\gamma}} < v < \frac{2t}{\bar{\gamma}}$, it can be shown that

$$\begin{aligned} F_T(t|l, \frac{t}{\bar{\gamma}} < v < \frac{2t}{\bar{\gamma}}) &\leq [e^{-\lambda \frac{t}{\bar{\gamma}}} - \frac{2\sqrt{t^2+t}\sqrt{\eta_2\eta_3}}{\bar{\gamma}} e^{-\frac{\lambda t}{\bar{\gamma}}} K_1(\frac{2\sqrt{t^2+t}\sqrt{\eta_2\eta_3}}{\bar{\gamma}})] \\ &\quad \times [(1-e^{-\lambda\frac{2t}{\bar{\gamma}}})^{L-1} - (1-e^{-\lambda\frac{t}{\bar{\gamma}}})^{L-1}]. \end{aligned} \tag{5.38}$$

On the other hand, apparently, one lower bound is $F_T(t|l, \frac{t}{\bar{\gamma}} < v < \frac{2t}{\bar{\gamma}}) \geq 0$. Finally, when $\frac{2t}{\bar{\gamma}} < v < (\sqrt{1/t+1}-1)^{-1}/\bar{\gamma}$, it can be readily proved that

$$\begin{aligned} 0 &\leq F_T(t|l, \frac{2t}{\bar{\gamma}} < v < (\sqrt{1/t+1}-1)^{-1}/\bar{\gamma}) \\ &\leq [\frac{2t\sqrt{\eta_2\eta_3}}{\bar{\gamma}} e^{-\frac{\lambda t}{\bar{\gamma}}} K_1(\frac{2t\sqrt{\eta_2\eta_3}}{\bar{\gamma}}) - \frac{2\sqrt{t^2+t}\sqrt{\eta_2\eta_3}}{\bar{\gamma}} e^{-\frac{\lambda t}{\bar{\gamma}}} K_1(\frac{2\sqrt{t^2+t}\sqrt{\eta_2\eta_3}}{\bar{\gamma}})] \\ &\quad \times [(1-e^{-\lambda\frac{h(t)}{\bar{\gamma}}})^{L-1} - (1-e^{-\lambda\frac{2t}{\bar{\gamma}}})^{L-1}] \end{aligned} \tag{5.39}$$

where $h(t) = (\sqrt{1/t+1}-1)^{-1}$. Integrating $F_T(t|l,V)$ over V, i.e., combining the aforementioned cases, we have a pair of bounds for $F_T(t|l)$. By recognizing that $F_T(t|l)$ are the same for all $l \in \{1, \cdots, L\}$, we have $F_T(t) = LF_T(t|l)$ and we obtain the upper bound and lower bound of $F_T(t)$ shown in (5.2) and (5.3), respectively.

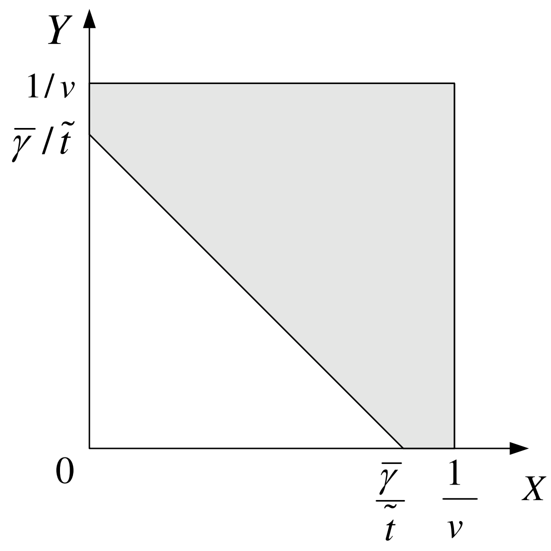

Figure 5.6: The grey region represents the integral area for $\widetilde{T} = (\bar{\gamma}|a_{s,r}|^2 \cdot \bar{\gamma}|a_{r,d}|^2)/(\bar{\gamma}|a_{s,r}|^2 + \bar{\gamma}|a_{r,d}|^2)$ when $0 < v < \frac{\tilde{t}}{\bar{\gamma}}$.

Appendix 5.B

Using the same notations as in Appendix 5.A, the cdf of $\widetilde{T}$ conditioned on l and V equals

$$\begin{aligned} F_{\widetilde{T}}(\tilde{t}|l, V) &= \Pr\left(\frac{1}{|a_{s,l}|^2} + \frac{1}{|a_{l,d}|^2} > \frac{\bar{\gamma}}{\tilde{t}}, |a_{s,l}|^2 > V, |a_{l,d}|^2 > V\right) \\ &= \Pr\left(X + Y > \frac{\bar{\gamma}}{\tilde{t}}, X < V^{-1}, Y < V^{-1}\right). \end{aligned} \tag{5.40}$$

To integrate the conditional cdf over V, we consider the following cases. When $0 < v < \frac{\tilde{t}}{\bar{\gamma}}$, as in Fig. 5.6, we have

$$F_{\widetilde{T}}(\tilde{t}|l, V = v) = e^{-\lambda v} - \frac{2\tilde{t}\sqrt{\eta_2\eta_3}}{\bar{\gamma}} e^{-\frac{\lambda\tilde{t}}{\bar{\gamma}}} K_1\left(\frac{2\tilde{t}\sqrt{\eta_2\eta_3}}{\bar{\gamma}}\right). \tag{5.41}$$

By integrating $F_{\widetilde{T}}(\tilde{t}|l, V)$ over $0 < v < \frac{\tilde{t}}{\bar{\gamma}}$, we obtain

$$\begin{aligned} F_{\widetilde{T}}(\tilde{t}|l, 0 < v < \frac{\tilde{t}}{\bar{\gamma}}) &= \left(e^{-\lambda\frac{\tilde{t}}{\bar{\gamma}}} - \frac{2\tilde{t}\sqrt{\eta_2\eta_3}}{\bar{\gamma}} e^{-\frac{\lambda\tilde{t}}{\bar{\gamma}}} K_1\left(\frac{2\tilde{t}\sqrt{\eta_2\eta_3}}{\bar{\gamma}}\right)\right)\left(1 - e^{-\lambda\frac{\tilde{t}}{\bar{\gamma}}}\right)^{L-1} \\ &\quad + \frac{1}{L}\left(1 - e^{-\lambda\frac{\tilde{t}}{\bar{\gamma}}}\right)^{L}. \end{aligned} \tag{5.42}$$

When $\frac{\tilde{t}}{\bar{\gamma}} < v < \frac{2\tilde{t}}{\bar{\gamma}}$, using the same technique as in the proof of Theorem 5.1, it can be readily shown that

$$\begin{aligned} F_{\widetilde{T}}(\tilde{t}|l, \frac{\tilde{t}}{\bar{\gamma}} < v < \frac{2\tilde{t}}{\bar{\gamma}}) \;\; &\leq \;\; [e^{-\lambda\frac{\tilde{t}}{\bar{\gamma}}} - \frac{2\tilde{t}\sqrt{\eta_2\eta_3}}{\bar{\gamma}} e^{-\frac{\lambda\tilde{t}}{\bar{\gamma}}} K_1(\frac{2\tilde{t}\sqrt{\eta_2\eta_3}}{\bar{\gamma}})] \\ &\times[(1 - e^{-\lambda\frac{2\tilde{t}}{\bar{\gamma}}})^{L-1} - (1 - e^{-\lambda\frac{\tilde{t}}{\bar{\gamma}}})^{L-1}], \end{aligned} \tag{5.43}$$

and $F_{\widetilde{T}}(\tilde{t}|l, \frac{\tilde{t}}{\bar{\gamma}} < v < \frac{2\tilde{t}}{\bar{\gamma}}) \geq 0$. Combining the above results, we have a pair of bounds of $F_{\widetilde{T}}(\tilde{t}|l)$. Since $F_{\widetilde{T}}(\tilde{t}|l)$ are the same for all $l \in \{1, \cdots, L\}$, suggesting $F_{\widetilde{T}}(\tilde{t}) = LF_{\widetilde{T}}(\tilde{t}|l)$, $F_{\widetilde{T}}(\tilde{t})$ is therefore upper-bounded and lower-bounded, respectively, by (5.11) and (5.12).

Chapter 6

Two-Way Relaying Systems

With an aim to integrating the benefits of relaying and network coding have been integrated, distributed space-time coding (STC) with modular network coding for two-way relaying systems has been proposed and referred to as the "partial decode-and-forward II (PDF II)" scheme [66]. To reflect the relaying strategy more precisely, in this thesis, we name such an relaying scheme as the "fully-distributed space-time two-way relaying (FDST-TR)" scheme. In the FDST-TR scheme, the two-way relaying is fulfilled in two time slots. In the first time slot, two sources broadcast their information frames to the common relays simultaneously. In the second time slot, some relays are selected to perform distributed STC and modular network coding, and the resulted signals are then broadcasted back to the two source nodes. It has been shown that the FDST-TR scheme can achieve the full diversity order if the number of symbols in a frame is no less than the number of relays. Furthermore, in order to achieve the optimal performance, the space-time codewords transmitted from different relays have to be orthogonal.

In this chapter, we propose a new two-way relaying protocol, namely opportunistic two-way relaying (O-TR) method, which is based on modular network coding and opportunistic relay selection. In the proposed O-TR protocol, no distributed

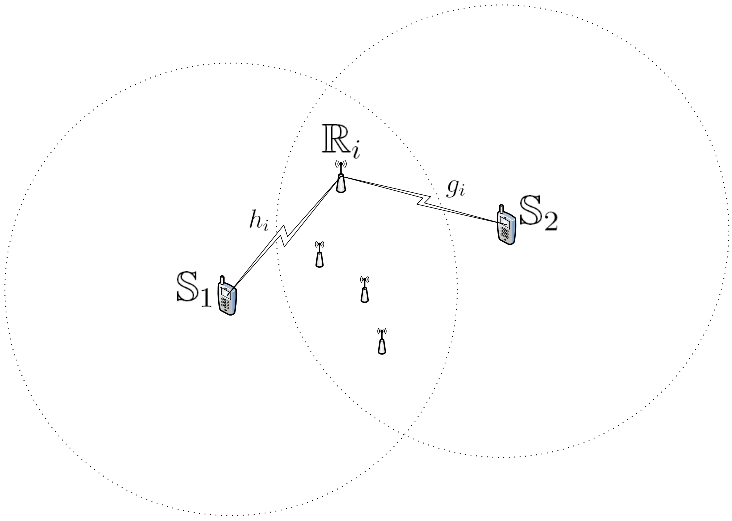

Figure 6.1: The system model of a multi-relay system with two sources and two-way communications.

space-time coding is needed. Therefore, the requirement that each relay should be assigned an orthogonal precoding matrix is removed. Instead of selecting a number of relays as in distributed space-time coding, the proposed O-TR protocol selects only one active relay to perform the network coding on the decoded symbols sent by the two sources and to forward the network-coded symbols back to the two sources. The decoding at the sources is also made simpler. Moreover, the proposed protocol imposes no restriction on the frame length, which results in a more flexible frame design at the sources. We will further show by analysis that the proposed O-TR protocol accomplishes the full diversity, and we compare the frame error error (FER) of the O-TR scheme with that of the FDST-TR method by simulations.

6.1 Two-Way Relaying with Decode-and-Forward Protocol

In this section, we briefly review the distributed space-time coded DF relaying strategy proposed in [66]. We consider the two-way relay network shown in Fig. 6.1, where

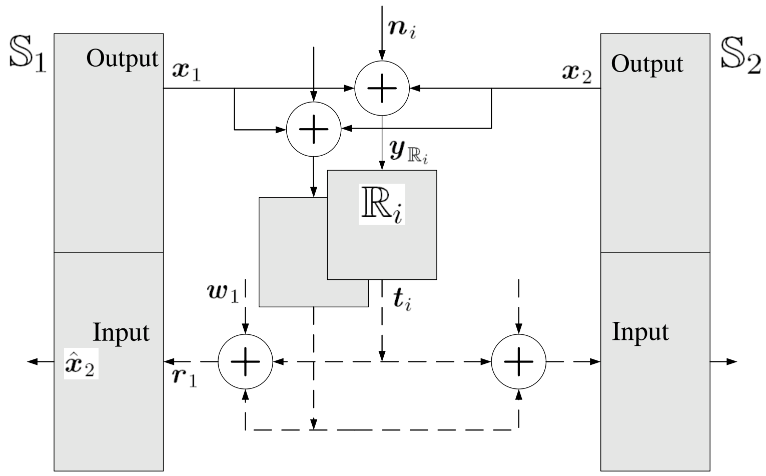

Figure 6.2: The block diagram of a two-way communications using FDST-TR.

two source nodes $\mathbb{S}_1$ and $\mathbb{S}_2$ exchange their information with the help of L relay nodes $\mathbb{R}_i$ $(i = 1, \cdots, L)$. We assume that all the relays are within the transmission ranges of both $\mathbb{S}_1$ and $\mathbb{S}_2$, but there is no direct link connecting $\mathbb{S}_1$ and $\mathbb{S}_2$. The link between $\mathbb{S}_1$ and $\mathbb{R}_i$ is characterized by the channel coefficient h_i, which accounts for the channel fading impairment and is modeled as a complex random variable following a complex Gaussian distribution with zero mean and unit variance, i.e., $\mathcal{CN}(0, 1)$. Meanwhile, the channel coefficient of the $\mathbb{S}_2$-to-$\mathbb{R}_i$ link is denoted by g_i which also follows a $\mathcal{CN}(0, 1)$ distribution.

We concentrate on a cooperative communication system in which both $\mathbb{S}_1$ and $\mathbb{S}_2$ employ the same modulation scheme and map each symbol to a corresponding energy-normalized signal $x \in \mathcal{X}$. We assume that the cardinality of the constellation $|\mathcal{X}| = M$, and that each transmission frame consists of N symbols. Also, we denote the minimum distance of the M-ary signal constellation by $d_{\min}$. In each transmission-time unit, $\mathbb{S}_1$ and $\mathbb{S}_2$ will exchange one frame of N symbols, which is fulfilled in two equal-duration time slots. Specifically, in the first time slot, $\mathbb{S}_1$ and $\mathbb{S}_2$ broadcast their signal frames $\boldsymbol{x}_1 = [x_1(1), \cdots, x_1(N)]^T$ and $\boldsymbol{x}_2 = [x_2(1), \cdots, x_2(N)]^T$, with powers P_1 and P_2, respectively, to all the relays at the same time, as shown in Fig. 6.2. At the ith relay, we denote the received signal frame by $\boldsymbol{y}_{\mathbb{R}_i} = [y_{\mathbb{R}_i}(1), \cdots, y_{\mathbb{R}_i}(N)]^T$. Then, $\boldsymbol{y}_{\mathbb{R}_i}$ is given by

$$\boldsymbol{y}_{\mathbb{R}_i} = \sqrt{P_1} h_i \boldsymbol{x}_1 + \sqrt{P_2} g_i \boldsymbol{x}_2 + \boldsymbol{n}_i \tag{6.1}$$

where $\boldsymbol{n}_i \in \mathcal{C}^N$ is a signal vector consisting of independent complex Gaussian noises with zero mean and variance N_0. In the second time slot, the relays process their received signal frames from both $\mathbb{S}_1$ and $\mathbb{S}_2$ and broadcast a new signal frame back to $\mathbb{S}_1$ and $\mathbb{S}_2$. Finally, $\mathbb{S}_1$ and $\mathbb{S}_2$ decode the sent symbols from its counterpart based on the received new signal frame.

In the FDST-TR protocol, the ith relay ($i = 1, \ldots, L$) will decode the received signal frame $\boldsymbol{y}_{\mathbb{R}_i}$ using a generalized sphere decoder [85]. The detection method is expressed by

$$[\hat{\boldsymbol{x}}_1^i, \hat{\boldsymbol{x}}_2^i] = \underset{[\boldsymbol{s}_1, \boldsymbol{s}_2]: \boldsymbol{s}_1, \boldsymbol{s}_2 \in \mathcal{X}^N}{\operatorname{argmin}} \parallel \boldsymbol{y}_{\mathbb{R}_i} - (\sqrt{P_1} h_i \boldsymbol{s}_1 + \sqrt{P_2} g_i \boldsymbol{s}_2) \parallel_2^2 \tag{6.2}$$

or simply

$$[\hat{x}_1^i(t), \hat{x}_2^i(t)] = \underset{[s_1, s_2]: s_1, s_2 \in \mathcal{X}}{\operatorname{argmin}} |y_{\mathbb{R}_i}(t) - (\sqrt{P_1} h_i s_1 + \sqrt{P_2} g_i s_2)|^2 \quad \text{for} \quad t = 1, 2, \ldots, N \tag{6.3}$$

where $\hat{\boldsymbol{x}}_1^i = [\hat{x}_1^i(1), \cdots, \hat{x}_1^i(N)]^T$ and $\hat{\boldsymbol{x}}_2^i = [\hat{x}_2^i(1), \cdots, \hat{x}_2^i(N)]^T$ are the decoded signal frames of $\boldsymbol{x}_1$ and $\boldsymbol{x}_2$, respectively. Afterwards, the ith relay will combine the two decoded signal frames into one frame by using modular network coding. The detailed modular network coding is presented as follows.

Recall that $M = |\mathcal{X}|$ is the cardinality of the signal constellation $\mathcal{X}$. Let $\mathcal{M} = \{0, 1, \ldots, M-1\}$ be a set containing M symbols. Define $\mathcal{A} : \mathcal{M} \mapsto \mathcal{X}$ as a one-to-one mapping with $\mathcal{A}(j) = x_j \in \mathcal{X}$ and $j \in \mathcal{M}$. For a vector $\boldsymbol{v}$ in which each element is a member of $\mathcal{M}$, $\mathcal{A}$ will map $\boldsymbol{v}$ on an element-by-element basis onto $\mathcal{X}$.

Denote the inverse mapping of $\mathcal{A}$ by $\mathcal{A}^{-1}$, which is also a one-to-one mapping. We can then map the decoded signal frames $\hat{\boldsymbol{x}}_1^i$ and $\hat{\boldsymbol{x}}_2^i$ to the decoded symbol vectors, which we denote by $\boldsymbol{v}_1^i$ and $\boldsymbol{v}_2^i$, respectively. Therefore, we have $\boldsymbol{v}_1^i = \mathcal{A}^{-1}(\hat{\boldsymbol{x}}_1^i)$ and $\boldsymbol{v}_2^i = \mathcal{A}^{-1}(\hat{\boldsymbol{x}}_2^i)$. Then the ith relay will determine whether the decoded symbol vectors satisfy the following equation:

$$\text{mod}\{\boldsymbol{v}_1^i + \boldsymbol{v}_2^i, M\} = \text{mod}\{\boldsymbol{v}_1 + \boldsymbol{v}_2, M\} \tag{6.4}$$

where $\boldsymbol{v}_1 = \mathcal{A}^{-1}(\boldsymbol{x}_1)$, $\boldsymbol{v}_2 = \mathcal{A}^{-1}(\boldsymbol{x}_2)$ and $\text{mod}\{\boldsymbol{x}, M\}$ denotes the modulo-M operation performing on each element in the vector $\boldsymbol{x}$. If the equation is satisfied, the ith relay is called a *successful relay* [1]. A successful relay will further linearly transform the networked-coded signal vector, i.e., $\mathcal{A}(\text{mod}\{\boldsymbol{v}_1^i + \boldsymbol{v}_2^i, M\})$, with a matrix $\boldsymbol{A}_i$ to obtain $\boldsymbol{t}_i$, i.e.,

$$\boldsymbol{t}_i = \sqrt{P_r}\boldsymbol{A}_i\mathcal{A}(\text{mod}\{\boldsymbol{v}_1^i + \boldsymbol{v}_2^i, M\}) \tag{6.5}$$

where P_r is the transmission power of each relay. Then, $\boldsymbol{t}_i$ is broadcasted back to the two source nodes.

The received signal vector at $\mathbb{S}_1$ is then given by

$$\boldsymbol{r}_1 = \sum_{k\in\mathcal{K}} h_k\boldsymbol{t}_k + \boldsymbol{w}_1 = \sum_{k\in\mathcal{K}} \sqrt{P_r}h_k\boldsymbol{A}_k\mathcal{A}(\text{mod}\{\boldsymbol{v}_1^k + \boldsymbol{v}_2^k, M\}) + \boldsymbol{w}_1 \tag{6.6}$$

where $\mathcal{K}$ is the set of successful relays, and $\boldsymbol{w}_1$ is a vector consisting of N independent complex Gaussian noises with zero mean and variance N_0. Based on $\boldsymbol{r}_1$, $\mathbb{S}_1$ estimates the transmitted signal vector from $\mathbb{S}_2$. Suppose the suboptimal detection method in

[1]Here, we assume that the condition (6.4) can be verified, for instance, by a cyclic-redundancy-check (CRC) error-detection code. If $\boldsymbol{v}_1$ and $\boldsymbol{v}_2$ are binary vectors, i.e., $M = 2$, the XOR between the CRCs of $\boldsymbol{v}_1$ and $\boldsymbol{v}_2$ is exactly the same as the CRC of $\text{mod}\{\boldsymbol{v}_1 + \boldsymbol{v}_2, M\}$ [66]. If $M = 2^r$ where r is an integer, the condition (6.4) can still be verified by mapping the M-ary symbol sequences $\boldsymbol{v}_1$ and $\boldsymbol{v}_2$ to binary vectors before performing a CRC detection. However, we have not considered the actual type of error-detection being used, which is outside the scope of this study. Consequently, the symbols in each frame are considered as independent and identically distributed, and the FER will be evaluated based on the transmitted symbols directly.

[66] is used, the decoded signal vector, denoted by $\hat{\boldsymbol{x}}_2$, will be given by

$$\hat{\boldsymbol{x}}_2 = \underset{\boldsymbol{x}=\mathcal{A}(\boldsymbol{v}_2')}{\operatorname{argmin}} \parallel \boldsymbol{r}_1 - \sum_{k\in\mathcal{K}} \sqrt{P_r} h_k \boldsymbol{A}_k \mathcal{A}(\mathrm{mod}\{\boldsymbol{v}_1 + \boldsymbol{v}_2', M\}) \parallel_2^2 . \tag{6.7}$$

Note that $\boldsymbol{v}_1$ is a function of the transmitted signal vector $\boldsymbol{x}_1$ from $\mathbb{S}_1$, and is therefore known to $\mathbb{S}_1$. With this suboptimal detection method, it has been proved that the FDST-TR relaying method can achieve the full diversity order [66].

However, in order to achieve the full diversity order in the FDST-TR relaying scheme, the frame length N is required to be no less than L. In other words, when L becomes large, the frame length has to be increased accordingly. This reduces the probability that the decoded symbol vectors at the relays meeting the condition (6.4) and hence degrades the system performance. Besides, whenever there is a new relay joining the active transmission, all other relays need to change their linear transformation matrices $\boldsymbol{A}_i$. Furthermore, the synchronization among all relays becomes more and more difficult when L is large.

6.2 Opportunistic Two-Way Relaying (O-TR) Method

To solve the problems inherent to the FDST-TR method, we propose a protocol based on modular network coding and opportunistic relay selection. In the proposed protocol, each relay will check if the modular condition (6.4) is satisfied after decoding the received signal vectors. Among the *successful relays*, only the "best relay" will be selected and will forward a combined signal frame back to the two sources.

Suppose the kth relay is the best relay, which can be selected based on the maxmin criterion, the maximize-harmonic-mean criterion or any other criteria [25, 43, 52, 60]. We further denote the transmitted signal frame from the kth relay by

$\check{\boldsymbol{t}}_k = \sqrt{LP_r}\mathcal{A}(\text{mod}\{\boldsymbol{v}_1^k + \boldsymbol{v}_2^k, M\})$, as shown in Fig. 6.3. Using (6.4), the received signal frame at the source $\mathbb{S}_1$ during the second time slot can be expressed as

$$\begin{aligned} \check{\boldsymbol{r}}_1 = h_k \check{\boldsymbol{t}}_k + \boldsymbol{w}_1 &= \sqrt{LP_r} h_k \mathcal{A}(\text{mod}\{\boldsymbol{v}_1^k + \boldsymbol{v}_2^k, M\}) + \boldsymbol{w}_1 \\ &= \sqrt{LP_r} h_k \mathcal{A}(\text{mod}\{\boldsymbol{v}_1 + \boldsymbol{v}_2, M\}) + \boldsymbol{w}_1. \end{aligned} \tag{6.8}$$

The suboptimal detection method is used and the received signal frame is decoded in favor of

$$\tilde{\boldsymbol{x}}_2 = \underset{\boldsymbol{x}=\mathcal{A}(\tilde{\boldsymbol{v}}_2)}{\text{argmin}} \parallel \check{\boldsymbol{r}}_1 - \sqrt{LP_r} h_k \mathcal{A}(\text{mod}\{\boldsymbol{v}_1 + \tilde{\boldsymbol{v}}_2, M\}) \parallel_2^2 . \tag{6.9}$$

Unlike the detection for the FDST-TR protocol (6.7), the detection for the proposed O-TR protocol (6.9) does not require the summing of different received signal vectors or any matrix transformations. Thus the decoding complexity is lower. Moreover, the average received power at each of the sources is equal to LP_r for the proposed O-TR protocol, and is no less than that for the FDST-TR protocol, which has a value of only KP_r ($L \geq K \geq 1$)). Therefore, intuitively the O-TR protocol should accomplish a better frame error rate (FER) performance than the FDST-TR protocol if the O-TR protocol can achieve the full diversity. In Sect. 6.3, we will further show the results when the average received powers at each of the sources for the proposed O-TR protocol and for the FDST-TR protocol are identical.

In summary, the benefit of the proposed protocol is threefold. Firstly, there is no restriction on the frame length N, which results in a more flexible frame design at the sources $\mathbb{S}_1$ and $\mathbb{S}_2$. Secondly, no distributed-space-time linear transformation is performed at the relays. Therefore, whenever there is a new relay entering the system, the matrix adjustment is not required. Thirdly, the decoding at the sources $\mathbb{S}_1$ and $\mathbb{S}_2$ is made simpler. In the following, we will continue our study by analyzing the upper-bound of the FER and the diversity order of the O-TR protocol.

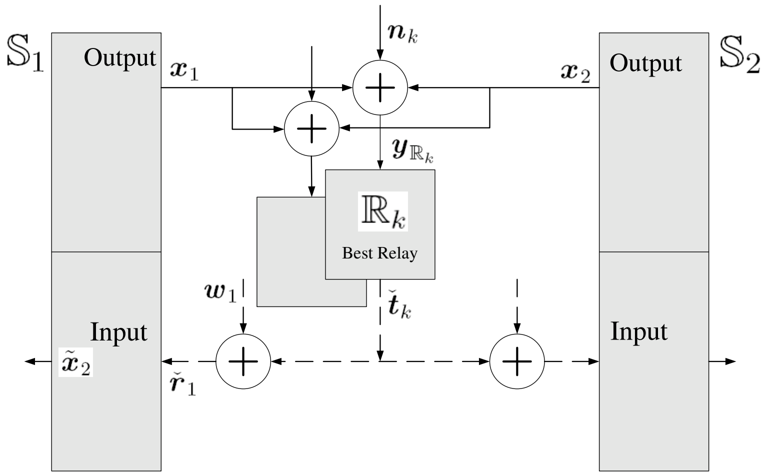

Figure 6.3: The block diagram of a two-way communications using O-TR.

6.2.1 Upper-bound of FER and diversity analysis

For simplicity, we assume that the transmission powers of the sources $\mathbb{S}_1$ and $\mathbb{S}_2$, and of the relays are identical, i.e., $P_1 = P_2 = P_r = P$. We also denote the SNR as $\bar{\gamma} = P/N_0$, where N_0 is the Gaussian noise variance. Furthermore, we will study the scenario when the maxmin criterion is used to select the "best relay" [43, 52]. The approach shown in the following can be applied to cases when another selection criterion is adopted.

6.2.1.1 FER at the relays $\mathbb{R}_i (i = 1, 2, \ldots, L)$

Considering the ith relay $\mathbb{R}_i$, we rewrite the detection equation (6.2) as

$$[\hat{\boldsymbol{x}}_1^i, \hat{\boldsymbol{x}}_2^i] = \underset{[\boldsymbol{s}_1, \boldsymbol{s}_2]: \boldsymbol{s}_1, \boldsymbol{s}_2 \in \mathcal{X}^N}{\operatorname{argmin}} \parallel \boldsymbol{y}_{\mathbb{R}_i} - \sqrt{P}[\boldsymbol{s}_1 \ \boldsymbol{s}_2][h_i \ g_i]^T \parallel_2^2 . \tag{6.10}$$

Recall that the signal frames $\boldsymbol{x}_1$ and $\boldsymbol{x}_2$ are transmitted from $\mathbb{S}_1$ and $\mathbb{S}_2$, respectively. We let $\boldsymbol{X} = [\boldsymbol{x}_1 \ \boldsymbol{x}_2]$ and $\boldsymbol{H} = [h_i \ g_i]^T$. Given that $\boldsymbol{X}$ has been transmitted and the estimation is in favor of a particular $\hat{\boldsymbol{X}} = [\hat{\boldsymbol{x}}_1^i \ \hat{\boldsymbol{x}}_2^i]$, by making use of the method described in Sect. IV of [34], it can be shown that the pairwise error probability

(PEP) is bounded above by the Chernoff bound, i.e.,

$$\begin{aligned}
\Pr\{\hat{\boldsymbol{X}} \neq \boldsymbol{X}|\hat{\boldsymbol{X}}, \boldsymbol{X}\} &\leq \min_{0<\delta<1} \left\{ \mathrm{E}_{h_i, g_i, \boldsymbol{n}_i} \left[e^{\delta(\ln p(\boldsymbol{y}_{\mathbb{R}_i}|\hat{\boldsymbol{X}}) - \ln p(\boldsymbol{y}_{\mathbb{R}_i}|\boldsymbol{X}))} \right] \right\} \\
&= \min_{0<\delta<1} \left\{ \mathrm{E}_{h_i, g_i} \left[e^{-\delta(1-\delta)\bar{\gamma}\boldsymbol{H}^*(\boldsymbol{X}-\hat{\boldsymbol{X}})^*(\boldsymbol{X}-\hat{\boldsymbol{X}})\boldsymbol{H}} \right] \right\} \\
&= \det{}^{-1}(\boldsymbol{I}_2 + \tfrac{\bar{\gamma}}{4}(\boldsymbol{X} - \hat{\boldsymbol{X}})^*(\boldsymbol{X} - \hat{\boldsymbol{X}})) \qquad (6.11)
\end{aligned}$$

where E[$\cdot$] is the expectation operation,

$$p(\boldsymbol{y}_{\mathbb{R}_i}|\tilde{\boldsymbol{X}}) = \tfrac{1}{\pi^{2N} N_0^{2N}} e^{-\frac{(\boldsymbol{y}_{\mathbb{R}_i} - \sqrt{P}\tilde{\boldsymbol{X}}\boldsymbol{H})^*(\boldsymbol{y}_{\mathbb{R}_i} - \sqrt{P}\tilde{\boldsymbol{X}}\boldsymbol{H})}{N_0}} \qquad (6.12)$$

and $\boldsymbol{y}_{\mathbb{R}_i}$ has been defined as in (6.1). Also, $\delta = 1/2$ is chosen to minimize the bound at the last step. Furthermore, applying the analysis that derives (50) in [66] to (6.11), we obtain

$$\Pr\{\hat{\boldsymbol{X}} \neq \boldsymbol{X}|\hat{\boldsymbol{X}}, \boldsymbol{X}\} \leq \tfrac{2}{\bar{\gamma} d_{\min}^2}. \qquad (6.13)$$

(Recall that $d_{\min}$ represents the minimum distance of the M-ary signal constellation.) Finally, considering all the cases where $\hat{\boldsymbol{X}} \neq \boldsymbol{X}$ in (6.13) (there are $(M^{2N} - 1)$ such $\hat{\boldsymbol{X}}$) and applying the union bound, we have

$$\Pr\{\hat{\boldsymbol{X}} \neq \boldsymbol{X}|\boldsymbol{X}\} = \sum_{\hat{\boldsymbol{X}}} \Pr\{\hat{\boldsymbol{X}} \neq \boldsymbol{X}|\hat{\boldsymbol{X}}, \boldsymbol{X}\} \leq \frac{2(M^{2N} - 1)}{\bar{\gamma} d_{\min}^2} \approx \frac{2M^{2N}}{\bar{\gamma} d_{\min}^2}. \qquad (6.14)$$

Consequently, the probability that the modular condition (6.4) is violated, denoted by p_{relay}, is bounded by

$$\begin{aligned}
p_{\text{relay}} &= \Pr\left\{ \mathcal{A}(\text{mod}\{\boldsymbol{v}_1^i + \boldsymbol{v}_2^i, M\}) \neq \mathcal{A}(\text{mod}\{\boldsymbol{v}_1 + \boldsymbol{v}_2, M\}) \right\} \\
&\leq \Pr\{\hat{\boldsymbol{X}} \neq \boldsymbol{X}|\boldsymbol{X}\} \leq \frac{2M^{2N}}{\bar{\gamma} d_{\min}^2}. \qquad (6.15)
\end{aligned}$$

6.2.1.2 FER at the sources $\mathbb{S}_1$ and $\mathbb{S}_2$

Suppose that there are K ($1 \le K \le L$) relays $\{i_1, \ldots, i_K\} \subset \{1, \ldots, L\}$ which can meet the modular condition (6.4). Assume that the maxmin criterion is used to select the "best relay", which is denoted as the i_kth relay. In other words, $i_k = \arg\max_{i \in \{i_1, \cdots, i_K\}}(\min(|h_i|^2, |g_i|^2))$. Furthermore, we define $U = \min(|h_{i_k}|^2, |g_{i_k}|^2)$. Since $|h_{i_1}|^2, \ldots, |h_{i_K}|^2$ and $|g_{i_1}|^2, \ldots, |g_{i_K}|^2$ are independent, identical exponential RVs with parameter $\lambda = 1$, the pdf of U is given [94] by

$$\begin{aligned} f_U(u) &= 2K \exp(-2u)[1 - \exp(-2u)]^{K-1} \\ &= 2K \sum_{k=0}^{K-1} \binom{K-1}{k} (-1)^k \exp(-2(k+1)u). \end{aligned} \tag{6.16}$$

At the sources $\mathbb{S}_1$ and $\mathbb{S}_2$, the signal frame received from the selected relay (i_kth relay) are given by $\sqrt{LP} h_{i_k} \mathcal{A}(\text{mod}\{\boldsymbol{v}_1 + \boldsymbol{v}_2, M\}) + \boldsymbol{w}_1$ and $\sqrt{LP} g_{i_k} \mathcal{A}(\text{mod}\{\boldsymbol{v}_1 + \boldsymbol{v}_2, M\}) + \boldsymbol{w}_2$, respectively, where $\boldsymbol{w}_2$ is a vector consisting of N independent complex Gaussian noises with zero mean and variance N_0. Denote the decoded symbol frame from $\mathbb{S}_2$ at $\mathbb{S}_1$ by $\tilde{\boldsymbol{v}}_2$ and the decoded symbol frame from $\mathbb{S}_1$ at $\mathbb{S}_2$ by $\tilde{\boldsymbol{v}}_1$. Using the decoding mechanism as in (6.9), the average conditional PEP can be shown equal to [66]

$$\begin{aligned} &\Pr\{\tilde{\boldsymbol{v}}_2 \neq \boldsymbol{v}_2 \cup \tilde{\boldsymbol{v}}_1 \neq \boldsymbol{v}_1 | \boldsymbol{v}_1, \boldsymbol{v}_2, \tilde{\boldsymbol{v}}_1, \tilde{\boldsymbol{v}}_2, U = u\} \\ = \;& \tfrac{1}{2} \Pr(\tilde{\boldsymbol{x}}_2 \neq \boldsymbol{x}_2 | \boldsymbol{x}_2, \tilde{\boldsymbol{x}}_2, U = u) + \tfrac{1}{2} \Pr(\tilde{\boldsymbol{x}}_1 \neq \boldsymbol{x}_1 | \boldsymbol{x}_1, \tilde{\boldsymbol{x}}_1, U = u) \\ \le \;& \tfrac{1}{2} [e^{-\frac{L}{4}\bar{\gamma} h_{i_k}^* (\tilde{\boldsymbol{x}}_2 - \boldsymbol{x}_2)^* (\tilde{\boldsymbol{x}}_2 - \boldsymbol{x}_2) h_{i_k}} + e^{-\frac{L}{4}\bar{\gamma} g_{i_k}^* (\tilde{\boldsymbol{x}}_1 - \boldsymbol{x}_1)^* (\tilde{\boldsymbol{x}}_1 - \boldsymbol{x}_1) g_{i_k}}] \\ \le \;& e^{-\frac{L}{4}\bar{\gamma} \min(|h_{i_k}|^2, |g_{i_k}|^2) d_{\min}^2} = e^{-\frac{L}{4}\bar{\gamma} u d_{\min}^2}. \end{aligned} \tag{6.17}$$

Combining the results in (6.16) and (6.17) and applying [73, Eq(3.312.1)], we obtain

$$\Pr\{\tilde{\boldsymbol{v}}_2 \neq \boldsymbol{v}_2 \cup \tilde{\boldsymbol{v}}_1 \neq \boldsymbol{v}_1 | \boldsymbol{v}_1, \boldsymbol{v}_2, \tilde{\boldsymbol{v}}_1, \tilde{\boldsymbol{v}}_2\} \le \int_0^\infty e^{-\frac{L}{4}\bar{\gamma} d_{\min}^2 u} f_U(u) \, \mathrm{d}u$$

$$= \quad K\mathbf{B}(\tfrac{L}{8}\bar{\gamma}d_{\min}^2 + 1, K) \qquad (6.18)$$

where $\mathbf{B}(\cdot,\cdot)$ is the Beta function [73]. Applying the union bound, the FER at $\mathbb{S}_1$ and $\mathbb{S}_2$, given that there are K successful relays, is upper-bounded as follows:

$$\begin{aligned} p_{\text{sources},K} &= \Pr(\tilde{\boldsymbol{v}}_2 \neq \boldsymbol{v}_2 \cup \tilde{\boldsymbol{v}}_1 \neq \boldsymbol{v}_1) \\ &= \sum_{\tilde{\boldsymbol{v}}_1, \tilde{\boldsymbol{v}}_2} \Pr\left\{\tilde{\boldsymbol{v}}_2 \neq \boldsymbol{v}_2 \cup \tilde{\boldsymbol{v}}_1 \neq \boldsymbol{v}_1 | \boldsymbol{v}_1, \boldsymbol{v}_2, \tilde{\boldsymbol{v}}_1, \tilde{\boldsymbol{v}}_2\right\} \\ &\leq M^N K\mathbf{B}(\tfrac{L}{8}\bar{\gamma}d_{\min}^2 + 1, K). \end{aligned} \qquad (6.19)$$

6.2.1.3 Overall system FER and diversity

Finally, the overall average FER of the two-way relaying system, denoted by $\bar{P}_{\text{FER}}$, is bounded by

$$\begin{aligned} \bar{P}_{\text{FER}} &= \sum_{K=0}^{L} \binom{L}{K} p_{\text{sources},K} \times (1 - p_{\text{relay}})^K \times p_{\text{relay}}^{L-K} \\ &\leq \sum_{K=0}^{L} \binom{L}{K} p_{\text{sources},K} \times p_{\text{relay}}^{L-K} \\ &\leq \left(\frac{2M^{2N}}{\bar{\gamma}d_{\min}^2}\right)^L + \sum_{K=1}^{L} \binom{L}{K} M^N K\mathbf{B}(\tfrac{L}{8}\bar{\gamma}d_{\min}^2 + 1, K) \left(\frac{2M^{2N}}{\bar{\gamma}d_{\min}^2}\right)^{L-K} \\ &= \left(\frac{2M^{2N}}{\bar{\gamma}d_{\min}^2}\right)^L + \sum_{K=1}^{L} \binom{L}{K} M^N K \frac{\Gamma(K)}{(\frac{L}{8}\bar{\gamma}d_{\min}^2 + 2)^K} \left(\frac{2M^{2N}}{\bar{\gamma}d_{\min}^2}\right)^{L-K} \\ &\leq M^N(\bar{\gamma}d_{\min}^2)^{-L}(8 + 2M^{2N})^L \end{aligned} \qquad (6.20)$$

where $\Gamma(\cdot)$ is the Gamma function [73]. In deriving the last inequality, we have applied $K\frac{\Gamma(K)}{(\frac{L}{8}\bar{\gamma}d_{\min}^2+2)^K} \leq K\frac{\Gamma(K)}{(\frac{L}{8}\bar{\gamma}d_{\min}^2)^K} \leq (\frac{8}{\bar{\gamma}d_{\min}^2})^K$. The results in (6.20) indicate that the upper bound of the average FER is proportional to $\bar{\gamma}^{-L}$. Thus, we can conclude that our proposed O-TR scheme for the two-way relaying system can achieve the full diversity even without employing distributed space-time coding.

6.2.2 FER analysis for BPSK modulation

In this section, we will study the average FER for the O-TR cooperative system analytically when the binary-phase-shift-keying (BPSK) modulation is used in the signal transmission.

We denote $p_{\mathbb{R}_i|h_i,g_i}$ as the FER at Relay $\mathbb{R}_i$ conditioned on h_i and g_i, i.e., the probability that the condition in (6.4) fails at Relay $\mathbb{R}_i$. We further define $V_i = \min(|h_i|^2, |g_i|^2)$. Then, $p_{\mathbb{R}_i|h_i,g_i}$ can be approximated by (see Appendix 6.A)

$$\begin{aligned} p_{\mathbb{R}_i|h_i,g_i} &\approx 1 - \left(1 - \mathrm{Q}(\sqrt{2\min(|h_i|^2, |g_i|^2)\bar{\gamma}})\right)^N \\ &= \sum_{n=1}^{N} \binom{N}{n} (-1)^{n+1} \mathrm{Q}^n \left(\sqrt{2V_i\bar{\gamma}}\right) \triangleq p_{\mathbb{R}_i|V_i}. \end{aligned} \tag{6.21}$$

We define $\mathcal{K} = \{i_m\}_{m=1}^K$ as a set of indices where $i_m \in \{1, \ldots, L\}$ and $K \leq L$. Define "$\mathbb{R}_\mathcal{K}$ successful" as the event that the relays $\{\mathbb{R}_{i_m}\}_{m=1}^K$ are successful while the relays $\{\mathbb{R}_j\}$ with $j \notin \mathcal{K}$ are not successful. The probability for such an event to occur can therefore be approximated by

$$\Pr\left(\mathbb{R}_\mathcal{K} \text{ successful}\right) \approx \prod_{i_m \in \mathcal{K}} (1 - p_{\mathbb{R}_{i_m}|V_{i_m}}) \times \prod_{j \notin \mathcal{K}} p_{\mathbb{R}_j|V_j}. \tag{6.22}$$

Furthermore, by applying $f_{V_i}(v) = 2\exp(-2v)$ and the approximation (6.34) in Appendix 6.B to (6.21), we can approximate the average FER at $\mathbb{R}_i$ as

$$\begin{aligned} p_\mathbb{R} &\triangleq p_{\mathbb{R}_i} \\ &= \mathrm{E}_{V_i}[p_{\mathbb{R}_i|V_i}] = \mathrm{E}_{V_i}\left[\sum_{n=1}^{N} \binom{N}{n} (-1)^{n+1} \mathrm{Q}^n \left(\sqrt{2V_i\bar{\gamma}}\right)\right] \\ &\approx \sum_{n=1}^{N} \binom{N}{n} (-1)^{n+1} \sum_{\substack{l_1, l_2, \ldots, l_8 \\ l_1 + l_2 + \cdots + l_8 = n}} 2\alpha_n\beta_n(2\bar{\gamma})^{\frac{\mu_n}{2}} \Gamma(\tfrac{\mu_n}{2} + 1)(n\bar{\gamma} + 2)^{-(\frac{\mu_n}{2}+1)} \end{aligned} \tag{6.23}$$

where $\alpha_n = n!/(l_1!l_2!\dots l_{m_a}!)$, $\beta_n = (c_1)^{l_1}\dots(c_{m_a})^{l_{m_a}}$ and $\mu_n = l_2 + 2l_3 + \cdots + (m_a-1)l_{m_a}$. As in Sect. 6.2.1.2, we denote $U = \max_{i_m\in\mathcal{K}}\{\min(|h_{i_m}|^2, |g_{i_m}|^2)\}$. Since only the best relay will transmit the coded signal vector back to the sources in the second time slot, the FER at the sources conditioned on the "$\mathbb{R}_\mathcal{K}$ successful" event is obtained by

$$
\begin{aligned}
p_{\text{sources}|\mathbb{R}_\mathcal{K}\text{ successful}} &\approx \tfrac{1}{2}(1-(1-\mathrm{Q}(\sqrt{2UL\bar{\gamma}}))^N) \\
&= \tfrac{1}{2}\sum\nolimits_{n=1}^{N}\tbinom{N}{n}(-1)^{n+1}\,\mathrm{Q}^n\left(\sqrt{2UL\bar{\gamma}}\right).
\end{aligned}
\tag{6.24}
$$

Note that the same approximation shown in Appendix 6.A has been used in the above derivation. Then, the average PEP at the sources over all $\{V_i\}_{i=1}^L$ when $\{\mathbb{R}_{i_m}\}_{m=1}^K$ are the successful relays, denoted by $p_{\text{sources},\mathbb{R}_\mathcal{K}\text{ successful},K}$, can be found using

$$
\begin{aligned}
&p_{\text{sources},\mathbb{R}_\mathcal{K}\text{ successful},K} \\
&= \mathrm{E}_{\{V_i\}_{i=1}^R}\left[p_{\text{sources}|\mathbb{R}_\mathcal{K}\text{ successful}}\times\Pr\left(\mathbb{R}_\mathcal{K}\text{ successful}\right)\right] \\
&= \mathrm{E}_{\{V_{i_m}\}_{i_m\in\mathcal{K}},\{V_j\}_{j\notin\mathcal{K}}}\left[p_{\text{sources}|\mathbb{R}_\mathcal{K}\text{ successful}}\times\prod_{i_m\in\mathcal{K}}(1-p_{\mathbb{R}_{i_m}|V_{i_m}})\times\prod_{j\notin\mathcal{K}}p_{\mathbb{R}_j|V_j}\right] \\
&= \mathrm{E}_{\{V_{i_m}\}_{i_m\in\mathcal{K}}}\left[p_{\text{sources}|\mathbb{R}_\mathcal{K}\text{ successful}}\times\prod_{i_m\in\mathcal{K}}(1-p_{\mathbb{R}_{i_m}|V_{i_m}})\right]\times\mathrm{E}_{\{V_j\}_{j\notin\mathcal{K}}}\left[\prod_{j\notin\mathcal{K}}p_{\mathbb{R}_j|V_j}\right] \\
&= \mathrm{E}_{\{V_{i_m}\}_{i_m\in\mathcal{K}}}\left[p_{\text{sources}|\mathbb{R}_\mathcal{K}\text{ successful}}\times\prod_{i_m\in\mathcal{K}}(1-p_{\mathbb{R}_{i_m}|V_{i_m}})\right]\times\prod_{j\notin\mathcal{K}}\mathrm{E}_{V_j}\left[p_{\mathbb{R}_j|V_j}\right] \\
&= \mathrm{E}_{\{V_{i_m}\}_{i_m\in\mathcal{K}}}\left[p_{\text{sources}|\mathbb{R}_\mathcal{K}\text{ successful}}\times\prod_{i_m\in\mathcal{K}}(1-p_{\mathbb{R}_{i_m}|V_{i_m}})\right]\times(p_\mathbb{R})^{L-K} \\
&= \mathrm{E}_U\left[\mathrm{E}_{\{V_{i_m}\}_{i_m\in\mathcal{K}}}\left[p_{\text{sources}|\mathbb{R}_\mathcal{K}\text{ successful}}\times\prod_{i_m\in\mathcal{K}}(1-p_{\mathbb{R}_{i_m}|V_{i_m}})\right]\times(p_\mathbb{R})^{L-K}\mid U=u\right] \\
&= \mathrm{E}_U\left[p_{\text{sources}|\mathbb{R}_\mathcal{K}\text{ successful}}\times\mathrm{E}_{\{V_{i_m}\}_{i_m\in\mathcal{K}}}\left[\prod_{i_m\in\mathcal{K}}(1-p_{\mathbb{R}_{i_m}|V_{i_m}})\mid U=u\right]\right]\times(p_\mathbb{R})^{L-K}.
\end{aligned}
\tag{6.25}
$$

By the definition of U, each V_{i_m} is no greater than U, i.e., $V_{i_m} \leq U$. Thus, the inner expectation in (6.25) can be written as

$$
\begin{aligned}
& \mathrm{E}_{\{V_{i_m}\}_{i_m\in\mathcal{K}}}\left[\prod_{i_m\in\mathcal{K}}(1-p_{\mathbb{R}_{i_m}|V_{i_m}})\middle| U=u\right] \\
\approx\ & \mathrm{E}_{\{V_{i_m}\}_{i_m\in\mathcal{K}}}\left[\prod_{i_m\in\mathcal{K}}\left(1-\mathrm{Q}(\sqrt{2v_{i_m}\bar{\gamma}})\right)^N\middle| U=u\right] \\
\approx\ & \prod_{i_m\in\mathcal{K}}\int_0^u [1-\tfrac{e^{-v_{i_m}\bar{\gamma}}}{12}-\tfrac{e^{-4v_{i_m}\bar{\gamma}/3}}{4}]\times[2\exp(-2v_{i_m})]\,\mathrm{d}v_{i_m} \\
\approx\ & \left(1-\tfrac{1}{6(\bar{\gamma}+2)}-\tfrac{1}{2(4\bar{\gamma}/3+2)}-e^{-2u}+\tfrac{e^{-(\bar{\gamma}+2)u}}{6(\bar{\gamma}+2)}+\tfrac{e^{-(4\bar{\gamma}/3+2)u}}{2(4\bar{\gamma}/3+2)}\right)^K.
\end{aligned}
\tag{6.26}
$$

Here, we have approximated $(1-\mathrm{Q}(\sqrt{2v_{i_m}\bar{\gamma}}))^N$ by $1-\mathrm{Q}(\sqrt{2v_{i_m}\bar{\gamma}})$. When $2v_{i_m}\bar{\gamma}$ is large, $\mathrm{Q}(\sqrt{2v_{i_m}\bar{\gamma}})$ approaches zero and the approximation becomes more accurate. The same is true when N is small. Further, we approximate $\mathrm{Q}(\sqrt{2v_{i_m}\bar{\gamma}})$ by $\frac{1}{12}e^{-v_{i_m}\bar{\gamma}}+\frac{1}{4}e^{-4v_{i_m}\bar{\gamma}/3}$ [95]. The accuracy of the approximations will be examined when we compare the analytical results with the simulations in Sect. 6.3. Then, by using (6.26) and (6.34), (6.25) can be expressed as

$$
\begin{aligned}
& p_{\text{sources},\mathbb{R}_{\mathcal{K}}\text{ successful},K} \\
=\ & \mathrm{E}_U\Big[\tfrac{1}{2}\textstyle\sum_{n=1}^{N}\binom{N}{n}(-1)^{n+1}\,\mathrm{Q}^n\left(\sqrt{2uL\bar{\gamma}}\right) \\
& \quad\times\left(1-\tfrac{1}{6(\bar{\gamma}+2)}-\tfrac{1}{2(4\bar{\gamma}/3+2)}-e^{-2u}+\tfrac{e^{-(\bar{\gamma}+2)u}}{6(\bar{\gamma}+2)}+\tfrac{e^{-(4\bar{\gamma}/3+2)u}}{2(4\bar{\gamma}/3+2)}\right)^K\Big](p_{\mathbb{R}})^{L-K} \\
\approx\ & \tfrac{1}{2}\textstyle\sum_{n=1}^{N}\binom{N}{n}(-1)^{n+1}\displaystyle\sum_{\substack{l_1,l_2,\ldots,l_8\\ l_1+l_2+\cdots+l_8=n}}\alpha_n\beta_n(2L\bar{\gamma})^{\frac{\mu_n}{2}}\sum_{k=0}^{K-1}2K\binom{K-1}{k}(-1)^k \\
& \times\sum_{\substack{j_1,j_2,j_3,j_4\\ j_1+j_2+j_3+j_4=K}}\tfrac{K!}{j_1!j_2!j_3!j_4!}\left(1-\tfrac{1}{6(\bar{\gamma}+2)}-\tfrac{1}{2(4\bar{\gamma}/3+2)}\right)^{j_1}(-1)^{j_2}(\tfrac{1}{6(\bar{\gamma}+2)})^{j_3}(\tfrac{1}{2(4\bar{\gamma}/3+2)})^{j_4} \\
& \times\Gamma(\tfrac{\mu_n}{2}+1)\,[nL\bar{\gamma}+2(k+j_2+1)+(\bar{\gamma}+2)j_3+(4\bar{\gamma}/3+2)j_4]^{-(\frac{\mu_n}{2}+1)}\times(p_{\mathbb{R}})^{L-K}.
\end{aligned}
\tag{6.27}
$$

Finally, by taking into account all possible cases of K, i.e., $K=1,2,\ldots,L$, and

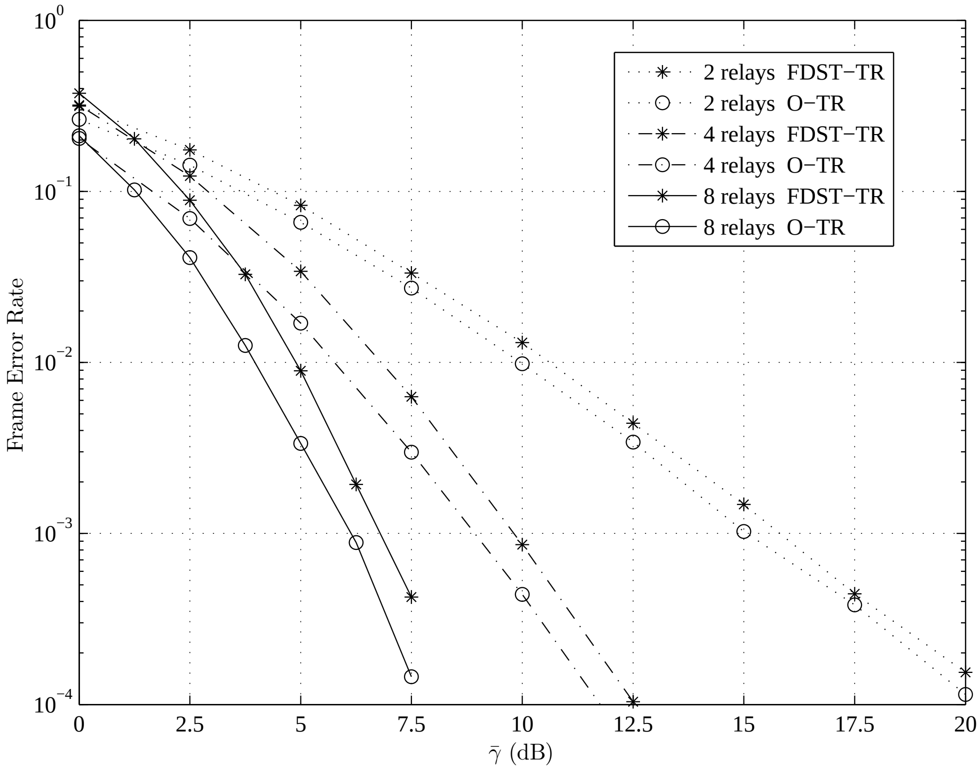

Figure 6.4: The frame error rate comparison between the fully-distributed space-time coded two-way relaying method (FDST-TR) and the proposed opportunistic two-way relaying method (O-TR) for three different systems: a 2-relay system (i.e., $L = 2$), a 4-relay system (i.e., $L = 4$) and an 8-relay system (i.e., $L = 8$). The frame length N is set to equal to the number of relays, i.e., $N = L$. BPSK modulation is used.

the number of possible combinations of $\{i_m\}_{m=1}^{K}$, the average FER for the O-TR relaying system when BPSK is applied, denoted by $\bar{P}_{\text{FER,BPSK}}$, can be estimated using

$$\begin{aligned}\bar{P}_{\text{FER,BPSK}} &= \sum_{K=0}^{L} \binom{L}{K} p_{\text{sources},\mathbb{R}_{\mathcal{K}}\text{ successful},K} \\ &= (p_{\mathbb{R}})^{L} + \sum_{K=1}^{L} \binom{L}{K} p_{\text{sources},\mathbb{R}_{\mathcal{K}}\text{ successful},K}. \end{aligned} \tag{6.28}$$

6.3 Simulation Results

In this section, we show the frame error rate (FER) results. First, we compare the FER performance of our proposed opportunistic two-way relaying (O-TR) method with that of the fully-distributed space-time coded two-way relaying (FDST-TR) method [66] by simulations. In Fig. 6.4, we show the simulated FER performance under three system settings: a 2-relay system with frame length $N = 2$, a 4-relay system with $N = 4$ and a 8-relay system with $N = 8$. We assume that the BPSK modulation scheme is used in all cases. For all the settings, orthogonal matrices are employed for the FDST-TR method [66]. The curves in Fig. 6.4 clearly show that the O-TR method can achieve the same full diversity order as the FDST-TR method. In addition, for all the settings being considered, the proposed O-TR method achieves better performance than the FDST-TR method in terms of FER.

In the FDST-TR scheme, for a given SNR, there will be an average of $\mathrm{E}[K]$ successful relays at each broadcasting session. The average transmission power of all the relays is therefore given by $\mathrm{E}[K]P_r$. In our proposed O-TR method, suppose the "best relay" transmits with a power identical to the average power of all the relays in the FDST-TR case, i.e., $\mathrm{E}[K]P_r$, we study the FER under such a scenario. (Note that in practice, it may not be feasible for the "best relay" to transmit with $\mathrm{E}[K]P_r$, which varies as the SNR changes [2].) In Fig. 6.5, we plot the FERs for a two-way relaying system with $L = 4$. The results indicate that our proposed O-TR method with the "best relay" transmitting with $\mathrm{E}[K]P_r$ still outperforms the FDST-TR scheme. The reason is that the "best relay" spends all the transmission power on the "best channels" while the relays in the FDST-TR scheme spend some

[2]In practice, the relays may not know the exact value of $\mathrm{E}[K]$ but can estimate it. We suppose that N_F two-way transmissions have been made and the ith relay has successfully decoded the frames for N_i times. Among these N_i occasions, the relay has only been selected as the "best" relay for m_i times. As N_F increases, it can be readily shown that $\lim_{N_F\to\infty} \frac{N_i}{m_i} = \mathrm{E}[K]$. Therefore, when the ith relay is selected as the "best" relay, it should transmit with the power $\frac{N_i}{m_i}P_r$, which is a good estimation of $\mathrm{E}[K]P_r$.

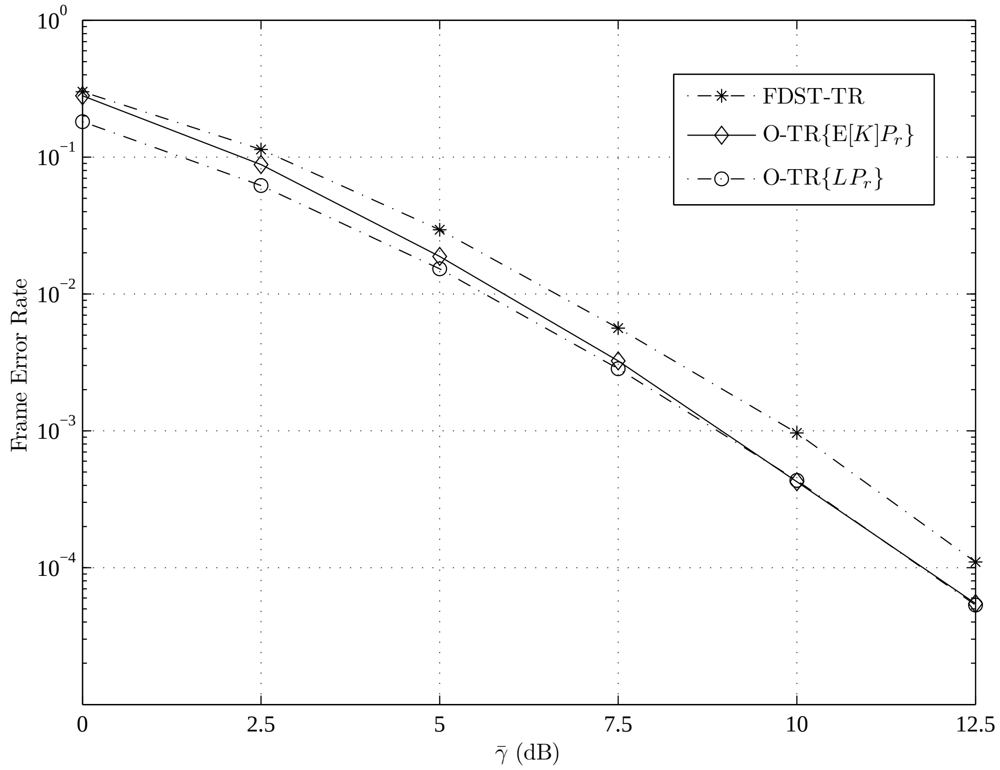

Figure 6.5: The frame error rate comparison between the fully-distributed space-time coded two-way relaying method (FDST-TR), the proposed opportunistic two-way relaying method with a relay transmission power of $\mathrm{E}[K]P_r$ (O-TR$\{\mathrm{E}[K]P_r\}$), and the proposed opportunistic two-way relaying method with a relay transmission power of LP_r (O-TR$\{LP_r\}$) for a 4-relay system (i.e., $L = 4$). The frame length N is set to equal to the number of relays, i.e., $N = L$. BPSK modulation is used.

of the transmission power on the comparatively "not-so-good" channels. Note also that as the SNR increases, the FER for the O-TR$\{\mathrm{E}[K]P_r\}$ converges to that for the O-TR$\{LP_r\}$. It is because when the SNR increases, the number of successful relays increases and approaches L.

We then examine the impact of the frame length N on the FER performance of the proposed O-TR method. In Fig. 6.6, we show the simulated FER performance of a four-relay system employing BPSK modulation under different frame length N. As expected, reducing the frame length improves the FER performance.

Finally, we compare the approximated FER performance (6.28) with the sim-

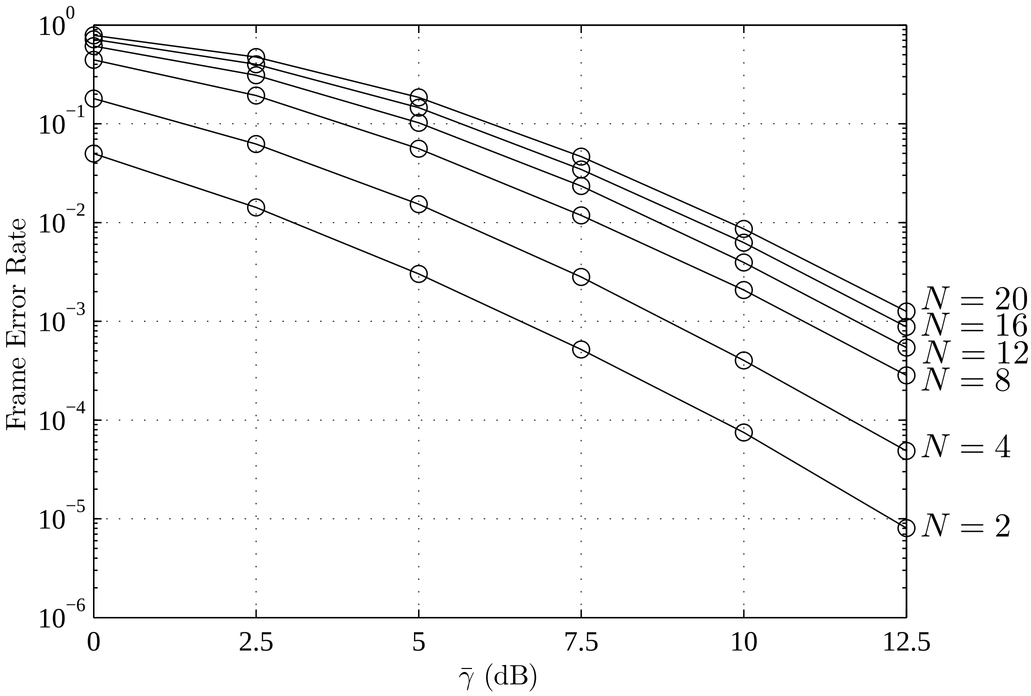

Figure 6.6: The frame error rate versus signal-to-noise ratio for a 4-relay system employing the O-TR method and the BPSK modulation scheme. Frame length $N = 2, 4, 8, 12, 16, 20$.

ulation results in the case of BPSK modulation. The results for a two-relay system and a four-relay system are illustrated in Fig. 6.7(a) and Fig. 6.7(b), respectively. The curves indicate that the FER approximation in (6.28) forms a lower-bound of the actual FER. We can further observe that for the same $\bar{\gamma}$, a smaller value of N gives a smaller absolutely difference between the simulated FER and approximated FER. The same observation occurs when we increase $\bar{\gamma}$ while keeping N constant. Such findings are consistent with a more accurate approximation of (6.26) (which forms part of (6.28)) when N is small and $\bar{\gamma}$ is large.

6.4 Summary

In this chapter, we have proposed a relaying method for a two-way relaying network, namely opportunistic two-way relaying (O-TR) method. It is based on the modular network coding method and the opportunistic relay selection. We have derived the upper frame error rate (FER) bound of the proposed O-TR method and have shown that the proposed method can accomplish the full diversity order. Simulation results have further shown that the proposed O-TR method outperforms the full distributed space-time two-way relaying method in terms of FER.

Appendix 6.A

At the time instance $1 \leq t \leq N$, the transmitted BPSK symbol from $\mathbb{S}_1$ and $\mathbb{S}_2$ are $x_1(t)$ and $x_2(t)$, respectively. To simplify the notation, in the following analysis we remove the time index and represent these symbols by x_1 and x_2. At the ith relay, the received signal is expressed as

$$\begin{bmatrix} \Re(y_{\mathbb{R}_i}) \\ \Im(y_{\mathbb{R}_i}) \end{bmatrix} = \sqrt{P} \begin{bmatrix} \Re(h_i) & \Re(g_i) \\ \Im(h_i) & \Im(g_i) \end{bmatrix} \begin{bmatrix} x_1 \\ x_2 \end{bmatrix} + \begin{bmatrix} \Re(n_i) \\ \Im(n_i) \end{bmatrix} \tag{6.29}$$

The corresponding decoded signal-vector results that made the modular condition (6.4) invalid are $\left[\begin{smallmatrix} -x_1 \\ x_2 \end{smallmatrix}\right]$ and $\big(\left[\begin{smallmatrix} x_1 \\ -x_2 \end{smallmatrix}\right]$. The probability that the detection result is $\left[\begin{smallmatrix} -x_1 \\ x_2 \end{smallmatrix}\right]$ given the transmission of $\left[\begin{smallmatrix} x_1 \\ x_2 \end{smallmatrix}\right]$ is given by (A.2, [4])

$$\begin{aligned} \Pr\big(\left[\begin{smallmatrix} -x_1 \\ x_2 \end{smallmatrix}\right] \big| \left[\begin{smallmatrix} x_1 \\ x_2 \end{smallmatrix}\right]\big) &\approx \mathrm{Q}\left(\| \sqrt{P}\left[\begin{smallmatrix} \Re(h_i) & \Re(g_i) \\ \Im(h_i) & \Im(g_i) \end{smallmatrix}\right]\left[\begin{smallmatrix} x_1 \\ x_2 \end{smallmatrix}\right] - \sqrt{P}\left[\begin{smallmatrix} \Re(h_i) & \Re(g_i) \\ \Im(h_i) & \Im(g_i) \end{smallmatrix}\right]\left[\begin{smallmatrix} -x_1 \\ x_2 \end{smallmatrix}\right] \| /(2\sqrt{1/2})\right) \\ &= \mathrm{Q}(\sqrt{2|h_i|^2\bar{\gamma}}). \end{aligned} \tag{6.30}$$

In the above derivation, we have made use of the fact that $|x_1| = 1$. Similarly, we have

$$\Pr\big(\left[\begin{smallmatrix} x_1 \\ -x_2 \end{smallmatrix}\right] \big| \left[\begin{smallmatrix} x_1 \\ x_2 \end{smallmatrix}\right]\big) \approx \mathrm{Q}(\sqrt{2|g_i|^2\gamma}). \tag{6.31}$$

Therefore the frame error rate of the signal frame detection at the relay $\mathbb{R}_i$ is calculated by

$$\begin{aligned} p_{r,i} &\approx 1 - \left(1 - \mathrm{Q}(\sqrt{2|h_i|^2\bar{\gamma}}) - \mathrm{Q}(\sqrt{2|g_i|^2\bar{\gamma}})\right)^N \\ &\approx 1 - \left(1 - \mathrm{Q}(\sqrt{2\min(|h_i|^2, |g_i|^2)\bar{\gamma}})\right)^N. \end{aligned} \tag{6.32}$$

Appendix 6.B

Using the approximations in [96], we can express the Gaussian Q-function as

$$\mathrm{Q}(x) \approx \exp(-x^2/2) \sum_{m=1}^{m_a} c_m x^{m-1} \tag{6.33}$$

where $c_m = \frac{(-1)^{m+1}A^m}{B\sqrt{\pi}(\sqrt{2})^{m+1}m!}$, and can approximate the n-th power of the Gaussian Q-function by

$$\mathrm{Q}^n(x) \approx \exp(-nx^2/2)(\sum_{m=1}^{m_a} c_m x^{m-1})^n = \exp(-nx^2/2) \sum_{\substack{l_1,l_2,\ldots,l_{m_a} \\ l_1+l_2+\cdots+l_{m_a}=n}} \alpha_n \beta_n x^{\mu_n} \quad (6.34)$$

where $\alpha_n = n!/(l_1!l_2!\ldots l_{m_a}!)$, $\beta_n = (c_1)^{l_1}\ldots(c_{m_a})^{l_{m_a}}$ and $\mu_n = l_2 + 2l_3 + \cdots + (m_a - 1)l_{m_a}$. In our analysis, we employ the following parameters: $m_a = 8$, $A = 1.98$ and $B = 1.135$, which has been found to be a good setting in approximating the Q-function [96].

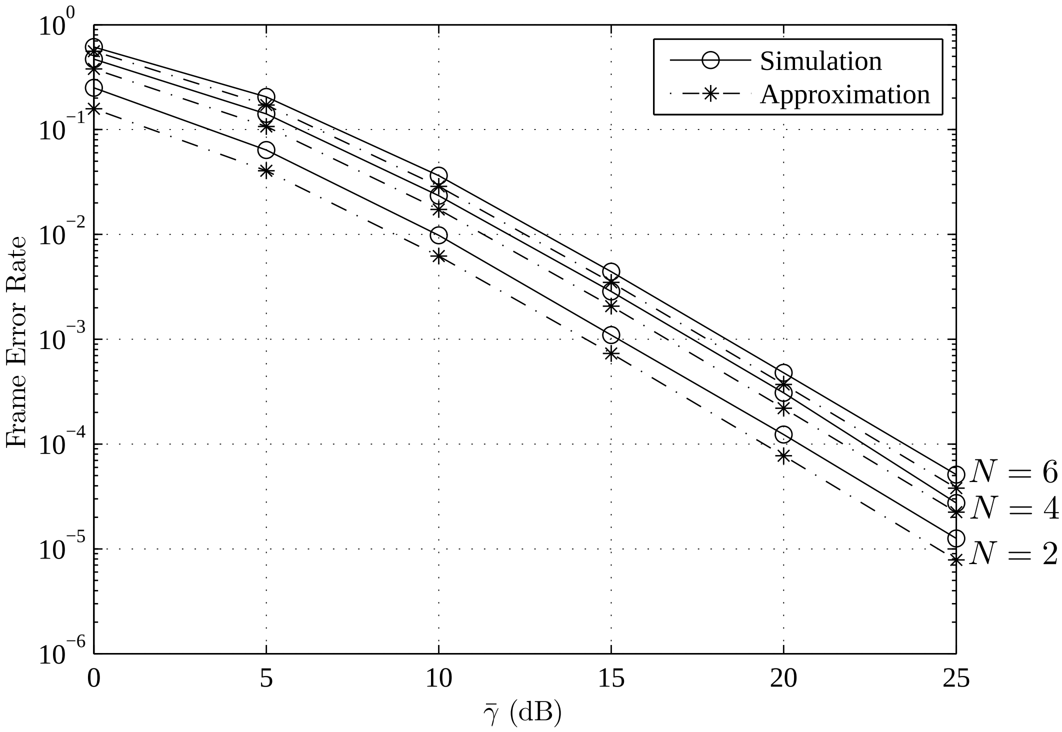

(a)

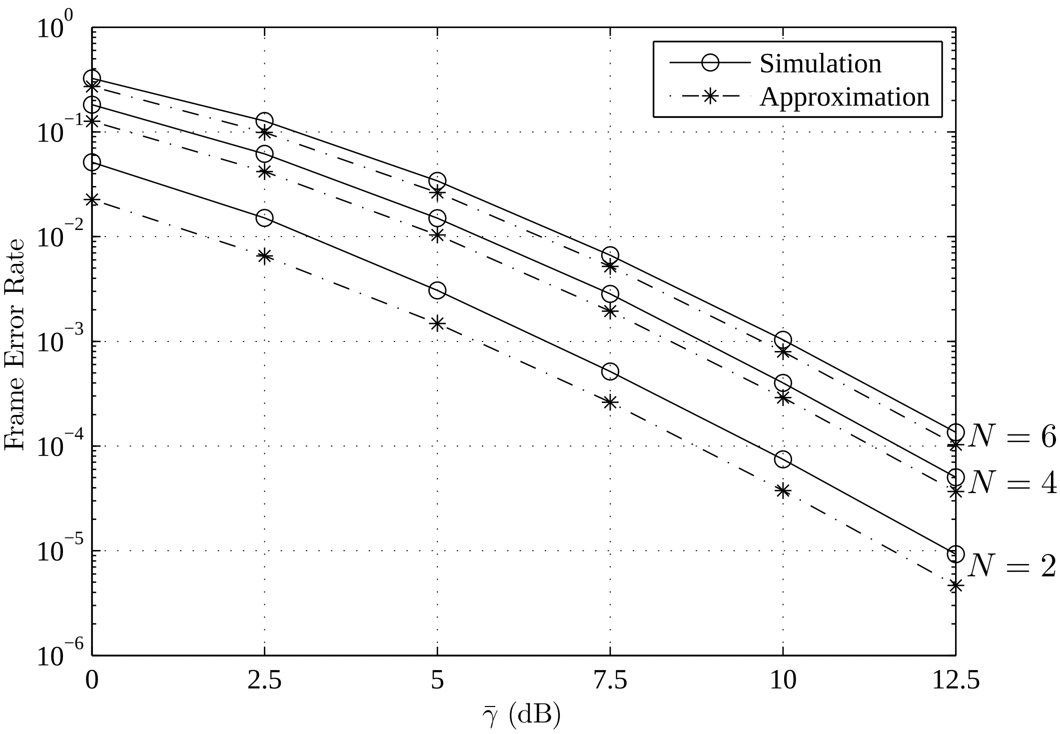

(b)

Figure 6.7: The simulated FER and the approximated FER for an O-TR two-way relaying system. All systems employ BPSK modulation. Frame length $N = 2, 4, 6$. (a) A 2-relay system; (b) a 4-relay system.

Chapter 7

Conclusions and Future Directions

7.1 Conclusions

Thanks to the channel capacity theorem, a milestone established by Shannon [1], the channel coding theory for point-to-point (P2P) communication systems has been comprehensively developed. Nowadays, some advanced channel coding methods can even approach the Shannon limit with negligible gaps. To wireless communication engineers and scientists, the challenge of developing faster communication systems is not to increase the transmission rates of the P2P channels of a network anymore, but to increase the overall throughput of the network by guiding the information streams within the network efficiently. As one of the simplest network models, the relay channel has attracted increasing academic and industrial interest.

In this thesis, we have investigated the relaying protocols for single-relay one-way networks, multi-relay one-way networks and multi-relay two-way networks. For single-relay networks, we have proposed two new relaying protocols, namely the incremental selection amplify-and-forward (ISAF) protocol and the joint incremental selection relaying (JISR) protocol. Theoretical asymptotic outage probability analyses have indicated that both ISAF and JISR are superior to incremental amplify-and-forward (IAF) for large SNR cases, and that JISR is no worse than ISAF over all SNR values. Moreover, the asymptotic outage probabilities have been verified by simulation results. The simulation results also show that ISAF is slightly better than IAF, and JISR is much better than ISAF at low SNR regime.

We have further examined the opportunistic relaying protocols for a cooperative communication network with multiple relays. We have extended the incremental selection amplify-and-forward (ISAF) and joint incremental selection relaying protocols (JISR) for use in opportunistic relaying, forming the opportunistic ISAF (OISAF) and opportunistic JISR (OJISR), respectively. We have shown that they outperform all other existing protocols (opportunistic decode-and-forward (ODF), opportunistic amplify-and-forward (OAF), opportunistic selection DF (OSDF) and opportunistic incremental AF (OIAF)). We have also derived the analytical expressions for the asymptotic outage probabilities of of six different protocols — ODF, OAF, OSDF, OIAF, OISAF and OJISR. By comparing the derived outage probabilities with the simulation results, we conclude that when the average SNR $\bar{\gamma}$ is large, the analytical asymptotic outage probabilities can provide accurate estimation of the actual performance of the protocols.

Furthermore, we have studied the CSI-assisted opportunistic AF relaying protocol that employs the maxmin relay-selection criterion and an MRC receiver at the destination. We have derived expressions for the upper and lower bounds for the outage probability, ergodic achievable rate and average SER of M-PSK, which are further verified by simulated results. Our performance analysis achieves better performance prediction than that obtained by conventional methods. The performance analyses here can be extended to the multi-relay systems with dissimilar fading, and also to the case when the energy fairness among the relays is taken into consideration.

Finally, we have proposed a relaying method for a two-way relaying network, namely opportunistic two-way relaying (O-TR) method. It is based on the modular network coding method and the opportunistic relay selection. We have derived the upper frame error rate (FER) bound of the proposed O-TR method and have shown that the proposed method can accomplish the full diversity order. Simulation results have further shown that the proposed O-TR method outperforms the fully-distributed space-time two-way relaying (FDST-TR) method in terms of FER. Compared to the FDST-TR method, the benefit of the proposed protocol is threefold. Firstly, there is no restriction on the frame length N, which results in a more flexible frame design at the sources. Secondly, no distributed-space-time linear transformation is performed at the relays. Therefore, whenever there is a new relay entering the system, the matrix adjustment is not required. Thirdly, the decoding at the sources is made simpler.

7.2 Future Directions

In the following, we propose some possible future directions.

- In this thesis, we have focused on the performance over Rayleigh fading channel model. As we know, the more general fading channel model is Nakagami-m fading model, in which Rayleigh fading is a special case. Thus, we can study the performance of these opportunistic relaying protocols over Nakagami-m fading channels.

- The performance bounds of OAF have been found. However, the bounds are not tight for the relaying systems with a large number of relays. Another research direction is therefore deriving more accurate closed-form analytical expressions for evaluating the performance of the OAF protocol.

- In our proposed opportunistic relaying protocol, we have considered the case in which the opportunistic relay is selected based on the maxmin criterion. Other selection criteria, such as harmonic-mean criterion, may also achieve the full diversity. It is worthwhile to discover the common features of the criteria which can provide the full diversity, and aim at categorizing them under an unified framework.

- Another research direction is to systematically study two-way relaying networks. We can identify/construct optimal relaying protocols with which the achievable rates can approach the upper bound of a two-way relaying network obtained by the cut-set theorem. We can then further implement these relaying protocols by exploiting existing channel coding methods.

Bibliography

[1] C. E. Shannon, “A mathematical theory of communication,” *Bell System Technical Journal*, vol. 27, pp. 379–423, 623–656, 1948.

[2] R. W. Yeung, *Information Theory and Network Coding.* Springer, 2008.

[3] T. M. Cover and J. A. Thomas, *Elements of Information Theory*, 2nd ed. Wiley-Interscience, 2006.

[4] D. Tse and P. Viswanath, *Fundamentals of Wireless Communication.* Cambridge University Press, 2005.

[5] S.-Y. Chung, J. Forney, G. D., T. J. Richardson, and R. Urbanke, “On the design of low-density parity-check codes within 0.0045 dB of the shannon limit,” *IEEE Commun. Lett.*, vol. 5, no. 2, pp. 58–60, Feb. 2001.

[6] E. C. van der Meulen, “Three-terminal communication channels,” *Adv. Appl. Prob.*, vol. 3, pp. 120–154, 1971.

[7] T. Cover and A. E. Gamal, “Capacity theorems for the relay channel,” *IEEE Trans. Inform. Theory*, vol. 25, no. 5, pp. 572–584, Sept. 1979.

[8] A. Sendonaris, E. Erkip, and B. Aazhang, “User cooperation diversity: Part I. System description,” *IEEE Trans. Commun.*, vol. 51, no. 11, pp. 1927–1938, Nov. 2003.

[9] ——, “User cooperation diversity. Part II. Implementation aspects and performance analysis,” *IEEE Trans. Commun.*, vol. 51, no. 11, pp. 1939–1948, Nov. 2003.

[10] J. N. Laneman, D. N. C. Tse, and G. W. Wornell, “Cooperative diversity in wireless networks: Efficient protocols and outage behavior,” *IEEE Trans. Inform. Theory*, vol. 50, no. 12, pp. 3062–3080, Dec. 2004.

[11] J. N. Laneman and G. W. Wornell, "Distributed space-time-coded protocols for exploiting cooperative diversity in wireless networks," *IEEE Trans. Inform. Theory*, vol. 49, no. 10, pp. 2415–2425, Oct. 2003.

[12] S. M. Alamouti, "A simple transmit diversity technique for wireless communications," *IEEE J. Select. Areas Commun.*, vol. 16, no. 8, pp. 1451–1458, Oct. 1998.

[13] G. J. Foschini and M. J. Gans, "On limits of wireless communications in a fading environment when using multiple antennas," *Wirel. Pers. Commun.*, vol. 6, no. 3, pp. 311–335, 1998.

[14] E. Telatar, "Capacity of multi-antenna Gaussian channels," *European Transactions on Telecommunications*, vol. 10, pp. 585–596, 1999.

[15] V. Tarokh, N. Seshadri, and A. R. Calderbank, "Space-time codes for high data rate wireless communication: Performance criterion and code construction," *IEEE Trans. Inform. Theory*, vol. 44, no. 2, pp. 744–765, Mar. 1998.

[16] V. Tarokh, A. Naguib, N. Seshadri, and A. R. Calderbank, "Space-time codes for high data rate wireless communication: Performance criteria in the presence of channel estimation errors, mobility, and multiple paths," *IEEE Trans. Commun.*, vol. 47, no. 2, pp. 199–207, Feb. 1999.

[17] V. Tarokh, H. Jafarkhani, and A. R. Calderbank, "Space-time block codes from orthogonal designs," *IEEE Trans. Inform. Theory*, vol. 45, no. 5, pp. 1456–1467, July 1999.

[18] A. Goldsmith, *Wireless Communications.* Cambridge University Press, 2005.

[19] L. Zheng and D. N. C. Tse, "Diversity and multiplexing: A fundamental tradeoff in multiple-antenna channels," *IEEE Trans. Inform. Theory*, vol. 49, no. 5, pp. 1073–1096, May 2003.

[20] P. A. Anghel and M. Kaveh, "Exact symbol error probability of a cooperative network in a Rayleigh-fading environment," *IEEE Trans. Wireless Commun.*, vol. 3, no. 5, pp. 1416–1421, Sept. 2004.

[21] J. Boyer, D. D. Falconer, and H. Yanikomeroglu, "Multihop diversity in wireless relaying channels," *IEEE Trans. Commun.*, vol. 52, no. 10, pp. 1820–1830, Oct. 2004.

[22] A. Ribeiro, X. Cai, and G. B. Giannakis, "Symbol error probabilities for general cooperative links," *IEEE Trans. Wireless Commun.*, vol. 4, no. 3, pp. 1264–1273, May 2005.

[23] N. C. Beaulieu and J. Hu, "A closed-form expression for the outage probability of decode-and-forward relaying in dissimilar Rayleigh fading channels," *IEEE Commun. Lett.*, vol. 10, no. 12, pp. 813–815, December 2006.

[24] S. Ikki and M. H. Ahmed, "Performance analysis of cooperative diversity wireless networks over Nakagami-m fading channel," *IEEE Commun. Lett.*, vol. 11, no. 4, pp. 334–336, April 2007.

[25] T. Wang, A. Cano, G. B. Giannakis, and J. N. Laneman, "High-performance cooperative demodulation with decode-and-forward relays," *IEEE Trans. Commun.*, vol. 55, no. 7, pp. 1427–1438, July 2007.

[26] A. K. Sadek, W. Su, and K. J. R. Liu, "Multinode cooperative communications in wireless networks," *IEEE Trans. Signal Processing*, vol. 55, no. 1, pp. 341–355, Jan. 2007.

[27] T. Wang, G. B. Giannakis, and R. Wang, "Smart regenerative relays for link-adaptive cooperative communications," *IEEE Trans. Commun.*, vol. 56, no. 11, pp. 1950–1960, Nov. 2008.

[28] F. Xu, Q. F. Zhou, F. C. M. Lau, D.-W. Yue, and S. F. Hau, "Performance analysis of serial cooperative communications with decode-and-forward relaying and blind-EGC reception under nakagami fading channels," *IEEE Trans. Wireless Commun.*, vol. 8, no. 11, pp. 5455–5460, Nov. 2009.

[29] G. Scutari and S. Barbarossa, "Distributed space-time coding for regenerative relay networks," *IEEE Trans. Wireless Commun.*, vol. 4, no. 5, pp. 2387–2399, Sept. 2005.

[30] P. A. Anghel, G. Leus, and M. Kaveh, "Distributed space-time cooperative systems with regenerative relays," *IEEE Trans. Wireless Commun.*, vol. 5, no. 11, pp. 3130–3141, Nov. 2006.

[31] S. Yiu, R. Schober, and L. Lampe, "Distributed space-time block coding," *IEEE Trans. Commun.*, vol. 54, no. 7, pp. 1195–1206, July 2006.

[32] B. Sirkeci-Mergen and A. Scaglione, "Randomized space-time coding for distributed cooperative communication," *IEEE Trans. Signal Processing*, vol. 55, no. 10, pp. 5003–5017, Oct. 2007.

[33] M. Uysal, O. Canpolat, and M. M. Fareed, "Asymptotic performance analysis of distributed space-time codes," *IEEE Commun. Lett.*, vol. 10, no. 11, pp. 775–777, November 2006.

[34] Y. Jing and B. Hassibi, "Distributed space-time coding in wireless relay networks," *IEEE Trans. Wireless Commun.*, vol. 5, no. 12, pp. 3524–3536, December 2006.

[35] P. A. Anghel and M. Kaveh, "On the performance of distributed space-time coding systems with one and two non-regenerative relays," *IEEE Trans. Wireless Commun.*, vol. 5, no. 3, pp. 682–692, March 2006.

[36] Z. Yi and I.-M. Kim, "Single-symbol ML decodable distributed STBCs for cooperative networks," *IEEE Trans. Inform. Theory*, vol. 53, no. 8, pp. 2977–2985, Aug. 2007.

[37] S. Wei, D. L. Goeckel, and M. C. Valenti, "Asynchronous cooperative diversity," *IEEE Trans. Wireless Commun.*, vol. 5, no. 6, pp. 1547–1557, June 2006.

[38] Y. Shang and X.-G. Xia, "Shift-full-rank matrices and applications in space-time trellis codes for relay networks with asynchronous cooperative diversity," *IEEE Trans. Inform. Theory*, vol. 52, no. 7, pp. 3153–3167, July 2006.

[39] Z. Li and X.-G. Xia, "A simple alamouti space-time transmission scheme for asynchronous cooperative systems," *IEEE Signal Processing Lett.*, vol. 14, no. 11, pp. 804–807, Nov. 2007.

[40] Y. Li and X.-G. Xia, "A family of distributed space-time trellis codes with asynchronous cooperative diversity," *IEEE Trans. Commun.*, vol. 55, no. 4, pp. 790–800, Apr. 2007.

[41] X. Guo and X.-G. Xia, "A distributed space-time coding in asynchronous wireless relay networks," *IEEE Trans. Wireless Commun.*, vol. 7, no. 5, pp. 1812–1816, May 2008.

[42] Z. Zhong, S. Zhu, and A. Nallanathan, "Distributed space-time trellis code for asynchronous cooperative communications under frequency-selective channels," *IEEE Trans. Wireless Commun.*, vol. 8, no. 2, pp. 796–805, Feb. 2009.

[43] A. Bletsas, A. Khisti, D. P. Reed, and A. Lippman, "A simple cooperative diversity method based on network path selection," *IEEE J. Select. Areas Commun.*, vol. 24, no. 3, pp. 659–672, March 2006.

[44] A. Bletsas and A. Lippman, "Implementing cooperative diversity antenna arrays with commodity hardware," *IEEE Commun. Mag.*, vol. 44, no. 12, pp. 33–40, Dec. 2006.

[45] A. Bletsas, H. Shin, and M. Z. Win, "Outage optimality of opportunistic amplify-and-forward relaying," *IEEE Commun. Lett.*, vol. 11, no. 3, pp. 261–263, March 2007.

[46] ——, "Cooperative communications with outage-optimal opportunistic relaying," *IEEE Trans. Wireless Commun.*, vol. 6, no. 9, pp. 3450–3460, September 2007.

[47] C. K. Lo, W. Heath, and S. Vishwanath, "Opportunistic relay selection with limited feedback," in *Proc. VTC2007-Spring Vehicular Technology Conference IEEE 65th*, Apr. 22–25, 2007, pp. 135–139.

[48] I. Krikidis and J. C. Belfiore, "Scheduling for amplify-and-forward cooperative networks," *IEEE Trans. Veh. Technol.*, vol. 56, no. 6, pp. 3780–3790, Nov. 2007.

[49] A. Bletsas, H. Shin, and M. Z. Win, "Outage analysis for co-operative communication with multiple amplify-and-forward relays," *Electronics Letters*, vol. 43, no. 6, pp. 51–52, March 15 2007.

[50] C. K. Lo, R. W. Heath, and S. Vishwawnath, "Hybrid-ARQ in multihop networks with opportunistic relay selection," in *Proc. IEEE International Conference on Acoustics, Speech and Signal Processing ICASSP 2007*, vol. 3, Apr. 15–20, 2007, pp. III–617–III–620.

[51] R. Madan, N. Mehta, A. Molisch, and J. Zhang, "Energy-efficient cooperative relaying over fading channels with simple relay selection," *IEEE Trans. Wireless Commun.*, vol. 7, no. 8, pp. 3013–3025, Aug. 2008.

[52] Q. F. Zhou, F. C. M. Lau, and S. F. Hau, "Asymptotic analysis of opportunistic relaying protocols," *IEEE Trans. Wireless Commun.*, vol. 8, no. 8, pp. 3915–3920, Aug. 2009.

[53] F. Xu, F. C. M. Lau, Q. F. Zhou, and D.-W. Yue, "Outage performance of cooperative communication systems using opportunistic relaying and selection combining receiver," *IEEE Signal Processing Lett.*, vol. 16, no. 2, pp. 113–116, Feb. 2009.

[54] B. Hassibi and B. M. Hochwald, "High-rate codes that are linear in space and time," *IEEE Trans. Inform. Theory*, vol. 48, no. 7, pp. 1804–1824, July 2002.

[55] M. Dohler, Y. Li, B. Vucetic, A. H. Aghvami, M. Arndt, and D. Barthel, "Performance analysis of distributed space-time block-encoded sensor networks," *IEEE Trans. Veh. Technol.*, vol. 55, no. 6, pp. 1776–1789, Nov. 2006.

[56] Y. Jing and H. Jafarkhani, "Using orthogonal and quasi-orthogonal designs in wireless relay networks," *IEEE Trans. Inform. Theory*, vol. 53, no. 11, pp. 4106–4118, Nov. 2007.

[57] O. Canpolat, M. Uysal, and M. Fareed, "Analysis and design of distributed spacectime trellis codes with amplify-and-forward relaying," *IEEE Trans. Veh. Technol.*, vol. 56, no. 4, pp. 1649–1660, July 2007.

[58] Y. Jing and H. Jafarkhani, "Distributed differential space-time coding for wireless relay networks," *IEEE Trans. Commun.*, vol. 56, no. 7, pp. 1092–1100, July 2008.

[59] R. Tannious and A. Nosratinia, "Spectrally-efficient relay selection with limited feedback," *IEEE J. Select. Areas Commun.*, vol. 26, no. 8, pp. 1419–1428, Oct. 2008.

[60] Z. Ding, Y. Gong, T. Ratnarajah, and C. F. N. Cowan, "On the performance of opportunistic cooperative wireless networks," *IEEE Trans. Commun.*, vol. 56, no. 8, pp. 1236–1240, Aug. 2008.

[61] R. Ahlswede, N. Cai, S.-Y. R. Li, and R. W. Yeung, "Network information flow," *IEEE Trans. Inform. Theory*, vol. 46, no. 4, pp. 1204–1216, July 2000.

[62] S.-Y. R. Li, R. W. Yeung, and N. Cai, "Linear network coding," *IEEE Trans. Inform. Theory*, vol. 49, no. 2, pp. 371–381, Feb. 2003.

[63] T. Ho, R. Koetter, M. Medard, D. R. Karger, and M. Effros, "The benefits of coding over routing in a randomized setting," in *Proc. IEEE International Symposium on Information Theory*, June 29–July 4, 2003, p. 442.

[64] S. Katti, H. Rahul, W. Hu, D. Katabi, M. Médard, and J. Crowcroft, "XORs in the air: practical wireless network coding," in *Proc. ACM SigComm'06*. Pisa, Italy: ACM, 2006, pp. 243–254.

[65] S. Zhang, S. C. Liew, and P. P. Lam, "Hot topic: Physical-layer network coding," in *Proc. ACM MobiCom'06*. Los Angeles, USA: ACM, 2006, pp. 358–365.

[66] T. Cui, F. Gao, T. Ho, and A. Nallanathan, "Distributed spacetime coding for two-way wireless relay networks," *IEEE Trans. Signal Processing*, vol. 57, no. 2, pp. 658–671, Feb. 2009.

[67] T. Wang, Y. Yao, and G. B. Giannakis, "Non-coherent distributed space-time processing for multiuser cooperative transmissions," *IEEE Trans. Wireless Commun.*, vol. 5, no. 12, pp. 3339–3343, December 2006.

[68] M. O. Hasna and M. S. Alouini, "End-to-end performance of transmission systems with relays over Rayleigh-fading channels," *IEEE Trans. Wireless Commun.*, vol. 2, no. 6, pp. 1126–1131, Nov. 2003.

[69] ——, "Harmonic mean and end-to-end performance of transmission systems with relays," *IEEE Trans. Commun.*, vol. 52, no. 1, pp. 130–135, Jan 2004.

[70] ——, "A performance study of dual-hop transmissions with fixed gain relays," *IEEE Trans. Wireless Commun.*, vol. 3, no. 6, pp. 1963–1968, Nov. 2004.

[71] H. Shin and J. B. Song, "MRC analysis of cooperative diversity with fixed-gain relays in Nakagami-m fading channels," *IEEE Trans. Wireless Commun.*, vol. 7, no. 6, pp. 2069–2074, June 2008.

[72] G. K. Karagiannidis, "Performance bounds of multihop wireless communications with blind relays over generalized fading channels," *IEEE Trans. Wireless Commun.*, vol. 5, no. 3, pp. 498–503, Mar. 2006.

[73] I. S. Gradshteyn and I. M. Ryzhik, *Table of Integrals, Series, and Products*, 7th ed. New York: Academic, 2007.

[74] M. K. Simon and M.-S. Alouini, *Digital Communication over Fading Channels*, 2nd ed. Wiley-IEEE Press, 2004.

[75] J. E. Smee and N. C. Beaulieu, "On the equivalence of the simultaneous and separate MMSE optimizations of a DFE FFF and FBF," *IEEE Trans. Commun.*, vol. 45, no. 2, pp. 156–158, Feb. 1997.

[76] ——, “Error-rate evaluation of linear equalization and decision feedback equalization with error propagation,” *IEEE Trans. Commun.*, vol. 46, no. 5, pp. 656–665, May 1998.

[77] J. Hammons, A. R. and H. El Gamal, “On the theory of space-time codes for PSK modulation,” *IEEE Trans. Inform. Theory*, vol. 46, no. 2, pp. 524–542, Mar. 2000.

[78] H.-F. Lu and P. V. Kumar, “A unified construction of space-time codes with optimal rate-diversity tradeoff,” *IEEE Trans. Inform. Theory*, vol. 51, no. 5, pp. 1709–1730, May 2005.

[79] Y. Zhao, R. Adve, and T. J. Lim, “Improving amplify-and-forward relay networks: Optimal power allocation versus selection,” *IEEE Trans. Wireless Commun.*, vol. 6, no. 8, pp. 3114–3123, August 2007.

[80] ——, “Symbol error rate of selection amplify-and-forward relay systems,” *IEEE Commun. Lett.*, vol. 10, no. 11, pp. 757–759, Nov. 2006.

[81] J. Hu and N. C. Beaulieu, “Performance analysis of decode-and-forward relaying with selection combining,” *IEEE Commun. Lett.*, vol. 11, no. 6, pp. 489–491, June 2007.

[82] B. Rankov and A. Wittneben, “Achievable rate regions for the two-way relay channel,” in *Proc. IEEE International Symposium on Information Theory*, July 9–14, 2006, pp. 1668–1672.

[83] ——, “Spectral efficient signaling for half-duplex relay channels,” in *Conference Record of the Thirty-Ninth Asilomar Conference on Signals, Systems and Computers*, Oct. 2005, pp. 1066–1071.

[84] B. Rankov and A. N. Wittneben, “Spectral efficient protocols for half-duplex fading relay channels,” *IEEE J. Select. Areas Commun.*, vol. 25, no. 2, pp. 379–389, February 2007.

[85] T. Cui and C. Tellambura, “An efficient generalized sphere decoder for rank-deficient MIMO systems,” *IEEE Commun. Lett.*, vol. 9, no. 5, pp. 423–425, May 2005.

[86] T. S. Rappaport, *Wireless Communications: Principles and Practice*, 2nd ed. Prentice Hall PTR, 2002.

[87] J. Proakis, *Digital Communications*, 4th ed. McGraw-Hill Science/Engineering/Math, 2001.

[88] Y. Zhao, R. Adve, and T. J. Lim, "Improving amplify-and-forward relay networks: Optimal power allocation versus selection," in *Proc. IEEE International Symposium on Information Theory*, July 2006, pp. 1234–1238.

[89] X. Liu and W. Su, "Optimum selection relaying protocols in cooperative wireless networks," in *Proc. IEEE Global Telecommunications Conference GLOBECOM '06*, Nov. 2006, pp. 1–5.

[90] K. Azarian, H. El Gamal, and P. Schniter, "On the achievable diversity-multiplexing tradeoff in half-duplex cooperative channels," *IEEE Trans. Inform. Theory*, vol. 51, no. 12, pp. 4152–4172, Dec. 2005.

[91] I.-H. Lee and D. Kim, "BER analysis for decode-and-forward relaying in dissimilar Rayleigh fading channels," *IEEE Commun. Lett.*, vol. 11, no. 1, pp. 52–54, Jan. 2007.

[92] D. S. Michalopoulos and G. K. Karagiannidis, "PHY-layer fairness in amplify and forward cooperative diversity systems," *IEEE Trans. Wireless Commun.*, vol. 7, no. 3, pp. 1073–1082, March 2008.

[93] D. Michalopoulos and G. Karagiannidis, "Performance analysis of single relay selection in Rayleigh fading," *IEEE Trans. Wireless Commun.*, vol. 7, no. 10, pp. 3718–3724, Oct. 2008.

[94] H. A. David, *Order Statistics.* John Wiley & Sons, 1970.

[95] M. Chiani, D. Dardari, and M. K. Simon, "New exponential bounds and approximations for the computation of error probability in fading channels," *IEEE Trans. Wireless Commun.*, vol. 2, no. 4, pp. 840–845, July 2003.

[96] Y. Isukapalli and B. Rao, "An analytically tractable approximation for the Gaussian Q-function," *IEEE Commun. Lett.*, vol. 12, no. 9, pp. 669–671, Sept. 2008.